AIRCRAFT PROPELLER HANDBOOK

By

KARL HANSSON FALK

BLADE DESIGNER FOR HAMILTON STANDARD PROPELLERS

REVISED EDITION

THE RONALD PRESS COMPANY

NEW YORK

Second Printing, January, 1944.

PRINTED IN THE UNITED STATES OF AMERICA

PREFACE

This second edition of the "Aircraft Propeller Handbook" has been brought up to date throughout and includes certain more advanced subject matter which has entered into the propeller field during the last five years.

The information is presented in the same style, understandable rather than extremely technical, which contributed to the success of the first edition. All equations are given in the most simplified forms, employing advanced mathematics only where it could not be avoided. The aim has been to meet the needs of engineers, draftsmen, students, pilots, service personnel and others in the aeronautic industry who wish to obtain concise, practical data without delving into propeller theory.

To Hamilton Standard Propellers the author is greatly indebted for information gained by daily contact over many years with its highly skilled engineering personnel. This Handbook, however, is in no sense a setting forth of the practices of this particular company, to which, indeed, in many instances, it does not conform. The author accepts the full responsibility of engineering judgment in what is presented in the Handbook.

KARL H. FALK

Hartford, Conn.
January 12, 1943

CONTENTS

ILLUSTRATIONS

AIRCRAFT PROPELLER HANDBOOK

CHAPTER 1

PROPELLER DESIGN

Two- or Three-Bladed Propellers. If possible, a two-bladed propeller should be used because of its lighter weight and greater efficiency. Three-bladed propellers are adopted when the limitations of the airplane design require a small diameter (for ground clearance) or when the tip-speed exceeds 1000 ft/sec., a condition which leads to a loss of efficiency and excessive noise. When conditions do not permit use of the theoretical diameter, it is necessary to absorb the power in some other manner—either by increasing the number of blades or by increasing the blade width.

Diameter. The diameter of a propeller may be computed from the formula:

$$D = d(\text{r.p.m.})\, d(\text{m.p.h.})\, d(\text{hp.})$$

Where D = propeller diameter, ft.
$d(\text{r.p.m.})$ = factor from r.p.m. curve, Figure 2
$d(\text{m.p.h.})$ = factor from m.p.h. curve, Figure 2a
$d(\text{hp.})$ = factor from hp. curve, Figure 2a
ρ_0/ρ = air density ratio, Figure 3 (multiply by hp. when the engine is rated at altitude)

TYPICAL METAL PROPELLER BLADES

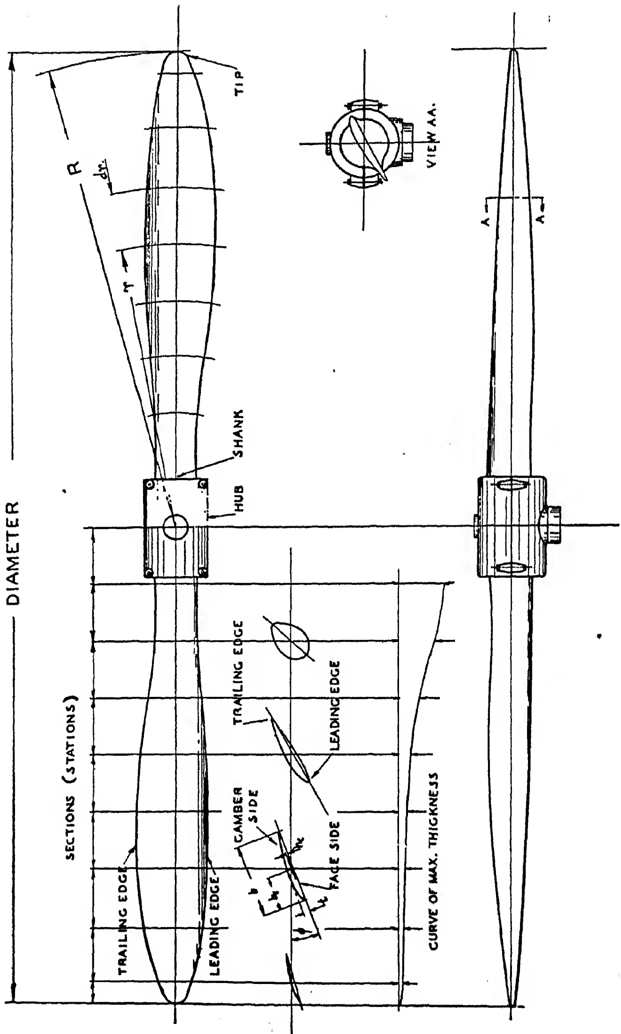

FIGURE I

'ACTOR OF R.P.M. FOR SELECTION OF
PROPELLER DIAMETER

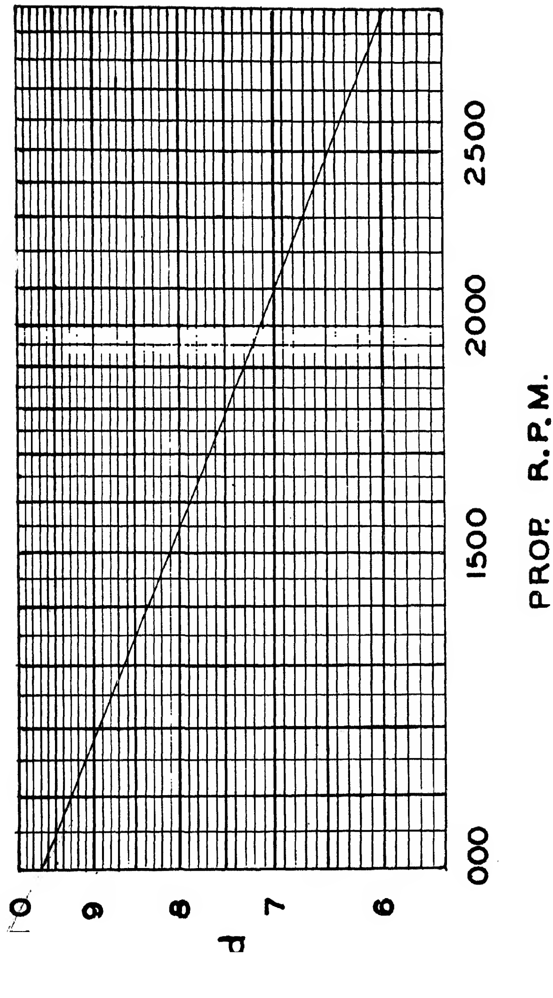

FIGURE 2

FACT S OF M.P.H. & H.P. FOR SELECTION OF PROPELLER DIAMETER

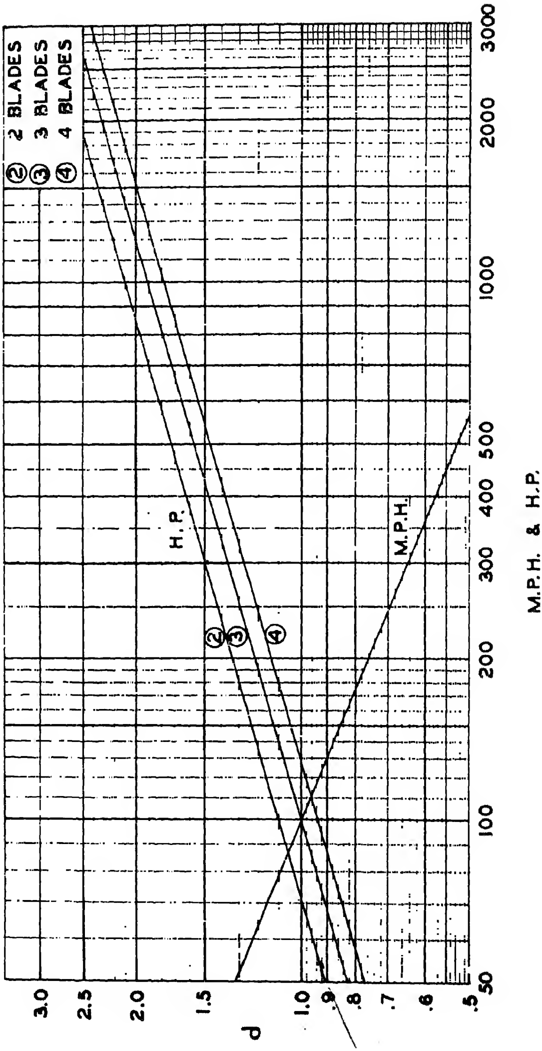

FIGURE 2a

ALTITUDE AIR DENSITY CURVE

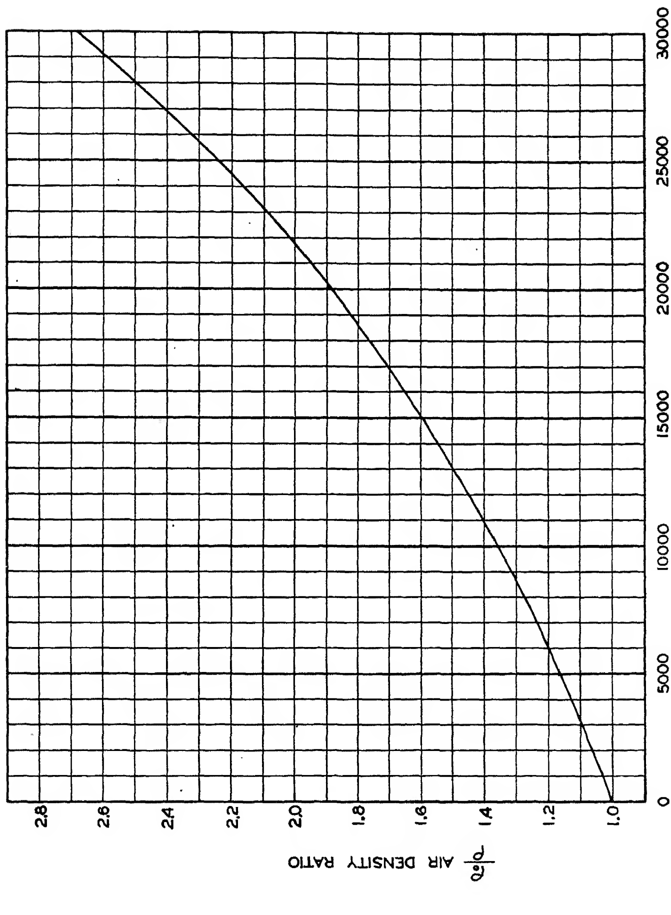

Width Ratio. The width ratio of a propeller blade is the blade width divided by the propeller diameter, Figure 4.

Blade Width. The blade width at each section may be calculated from

$$b = D \times \frac{b}{D}$$

Where D = propeller diameter, in.
b = blade width, in.

$\frac{b}{D}$ may be obtained from the width-ratio curve, Figure 4, in which the respective curves represent:

Narrow = high speed
Medium = fairly high speed and take-off
Wide = take-off and climb

Camber Ratio. The camber ratio or the thickness ratio of a propeller section is the thickness divided by the width, Figure 5.

Blade Thickness. The blade thickness at each section may be calculated from

$$t = b \times \frac{t}{b}$$

t = blade thickness, in.
b = blade width, in.

$\frac{t}{b}$ may be obtained from the camber-ratio curve, Figure 5.

Aspect Ratio. The aspect ratio (A.R.) of a propeller blade is the tip radius divided by maximum blade width.

WIDTH RATIO

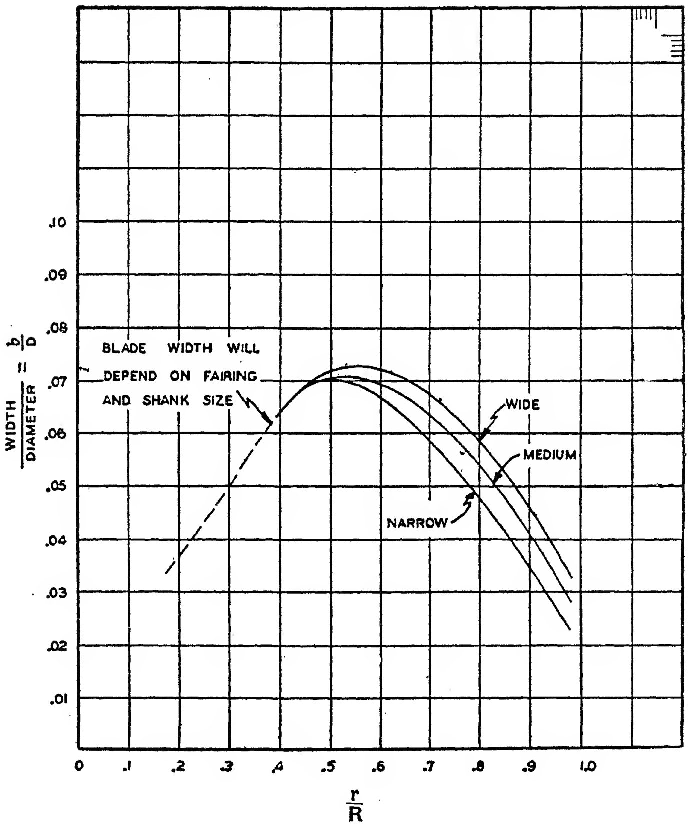

FIGURE 4

CAMBER RATIO

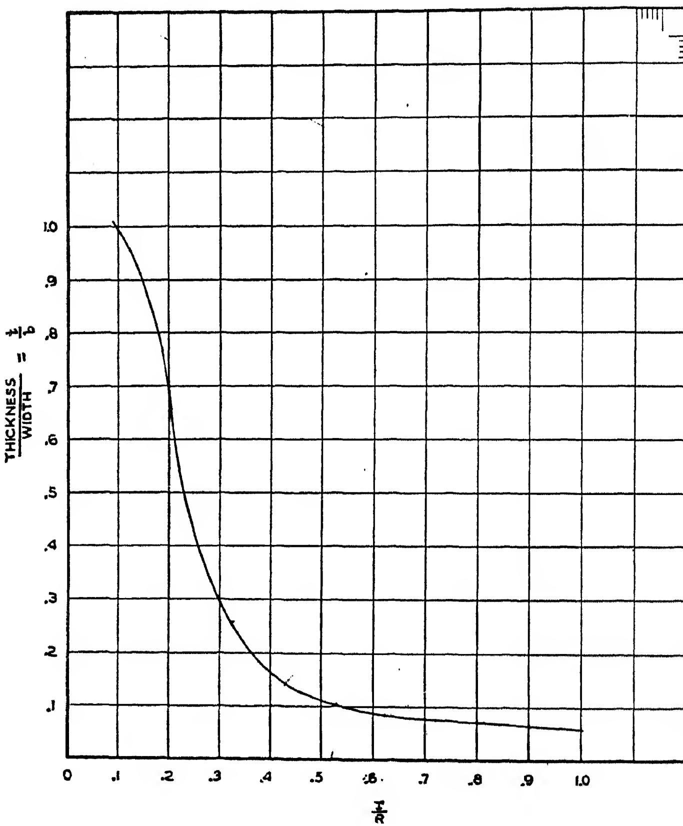

FIGURE 5

DIMENSIONS AND SECTION PROPERTIES FOR CLARK-Y SECTIONS

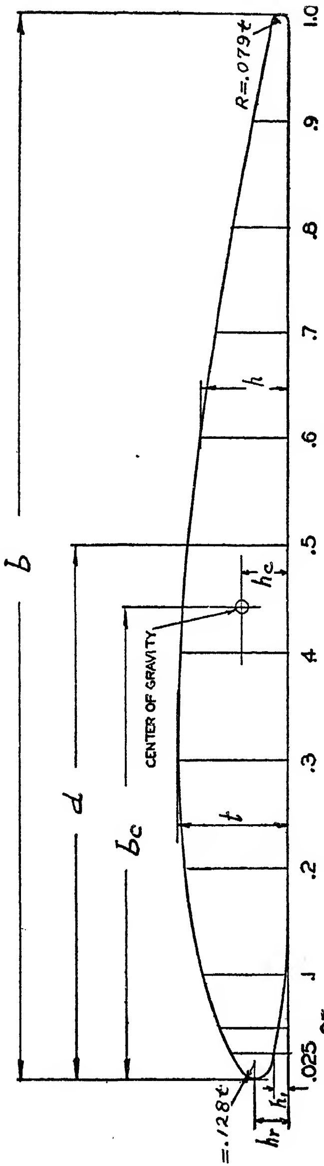

FIGURE 6

Ordinates of Section. (See Figure 6)

d/b	hr.	.025	.050	.1	.2	.3	.4	.5	.6	.7	.8	.9
h/t	.300	.549	.663	.806	.957	.995	.983	.928	.829	.684	.521	.337
h/t		.128	.081	.038	.008							

Center of Gravity of Section. (Clark-Y airfoil)

$$\text{c.g. above chord } (h_c) = 0.416\,t$$
$$\text{c.g. from leading edge } (b_c) = 0.4405\,b$$

t = blade thickness, in.
b = blade width, in.

The constant as given for locating the center of gravity of the blade section applies only to sections that have a flat face. For sections other than the flat-face type, the center of gravity can be determined either by experiment or by calculations as given on page 13. (Figure 7)

Cross-Sectional Area of Blade Section. (Clark-Y airfoil)

$$A = 0.7245\,b\,t$$

A = area, sq. in.
b = blade width, in.
t = blade thickness, in.

The above equation applies only to sections that have a flat face. For sections other than the flat-face type, see page 13. (Figure 7)

Moment of Inertia of Section. (Clark-Y airfoil, Figure 8)

$$\left.\begin{aligned} I\text{-major} &= 0.0418\,b^3\,t \\ I\text{-minor} &= 0.0454\,b\,t^3 \end{aligned}\right. \quad \text{Moment of inertia, in.}^4$$

b = blade width, in.
t = blade thickness, in.

AREA, CENTER OF GRAVITY AND MOMENT OF INERTIA OF ANY BLADE SECTION

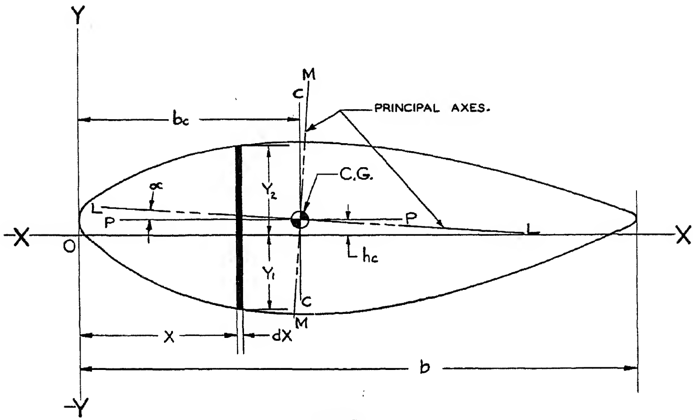

FIGURE 7

CROSS SECTIONAL AREA:

$$A = \int_0^b (Y_2 - Y_1)\,dx$$

CENTER OF GRAVITY:

$$b_c = \frac{\int_0^b (Y_2 - Y_1)\,x\,dx}{\int_0^b (Y_2 - Y_1)\,dx} \qquad h_c = \frac{\int_0^b (Y_2^2 - Y_1^2)\,dx}{2\int_0^b (Y_2 - Y_1)\,dx}$$

MOMENT OF INERTIA:

$$I_{XX} = \frac{1}{3}\int_0^b (Y_2^3 - Y_1^3)\,dx \qquad I_{YY} = \int_0^b (Y_2 - Y_1)\,x^2\,dx$$

ABOUT C. G.

$$I_{PP} = I_{XX} - h_c^2 \cdot A \qquad I_{CC} = I_{YY} - b_c^2 \cdot A$$

ABOUT PRINCIPAL AXES:

$$\alpha = \frac{1}{2}\,\mathrm{TAN}^{-1}\frac{\int_0^b (Y_2^2 - Y_1^2)\,x\,dx - 2\,b_c \cdot h_c \cdot A}{(I_{CC} - I_{PP})}$$

$$I_{LL} = I_{PP}\,\mathrm{COS}^2\alpha + I_{CC}\,\mathrm{SIN}^2\alpha \qquad I_{MM} = I_{PP}\,\mathrm{SIN}^2\alpha + I_{CC}\,\mathrm{COS}^2\alpha$$

The above equation applies only to sections that have a flat face. For sections other than the flat-face type, see page 13. (Figure 7)

MOMENTS OF INERTIA ABOUT THE PRINCIPAL AXES OF A BLADE SECTION

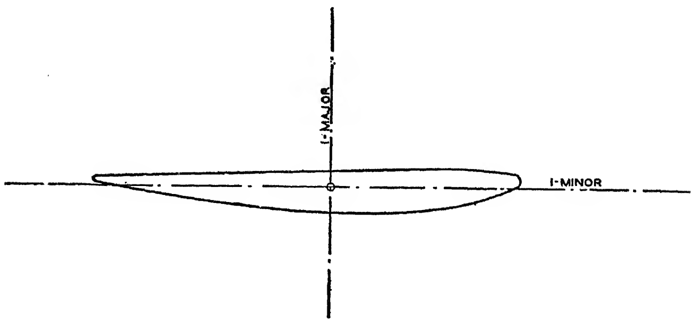

FIGURE 8

Ordinates of Section. (Figure 9)

d/b	.025	.050	.1	.2	.3	.4	.5	.6	.7	.8	.9
h/t	.410	.590	.790	.950	1.00	.990	.950	.870	.740	.560	.350

Center of Gravity of Section. (R.A.F.–6, airfoil)

c.g. above chord (h_c) $= 0.421\, t$

c.g. from leading edge (b_c) $= 0.446\, b$

t = blade thickness, in.

b = blade width, in.

The constant as given for locating the center of gravity of the blade sections applies only to sections that have a flat face. For sections other than the flat-face type, the center of gravity can be determined either by experiment or calculations as given on page 13. (Figure 7)

DIMENSION AND SECTION PROPERTIES FOR R.A.F.-6 SECTIONS

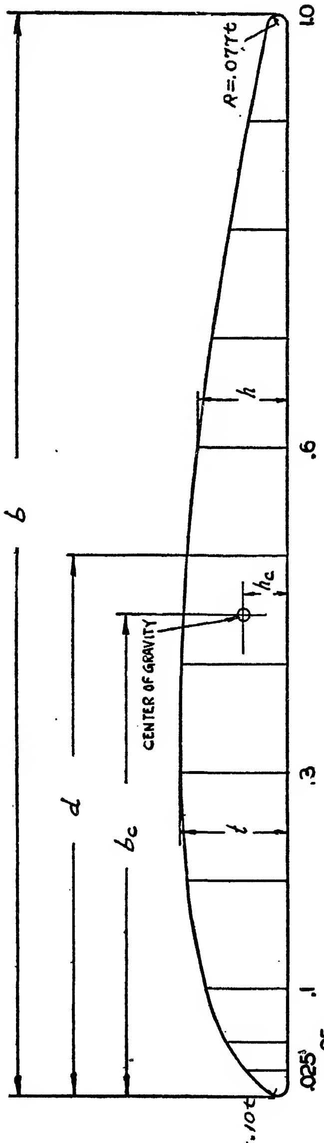

FIGURE 9

Cross-Sectional Area of Blade Section. (R.A.F.–6, airfoil)

$$A = 0.738\ b\ t$$

A = area, sq. in.
b = blade width, in.
t = blade thickness, in.

For other than the flat-face type sections, see page 13. (Figure 7)

Moment of Inertia of Section. (R.A.F.–6, airfoil)

$$\left.\begin{aligned} I\text{-major} &= 0.0446\ b^3\ t \\ I\text{-minor} &= 0.0464\ b\ t^3 \end{aligned}\right\} \text{Moment of inertia, in.}^4$$

b = blade width, in.
t = blade thickness, in.

For other than the flat-face type sections, see page 13. (Figure 7)

Blade Angle. The blade angle of a propeller is the acute angle between the chord of a propeller section and the plane of rotation. (Figure 10)

Effective Pitch. (Figure 10) The effective pitch angle is the distance an aircraft advances along its flight path and is the angle used for the designed pitch distribution. The effective pitch at each section is then:

$$\tan \Theta = \frac{V_1}{V} = \frac{V_1}{2\pi \times r/12 \times n} = \frac{\text{m.p.h.} \times 168}{r\ N}$$

Angle of Attack. The angle of attack is the difference between the blade angle and the effective pitch angle. (Figure 10)

Add an angle of attack from 0°–3°, depending on propeller characteristics, to the calculated effective pitch.

V_1 = forward speed, ft/sec.
V = rotation speed, ft/sec.
r = radius, in.
n = rev. per sec.
N = r.p.m.

ILLUSTRATION OF EFFECTIVE PITCH, BLADE ANGLE AND ANGLE OF ATTACK

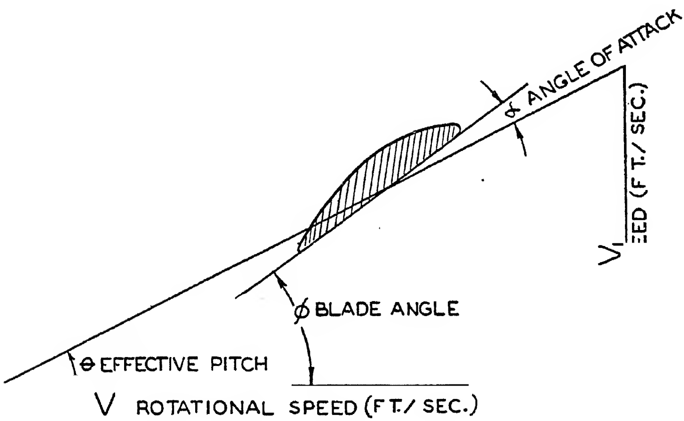

FIGURE 10

Blade Angle at the 42-In. Section. The blade angle at the 42-in. section may be obtained from Figure 11. A simplified method to check the angle at the 42-in. section is:

$$\tan \Theta = \frac{\text{m.p.h.} \times 4}{N}$$

NOMOGRAM FOR BLADE ANGLE AT 42" RADIUS

(ADD ANGLE OF ATTACK FROM 0° TO 3° DEPENDING
ON PROPELLER CHARACTERISTICS)

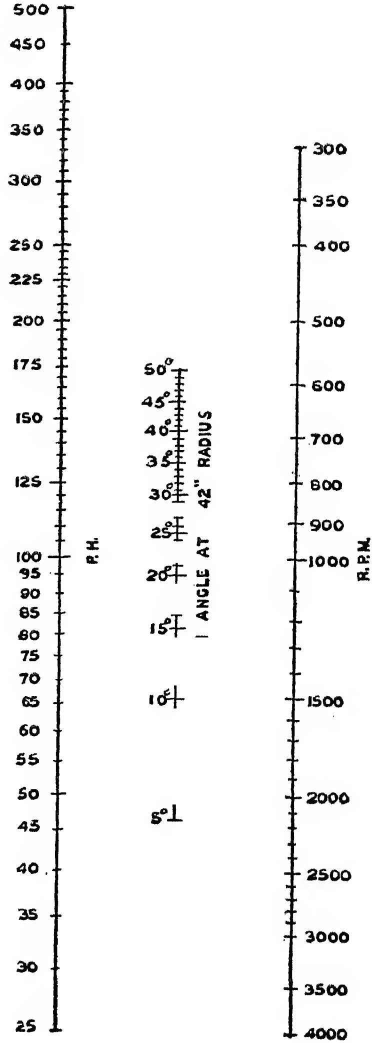

FIGURE 11

RELATION BETWEEN PROPELLER PITCH IN FEET AND BLADE ANGLE IN DEGREES AT THE 42" STATION

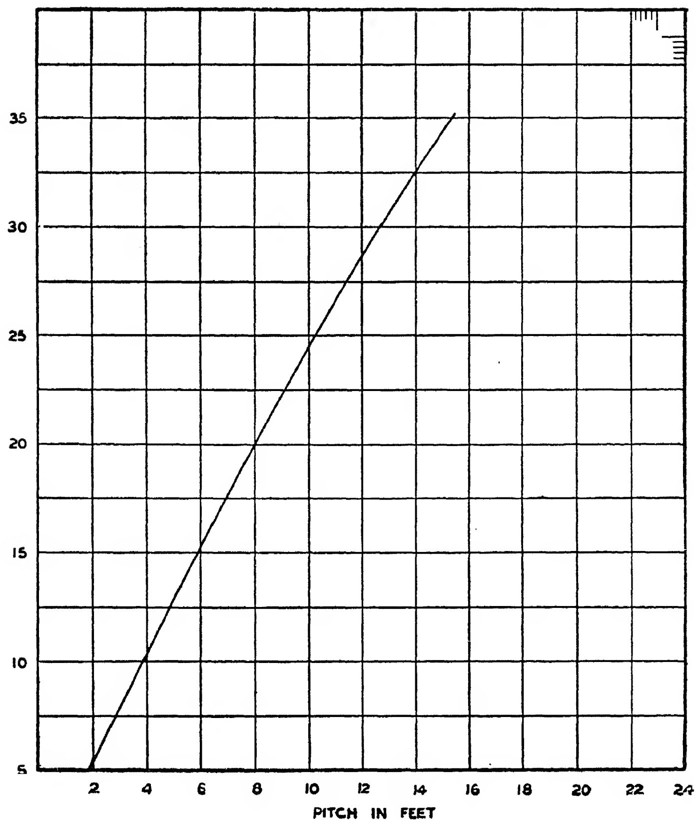

FIGURE 12

Blade Pitch. The blade angle may be determined by the pitch in feet or the angle in degrees from the curve (Figure 12) or may be calculated at any section from the formula:

$$2\pi \times \frac{r}{12} \times \tan \Theta = \text{pitch, ft.}$$

Blade Shank. When selecting the shank size, the determining factors are tip-speed and horsepower.

Shank size in relation to tip-speed is computed from the formula:

$$A = \frac{a}{f}$$

Where A = area of shank, sq. in.
a = area of section at 75% radius
f = factor from Figure 13

Shank size in relation to horsepower is obtained from Figure 14, where the engine horsepower is divided by the number of blades and the shank area is found directly on the curve.

The maximum shank area obtained is of course the fundamental basis for shank design. If the computed area for tip-speed is less than the area obtained from the horsepower curve, the tip-speed area then may be used for computing the root diameter of the retaining shoulder inside of the hub, which is subject only to tension.

RELATION OF SHANK SIZE TO TIP-SPEED

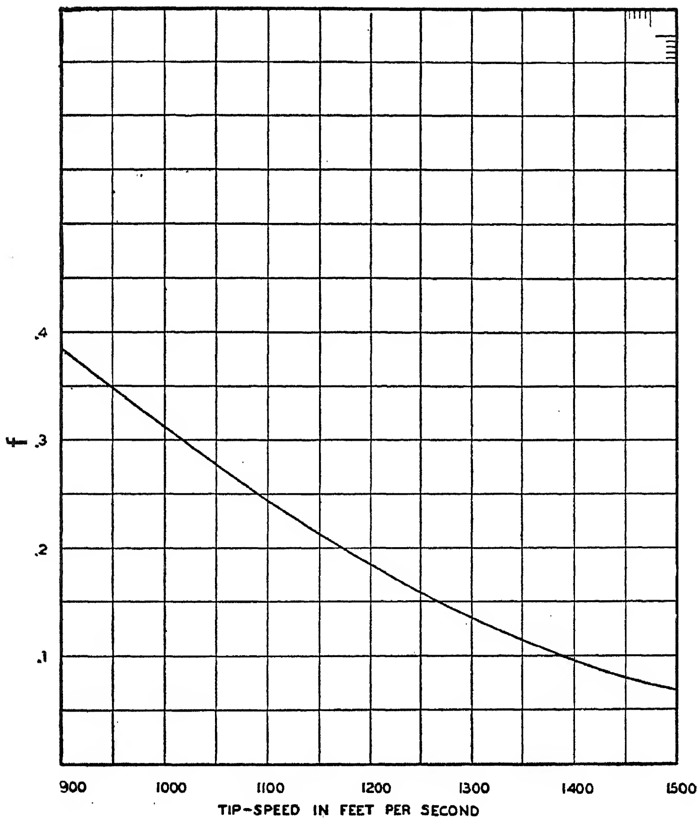

FIGURE 13

RELATION OF SHANK SIZE TO HP.

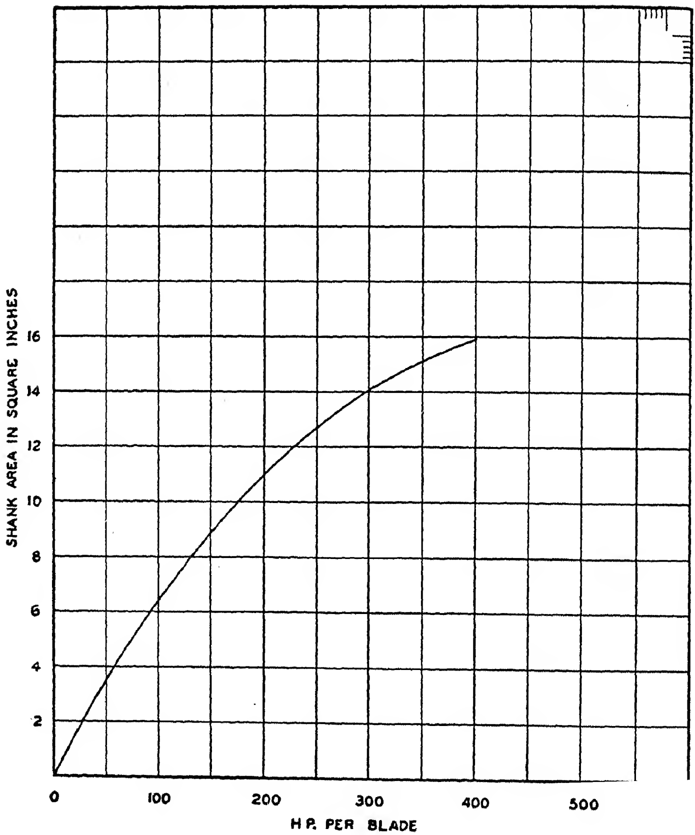

FIGURE 14

Blade Weight. Plot a curve of the area at each section against the radius; integrate graphically from shank to tip; and then multiply by the density of the material.

$$W = \delta \int_{O}^{R} A \, dr$$

W = weight, lb.
A = area of section, sq. in.
δ = density of material, lb/cu. in.

CHAPTER 2

STATIC AND GYROSCOPIC CHARACTERISTICS

Static Moment. The static moment of a propeller blade is obtained by plotting a curve of the area times the radius against the radius. The integration under the curve times the density of the material gives the static moment.

$$M = \delta \int_{O}^{R} A\ r\ dr$$

Where M = static moment, in-lb.
A = area of section, sq. in.
r = radius, in.
δ = density of material, lb/cu. in.

Static Moment. The static moment also may be obtained, if the center of gravity and the weight of the blade are known, as follows:

$$M = L\ W$$

L = distance from center of rotation to center of gravity of the blade, in.
W = weight of blade, lb.

Center of Gravity. The center of gravity of a propeller blade is calculated from the static moment and the blade weight.

$$L = \frac{M}{W}$$

L = distance from center of rotation to the center of gravity of blade, in. (Figure 15)

W = weight of blade, lb.

M = static moment, in-lb.

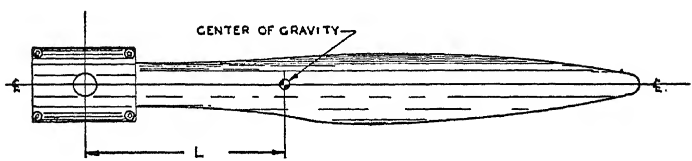

FIGURE 15

Polar or Mass Moment of Inertia. The polar moment of inertia of a propeller blade is one of the controlling factors in determining the gyroscopic force acting on the engine crankshaft.

Major Polar Moment of Inertia, Figure 16a.

$$I_z = \delta \int_0^R A\, r^2\, dr$$

Minor Polar Moment of Inertia, Figure 16a.

$$I_y = \frac{\delta}{144} \int_0^R (I_{maj} + I_{min}) dr$$

I_z & I_y = polar moment, lb-ft.^{2}, per blade
A = area of section, sq. in.
r = radius, ft.
δ = density of material, lb/cu. in.
I_{maj} = moment of inertia about major axis
I_{min} = moment of inertia about minor axis

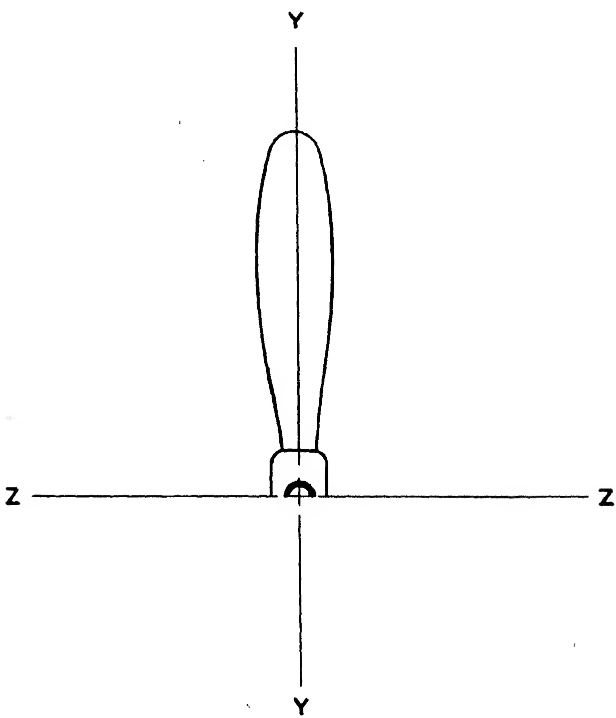

FIGURE 16a

EXAGGERATED SKETCH SHOWING THE EFFECT
OF PROPELLER POLAR MOMENT

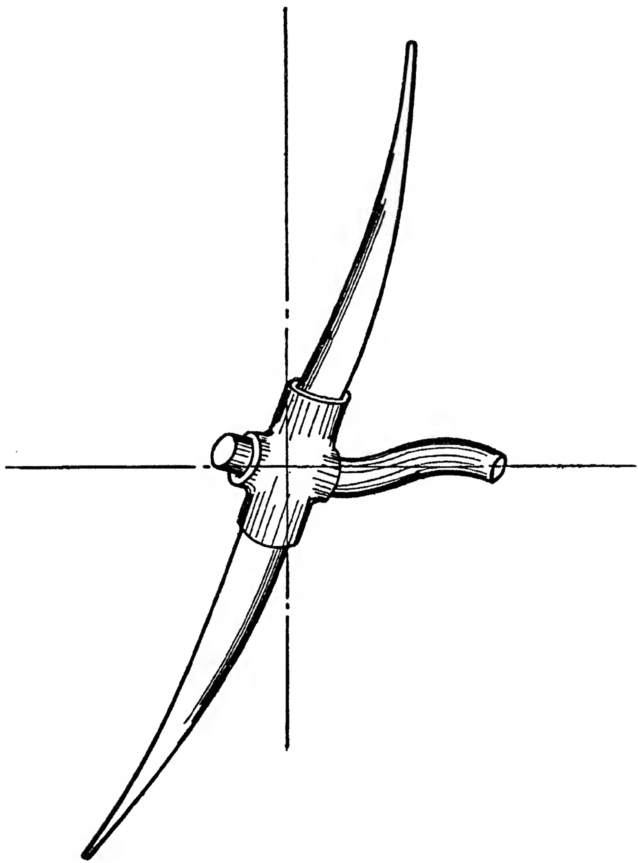

FIGURE 16

Polar Moment. (Approximate Method) May be computed by the following equation:

$$I_p = \frac{.135\ c\ D^5}{\text{A.R.}}$$

D = diameter of propeller, ft.
c = camber ratio, (t/b at 75% radius)
A.R. = aspect ratio, (R/b_{max})

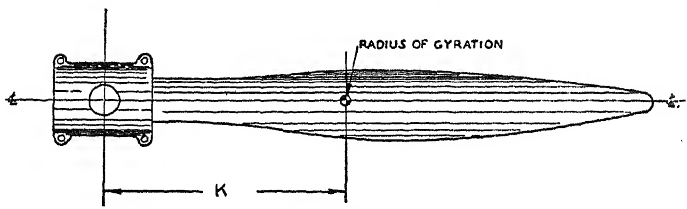

FIGURE 17

Radius of Gyration.

$$I_p = \delta \int_O^R A\ r^2\ dr = K^2\ W$$

Where K is the radius of gyration (Figure 17) and the moment of inertia remains the same.

From the above formula:

$$K = \sqrt{\frac{I_p}{W}}$$

I_p = polar moment, lb-ft.^{2}
K = radius of gyration, ft.
W = weight of blade, lb.

The radius of gyration of a propeller blade is the distance from the axis at which all of the mass of the blade could be concentrated and have the same moment of inertia.

CHAPTER 3

AERODYNAMIC CHARACTERISTICS

Efficiency. The approximate efficiency may be obtained from Figure 18. Where:

$$\frac{V}{N\,D} = \frac{\text{m.p.h.} \times 88}{\text{r.p.m.} \times D}$$

D = propeller diameter, ft.

Thrust at Top Speed. The component parallel to the propeller axis of the total air forces:

$$T = \frac{\text{hp.} \times e \times 375}{V}$$

T = thrust, lb. per propeller
e = efficiency from Figure 18
V = design speed, m.p.h.

Static Thrust and Blade Angle at Static Condition. Static thrust is the thrust developed by a propeller when rotating at a fixed point.

The following method in calculating the static thrust is based on a tip-speed of 900 feet per second, normal plan-form, thickness ratio of 0.075 at the 75% radius and a ratio of body diameter to propeller diameter of approximately 0.42.

The static thrust is computed by first determining the power coefficient (C_p), which is obtained by,

$$C_p = P_{(\text{hp.})} \times P_{(N)} \times P_{(D)} \text{ From Figure 19}$$

The static thrust is then calculated by,

$$T_s = \frac{K \times \text{hp.}}{N\,D}$$

The value of K and blade angle at the 75% radius are determined by projecting the computed power coefficient from the C_p curve (as shown in Figure 19a), depending upon the number of blades used. However, should the blade angle at the 75% radius be known, the value of K may be found directly from Figure 19a.

T_s = static thrust per propeller, lb.
K = thrust coefficient from Figure 19a
hp. = horsepower
N = r.p.m.
D = propeller diameter, ft.
$P_{(\text{hp.})}$ = horsepower coefficient from Figure 19
$P_{(N)}$ = r.p.m. coefficient from Figure 19
$P_{(D)}$ = diameter coefficient from Figure 19

Rotational Tip-Speed. The propeller tip-speed may be obtained from Figure 20, or calculated from the equation:

$$V_t = \frac{\pi\,N\,D}{60} = 0.0524\ N\,D \text{ ft/sec.} = 3.141\ N\,D \text{ ft/min.}$$

APPROXIMATE EFFICIENCY
FOR
METAL PROPELLERS

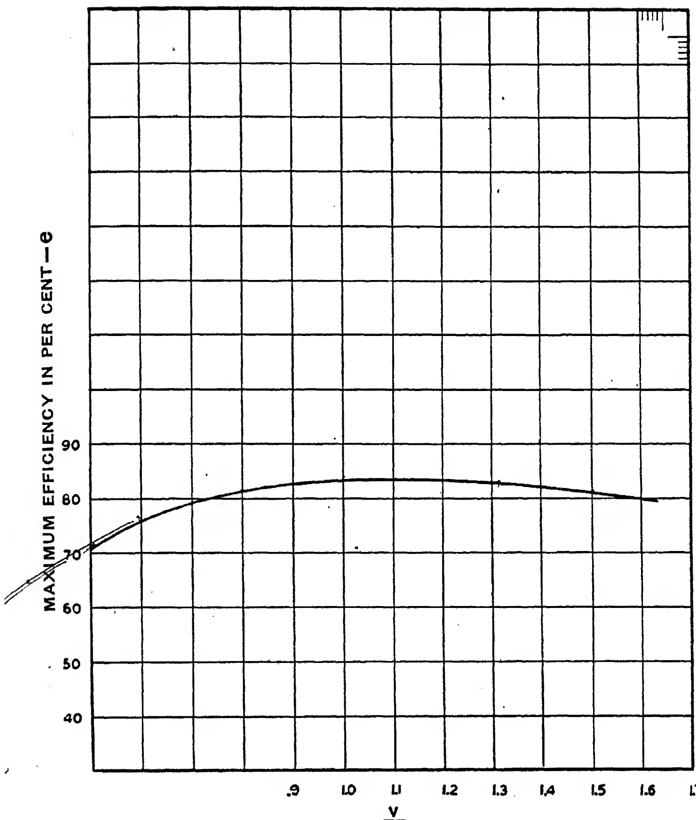

FIGURE 18

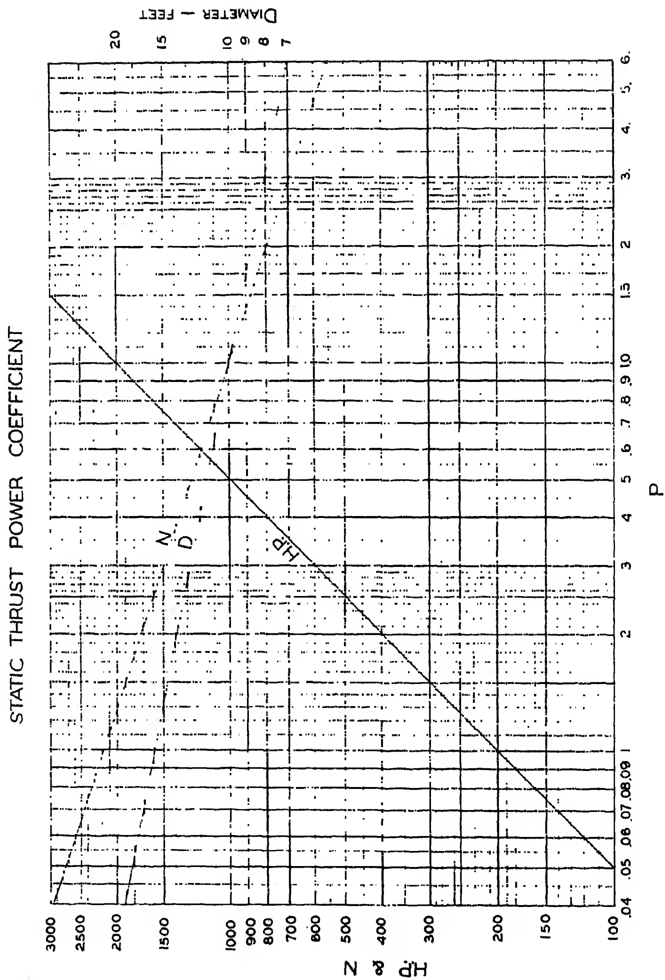
STATIC THRUST POWER COEFFICIENT
DIAMETER — FEET
20
15
10
9
8
7
N
D
H.P.
HP & N
3000
2500
2000
1500
1000
900
800
700
600
500
400
300
200
150
100
.04
.05
.06
.07
.08
.09
1
1.5
2
3
4
5
.6
.7
.8
.9
1.0
P

FIGURE 19

VARIATION OF BLADE ANGLE WITH

POWER AND STATIC THRUST COEFFICIENT

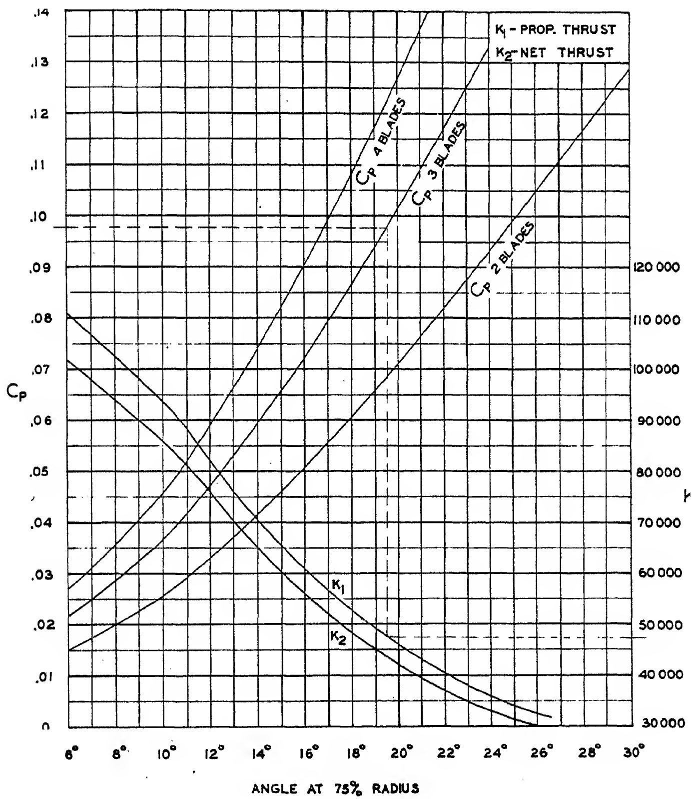

FIGURE 19a

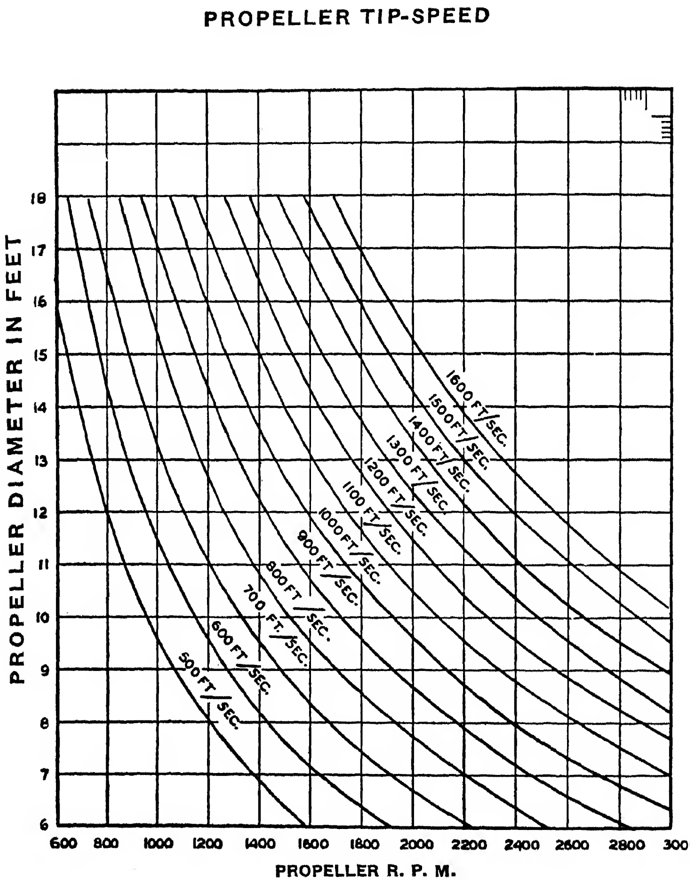
PROPELLER TIP-SPEED
PROPELLER DIAMETER IN FEET
18
17
16
15
14
13
12
11
10
9
8
7
6
600
800
1000
1200
1400
1600
1800
2000
2200
2400
2600
2800
3000
PROPELLER R. P. M.
500 FT/SEC.
600 FT/SEC.
700 FT./SEC.
800 FT/SEC.
900 FT/SEC.
1000 FT/SEC.
1100 FT/SEC.
1200 FT/SEC.
1300 FT/SEC.
1400 FT/SEC.
1500 FT/SEC.
1600 FT/SEC.

FIGURE 20

Helical Tip-Speed. The helical tip-speed is the resultant of the rotational and forward speeds.

The helical tip-speed is procured by selecting the rotational and forward speed coefficient from Figure 20a. Summing the coefficient, the helical tip-speed may be obtained from Figure 20b.

The helical tip-speed also may be calculated from equation:

$$V_r = \sqrt{\left(\frac{\pi\, N\, D}{60}\right)^2 + V^2} \text{ ft/sec.}$$

N = r.p.m.
D = propeller diameter, ft.
V = forward speed, ft/sec.

Torque. The moment produced on the propeller by the engine shaft:

$$Q = \frac{\text{hp.} \times 63{,}000}{\text{r.p.m.}}$$

Q = torque, lb-in.

The torque force at tip radius:

$$F_q = \frac{Q}{B\, R}$$

F_q = force, lb.
B = number of blades
R = tip radius, in.

Torque moment at stations:

$$M_q = F_q\, d$$

M_q = moment at stations, lb-in.
F_q = force, lb.
l = distance from tip to the station, in.

TIP-SPEED COEFFICIENTS

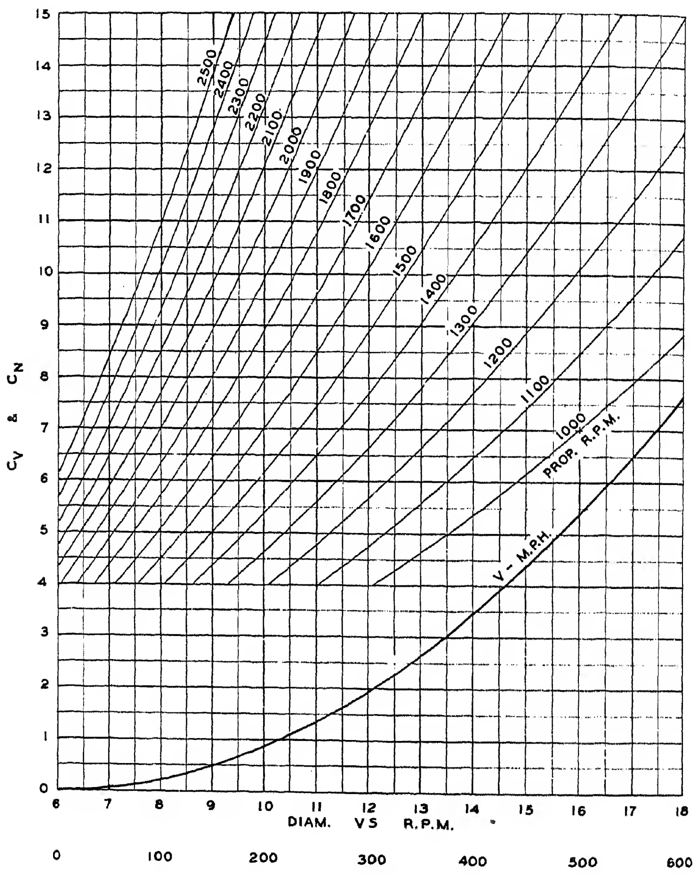

FIGURE 20a

HELICAL TIP-SPEED

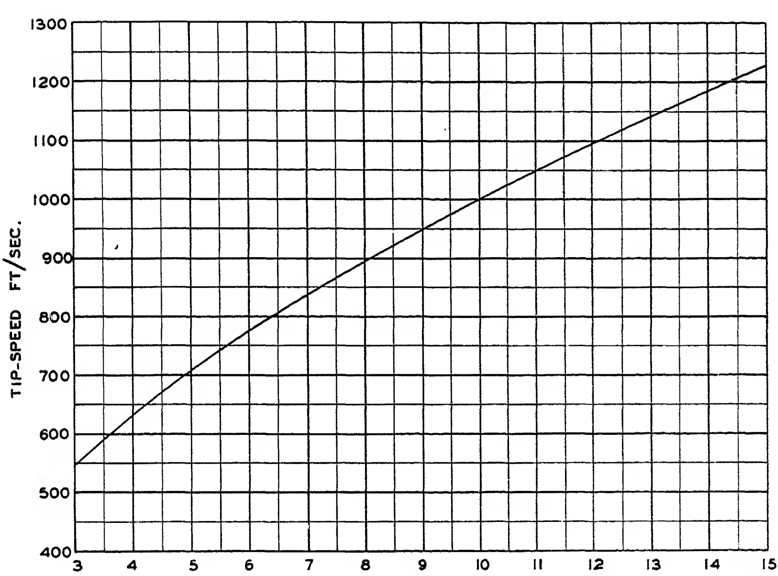

FIGURE 20b

CHAPTER 4

TWISTING MOMENTS

Centrifugal Twisting Moment. In a typical blade with the center of gravity of the sections along the center line of blade rotation, the centrifugal twisting moment introduced by the centrifugal load tends to force the blade into a low pitch position. The blade may also be designed to partially balance this condition by initially offsetting, or sweeping, the blade.

ILLUSTRATED EFFECT OF CENTRIFUGAL TWISTING MOMENT

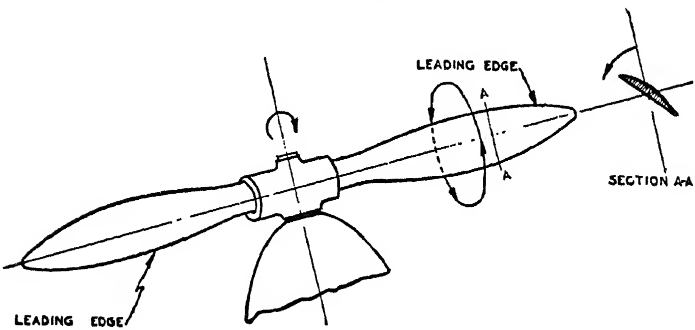

FIGURE 21

Determine the centrifugal twisting moments from equation 1 or 2 for the desired angle settings. Then from the following equations, 3, 4, 5 and 6, the moments may be computed for any desired condition.

TYPICAL SECTION WITH C.G. IN PLANE OF ROTATION

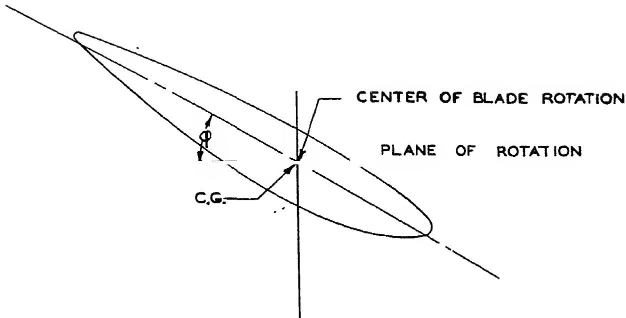

$$T_Q = .102\,\delta n^2 \int^{R} \left(I_{MAJ} - I_{MIN}\right) \sin\varphi \cos\varphi \, dr \tag{1}$$

FIGURE 22a

TYPICAL SECTION WITH INITIAL OFFSET OR SWEEP

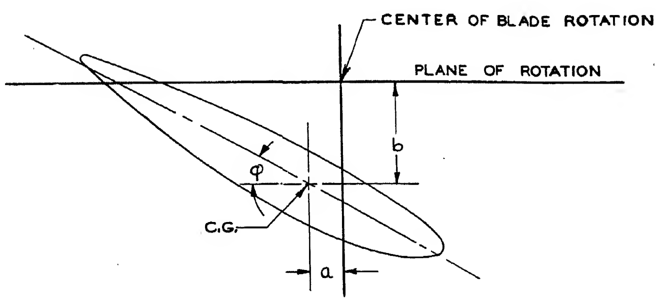

$$T_Q = .102\,\delta n^2 \int^{R} \left[\left(I_{MAJ} - I_{MIN}\right) \sin\varphi \cos\varphi - A \cdot a \cdot b\right] dr \tag{2}$$

FIGURE 22b

TWISTING MOMENT PER BLADE

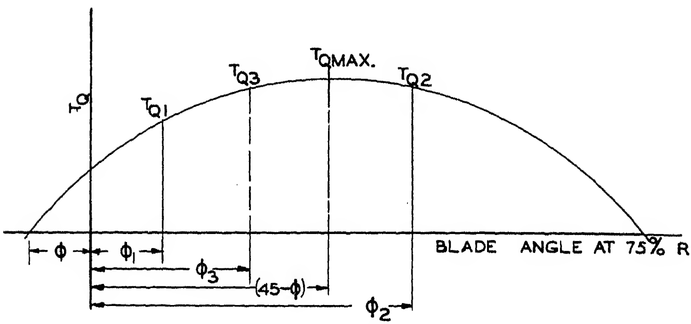

BLADE ANGLE AT ZERO MOMENT:

(3) $$\phi = \frac{1}{2}\,TAN^{-1}\left(\frac{T_{Q2}\,SIN\,2\phi_1 - T_{Q1}\,SIN\,2\phi_2}{T_{Q1}\,COS2\phi_2 - T_{Q2}COS2\phi_1}\right)$$

MAXIMUM MOMENT:

(4) $$T_{QMAX.} = \frac{T_{Q1}}{SIN2(\phi+\phi_1)} = \frac{T_{Q2}}{SIN\,2\,(\phi+\phi_2)} = \frac{T_{QN}}{SIN\,2(\phi+\phi_N)}$$

MOMENT AT ANY BLADE ANGLE:

(5) $$T_{Q3} = T_{QMAX.}\,SIN\,2(\phi+\phi_3)$$

MOMENT AT ANY DESIRED R.P.M.

(6) $$T_{Q\,n} = T_Q\,\frac{N_n^2}{N^2}$$

FIGURE 22c

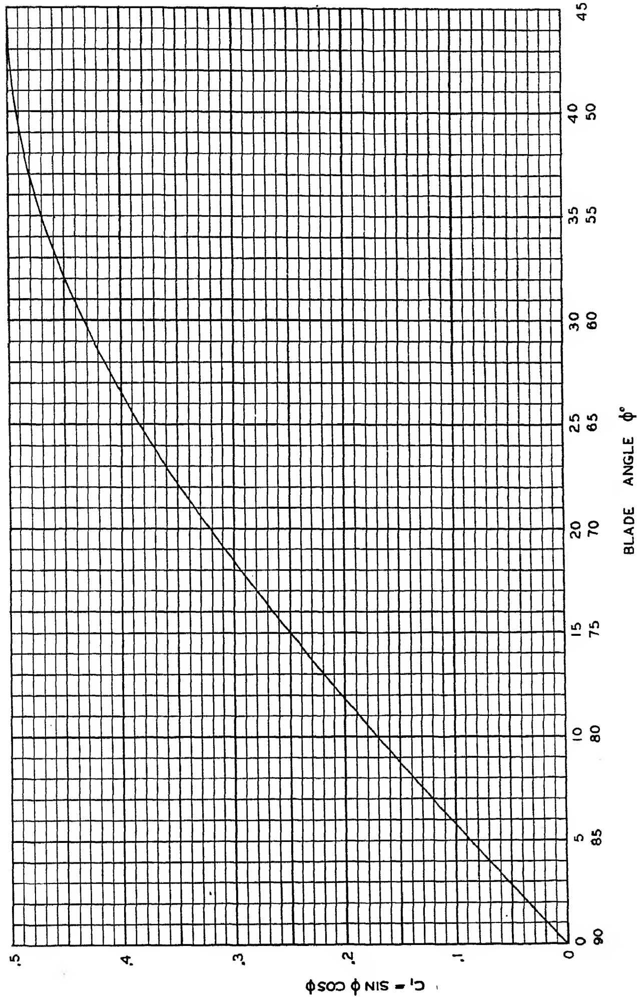
.5
.4
.3
.2
.1
0
$C_1 = \sin\phi \cos\phi$
0 5 10 15 20 25 30 35 40 45
90 85 80 75 70 65 60 55 50
BLADE ANGLE $\phi°$

FIGURE 23

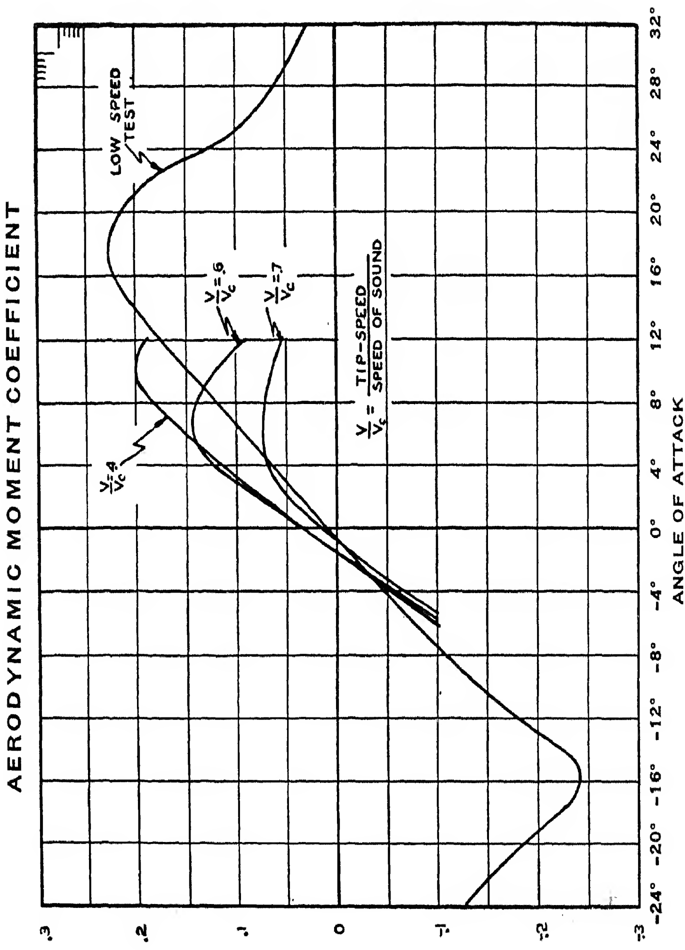

AERODYNAMIC MOMENT COEFFICIENT
ANGLE OF ATTACK
LOW SPEED TEST
V/Vc = .6
V/Vc = .7
V/Vc = .4
V/Vc = TIP-SPEED / SPEED OF SOUND
.3
.2
.1
0
-.1
-.2
-.3
-24°
-20°
-16°
-12°
-8°
-4°
0°
4°
8°
12°
16°
20°
24°
28°
32°

FIGURE 24

T_Q = centrifugal twisting moment per blade lb-in.
n = propeller rev. per sec.
I_{maj} = moment of inertia about major axis
I_{min} = moment of inertia about minor axis
δ = density of material, lb/cu. in.
ϕ = blade angle—values of $\sin\phi\cos\phi = c_1$ (Figure 23)
A = area of section
a = distance from center of blade rotation to center of gravity of blade section parallel to plane of rotation
b = distance from center of blade rotation to center of gravity of blade section perpendicular to plane of rotation

Aerodynamic Twisting Moment. The aerodynamic twisting moment tends at normal and positive angles of attack to force the blade into the high-pitch position. At high negative angles of attack, it tends to force the blade into the low-pitch position.

$$M_T = \int_O^R C_m b^2 \times \rho/_2 \times W^2 \, dr$$

M_T = aerodynamic twisting moment
b = blade width, ft.
ρ = air density

$$W = \frac{V_1}{\sin\phi} - \frac{\text{m.p.h.} \times 1.466}{\sin\phi}$$

C_m = moment coefficient, Figure 24
ϕ = blade angle

CHAPTER 5

THE STRENGTH OF PROPELLERS

Centrifugal Force. (Figure 25) The direct tension due to centrifugal force is obtained by plotting a curve of centrifugal force per inch of radius against the radius in inches.

CENTRIFUGAL FORCE

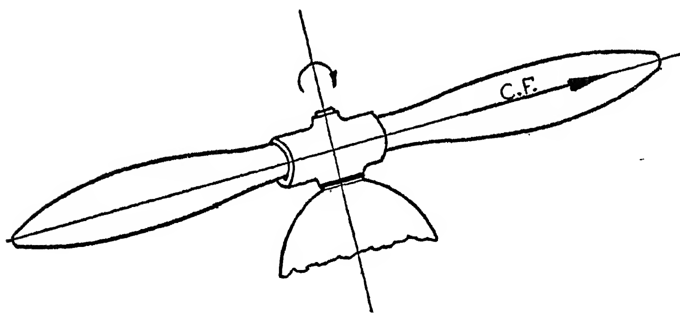

FIGURE 25

Integration under this curve from the propeller tip to the section under consideration gives the total centrifugal load on any section. The centrifugal force on any element of the blade is:

$$\frac{\delta\ A\ dr}{g}\left(2\ \pi\ n\right)^2\frac{r}{12} = 0.102\ \delta\ A\ r\ n^2\ dr$$

The total centrifugal force at any station is therefore,

$$\int_{R}^{r} 0.102\, \delta\, A\, r\, n^2\, dr$$

Where A = area of section, sq. in.
r = radius, in.
n = rev. per sec.
δ = density of material, lb/cu. in.

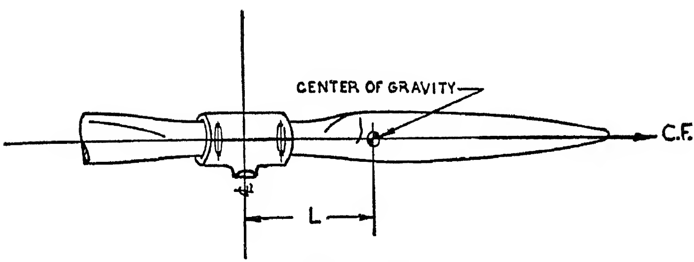

FIGURE 26

Centrifugal Force. (Simplified Method) The total centrifugal force of the blade may be obtained if the weight and center of gravity of the blade are known.

$$\text{C.F.} = 1.227\, W\, L\, n^2$$

W = weight of blade, lb.
L = distance from axis of rotation to c.g. of blade, ft. (Figure 26)
n = rev. per sec.

Centrifugal Stress. The centrifugal force load at each section divided by the area of the cross-section at the corresponding radius gives the direct tensile stress.

$$f_t = \frac{\text{C.F.}}{A}$$

f_t = tensile stress due to centrifugal force, lb/sq. in.
A = area of section, sq. in.
C.F. = centrifugal force load, lb.

Air Load. (Figure 27) The air load per inch is assumed to be proportional to

$$r^2\, b$$

then the total load at any section is:

$$\int_R^r r^2\, b\, dr$$

Plot this function against the radius and by integration the total load (P) in uncorrected form is found.

AIR LOAD'S EFFECT ON PROPELLER BLADE

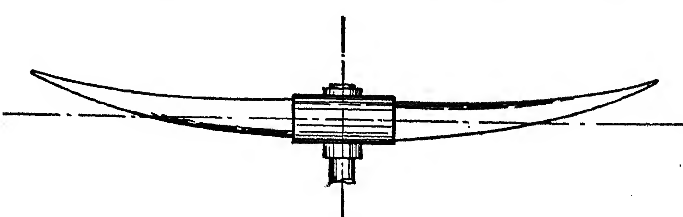

FIGURE 27

True Air Load. The true air load is obtained from the correction factor (f).

$$f = 1.042\ (t_s/P)$$

The true air load is then:

$$\int_R^r f\, r^2\, b\, dr$$

r = radius, in.
b = blade width, in.
P = uncorrected air load
t_s = static thrust per blade

Shear. By integration of the true air-load curve, $\int_R^r f r^2 b\, dr$, from the propeller tip to the section under consideration, the shear at any section is obtained.

Bending Moment. (Due to air load only.) By integrating the shear curve with respect to the radius, the bending moment at any section is determined as follows:

$$\text{B.M.} = \int_R^r \int_R^r f\, r^2\, b\, dr\, dr$$

Curvature. The curvature at each section is then determined by,

$$\frac{\text{B.M.}}{E \cdot I_{min}}$$

E = modulus of elasticity
I_{min} = moment of inertia about minor axis

Slope. Integrating the curvature with respect to the radius, the slope is determined at each station by,

$$\int_0^r \frac{\text{B.M.}}{E \cdot I_{min}} \, dr$$

Deflection. The deflection of each section is determined by integrating the slope with respect to the radius as follows:

$$\int_0^r \int_0^r \frac{\text{B.M.}}{E \cdot I_{min}} \, dr \, dr$$

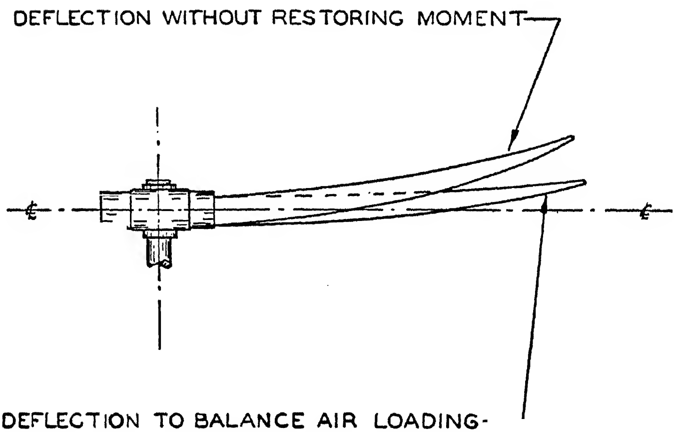

FIGURE 28

Restoring Moment. When the centrifugal force opposes the air force, a moment commonly known as "restoring moment" is produced. (Figure 28.) This restoring moment reduces the deflection which has been induced by the air forces and is determined by integrating the following equation from the tip to the section under consideration.

$$M_R = \int_R^r F_c \, dy$$

F_c = centrifugal force in pounds
y = deflection in inches

Correction Factor. To obtain the true bending moment, the previously computed bending moment must be multiplied by a restoring moment correction factor,

$$Z = \frac{\text{B.M.}}{\text{B.M.} + M_R}$$

$$C_R = \frac{Z^2}{Z_{average}} = \text{empirical correction factor}$$

True Bending Moment.

$$M = C_R \cdot \text{B.M.}$$

True Curvature.

$$\frac{M}{E \cdot I_{min}}$$

True Slope.

$$\int_0^r \frac{M}{E \cdot I_{min}}$$

True Deflection.

$$\int_0^r \int_0^r \frac{M}{E \cdot I_{min}}\, dr\, dr$$

Bending Stress.

$$f_b = \frac{M \cdot h_c}{I_{min}}$$

h_c = distance from neutral axis to outermost fibre

Initially Offset Blades. Sometimes it is advisable to initially offset the center of gravity of a blade from its center of rotation, in the direction of thrust, to relieve a high bend-

ing stress about the minor axis. For a blade with such an offset, the restoring moment correction factor becomes:

$$Z_1 = \frac{\text{B.M.} - \int F_c \, dy_o}{\text{B.M.} + \int F_c \, dy}$$

$$C_{R1} = \frac{Z_1^2}{Z_{1\ average}}$$

y_o = initial offset of the center of gravity from the center line of blade rotation

True Bending Moment.

$$M_1 = C_{R1} \cdot \text{B.M.}$$

However, should this blade be used at reverse blade angles for a negative thrust condition, the correction factor then becomes:

$$Z_2 = \frac{\text{B.M.} + \int F_c \, dy_o}{\text{B.M.} + \int F_c \, dy}$$

$$C_{R2} = \frac{Z_2^2}{Z_{2\ average}}$$

True Bending Moment.

$$M_2 = C_{R2} \cdot \text{B.M.}$$

Initially Swept Blades. The sweep-back found in wood blades and some metal blades introduces the following sweep moment:

$$M_s = \int F_c \, ds$$

s = the offset of the center of gravity from the center line of rotation along the major axis

Sweep Stress.

$$f_s = \frac{M_s \cdot h_b}{I_{maj}}$$

h_b = distance from neutral axis to outermost fibre
I_{maj} = moment of inertia about the major axis

Gyroscopic Bending Moment. The gyroscopic bending moment induced on a propeller blade by the angular velocity of the aircraft may be determined as follows:

Gyroscopic Moment.

$$M_{g1} = 19.1 \frac{\Omega}{N} \int_R^r F_c \, dr \text{ where,}$$

Ω = angular velocity of the aircraft in radians per second
N = propeller r.p.m.
F_c = centrifugal force

Gyroscopic Deflection.

$$Y_{g1} = \int_O^r \int_O^r \frac{M_{g1}}{E \cdot I_{min}} \, dr \, dr \text{ where,}$$

E = modulus of elasticity
I_{min} = minor moment of inertia of blade sections

Rectifying Moment. When the centrifugal and inertia forces oppose the gyroscopic force, a moment is produced which tends to decrease the gyroscopic deflection and moment. This rectifying moment is determined by,

$$M_{R1} = \int_{\left(\frac{Y_{g1}}{R}\right)}^{\left(\frac{Y_{g1}}{r}\right)} F_c \, d\left(\frac{Y_{g1}}{r}\right)$$

Rectifying Factor.

$$C_1 = \frac{M_{g1}}{M_{g1} + r \cdot M_{R1}}$$

and since this factor is merely a first approximation,

$$M_{g2} = C_1 \cdot M_{g1}$$

$$Y_{g2} = \int_0^r \int_0^r \frac{M_{g2}}{E \cdot I_{min}} \, dr \, dr$$

$$M_{R2} = \int_{\left(\frac{Y_{g2}}{R}\right)}^{\left(\frac{Y_{g2}}{r}\right)} F_c \, d\left(\frac{Y_{g2}}{r}\right)$$

$$C_2 = \frac{M_{g1}}{M_{g2} + r \cdot M_{R2}}$$

$M_{g3} = C_2 \cdot M_{g2}$, and similarly C_3, C_4 . . . . C_n may be computed. However, when C becomes 1 along the entire blade, the final "Rectifying factor" is determined by,

$$C_R = [C_1 \cdot C_2 \cdot C_3 \cdot \; . \; . \; . \; . \; C_n]$$

Gyroscopic Bending Moment.

$$M_G = C_R \cdot M_{g1}$$

Tensile Stress Due to Gyroscopic Bending Moment.

$$f_G = \frac{M_G \cdot h_c}{I_{min}}$$

h_c = distance from neutral axis to outermost fibre

CHAPTER 6

VIBRATION

Bending Moment Due to Weight of Blade. When propeller blades are vibrating in the fundamental mode, it is assumed that the form of deflection is the same as if the blade were supported at the hub and allowed to sag under its own weight (Figure 29).

DEFLECTION DUE TO WEIGHT OF BLADE

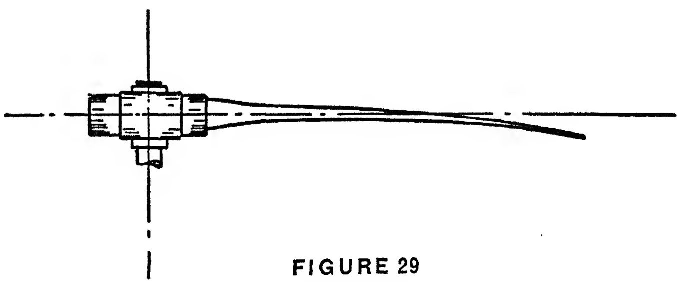

FIGURE 29

The weight load per inch is assumed to be $\delta\, A\, dr$; then the total load at any station is:

$$\int_R^r \delta\, A\, dr$$

By graphical integration of this function, the shear at any section can be found. By plotting the shear against radius

$$\int_R^r \int_R^r \delta\ A\ dr\ dr$$

and integrating, the weight-load bending moment at any section is obtained.

Deflection Due to Weight of Blade. The curvature of each section may be obtained from the value $M/E\ I$, where M is the moment due to blade weight, E the modulus of elasticity in tension, and I the minor and major moments of inertia for flatwise and edgewise frequencies, respectively. For torsional frequencies the curvature is assumed proportional to M/GI_p, where M is again the moment due to blade weight, G the modulus of elasticity in shear and I_p the polar moment of inertia. By plotting the curvature against the radius and integrating from the axis out to various stations, the slope at each station may be obtained. By plotting these values against the radius and integrating as before, a curve of deflection Δ may be obtained.

Potential Energy. If the propeller tip sags under its own weight it may be made to do positive work by returning to its zero position. This work is due to the stressed condition of the blade which is said to possess energy of position or "potential energy."

The potential energy may be obtained by plotting a curve of area of the cross-section times the deflection due to weight of blade at the corresponding radius.

$$\int_O^R A\ \Delta\ dr$$

This function is plotted against radius and the result is obtained by integration.

Kinetic Energy. When the propeller tip returns from the potential energy location to its zero position, it moves with some velocity, thereby obtaining energy. Thus energy possessed by the propeller blade on account of its motion is "kinetic" or actual energy.

The kinetic energy is obtained from the deflection due to the weight of the blade squared times the area under the corresponding radius.

$$\int_O^R A\ \Delta^2\, dr$$

Plot this function against the radius and obtain the result by integration.

Fundamental Flatwise Frequency. The fundamental flatwise frequency is calculated from the equation:

$$f = 187.86 \quad \frac{\int A \cdot \Delta}{\int A \cdot \Delta^2} \quad \text{where,}$$

f = natural period of vibration, cycles per min.
$\int A \quad \Delta$ = potential energy
$\int A \quad \Delta^2$ = kinetic energy

Fundamental Edgewise Frequency. The fundamental edgewise frequency is calculated from the equation:

$$f = 187.86 \cos \phi \sqrt{\frac{\int A \cdot \Delta}{\int A \cdot \Delta^2}} \quad \text{where,}$$

f = natural period of vibration, cycles per min.
ϕ = angular difference between the 0.5 t/b station and the tip
$\int A \cdot \Delta$ = potential energy
$\int A \cdot \Delta^2$ = kinetic energy

Fundamental Torsional Frequency. The fundamental torsional frequency is calculated from the equation:

$$f = 187.86 \frac{D}{3.636 \cos \phi} \sqrt{\frac{\int A \cdot \Delta}{\int A \cdot \Delta^2}} \quad \text{where,}$$

f = natural period of vibration, cycles per min.
D = diameter of propeller in feet
ϕ = angular difference between the 0.5 t/b station and the tip
$\int A \cdot \Delta$ = potential energy
$\int A \cdot \Delta^2$ = kinetic energy

CHAPTER 7

EXAMPLES

Propeller blades are designed by incorporating sections at 6-in. intervals of the blade length. These sections are commonly referred to as stations. To save space in this example, the design shall be handled with stations at 12-in. intervals. It should be noted that the following design is merely to show the method as outlined in the previous chapters.

Design and calculations are based on the following requirements:

400 hp. (sea level), 1760 r.p.m. @ 150 m.p.h.

Assuming a 2-bladed propeller and Clark-Y airfoil sections, select a medium blade width from Figure 4.

Material: aluminum alloy with a density of 0.102 lb/cu. in., modulus of elasticity $E = 10{,}000{,}000$.

In the following examples, the integrated values are multiplied by a scale factor which is obtained by multiplying the unit of the ordinate by the unit of the abscissa per inch.

Diameter. The propeller diameter is computed from the equation:

$$D = d(\text{r.p.m}) \; d(\text{m.p.h.}) \; d(\text{hp.}) = 1.62 \times 7.55 \times 0.85 = 10.4'$$

For simplicity a diameter of 10 feet is used here.

Width and Thickness of Blade. (Figure 30)

	Stations 12 in.	24 in.	36 in.	48 in.
r/R	.2	.4	.6	.8
b/D (from Figure 4)	.0367	.063	.069	.0535
$b = 120 \times b/D$	4.4	7.55	8.28	6.42
t/b (from Figure 5)	.685	.165	.089	.07
$t = b \times t/b$	3.01	1.245	.736	.449

Section Ordinates. The sections are divided into ten equal divisions with the division nearest the leading edge subdivided into halves and quarters. For section ordinates see Clark-Y airfoil section, Figure 6.

Center of Gravity of Sections.

	Stations 12 in.	24 in.	36 in.	48 in.
t	3.01	1.245	.736	.449
$h_c = 0.416\ t$	1.5	.52	.306	.187
b	4.4	7.55	8.28	6.42
$b_c = 0.4405\ b$	2.03	3.32	3.65	2.82

The constant as given for locating the center of gravity of the blade section applies only to sections that have a flat face. For sections other than the flat-face type, the center of gravity can be determined either by experiment or calculations as given on page 13.

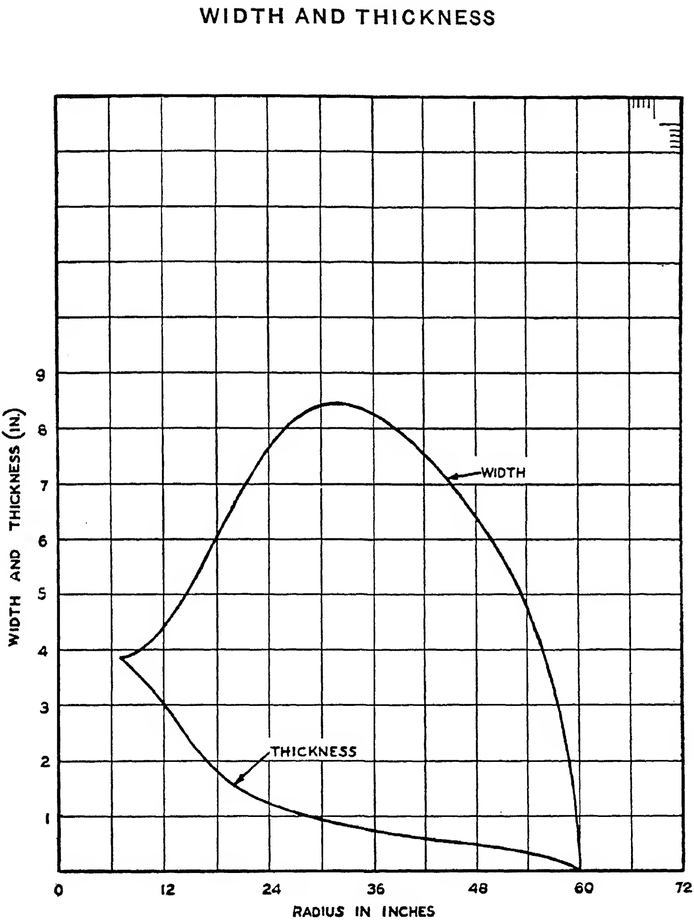
WIDTH AND THICKNESS
WIDTH AND THICKNESS (IN.)
9
8
7
6
5
4
3
2
1
0
12
24
36
48
60
72
RADIUS IN INCHES
WIDTH
THICKNESS

FIGURE 30

AREA CURVE

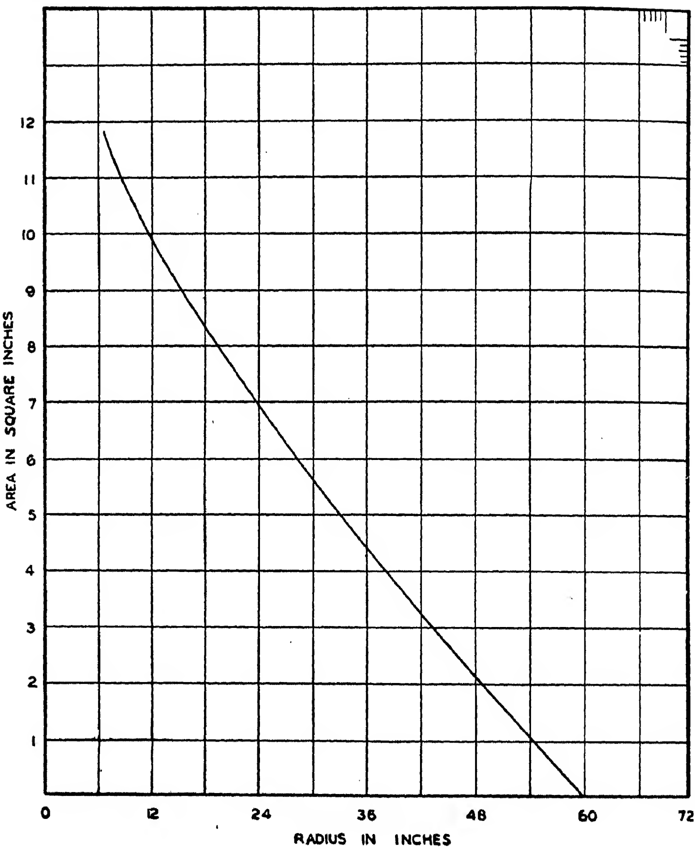

FIGURE 31

Area of Sections. (Figure 31)

	Stations			
	12 in.	24 in.	36 in.	48 in.
b	4.4	7.55	8.28	6.42
t	3.01	1.245	.736	.449
$A = 0.7245\ b\ t$	9.9	6.83	4.42	2.09

Moments of Inertia of Sections. (Figure 32)

	Stations			
	12 in.	24 in.	36 in.	48 in.
b	4.4	7.55	8.28	6.42
b^3	85.2	430.0	567.6	264.6
t	3.01	1.245	.736	.449
$I_{maj} = 0.0418\ b^3\ t$	11.2	22.40	17.45	4.96
t^3	27.27	1.95	.398	.09
$I_{min} = 0.0454\ b\ t^3$	5.7	.667	.15	.026

Blade Angle Distribution. (Figure 33)

$$\tan \Theta = \frac{V_1}{V} = \frac{150 \times 168}{r \times 1760}$$

	Stations			
	12 in.	24 in.	36 in.	48 in.
$\tan \Theta$	1.195	.596	.398	.299
Blade angle (Designed)	50.08°	30.8°	21.7°	16.65°

Blade Angle at the 42-In. Station.

$$\tan \Theta = \frac{\text{m.p.h.} \times 4}{N} = \frac{150 \times 4}{1760} = 0.341$$

Angle at the 42-in. station = 18.83°

Pitch in Feet at the 42-In. Station.

Tan Θ at the 42-in. station = 0.341
Radius, ft. = 42/12 = 3.5
Pitch, ft. = $2\ \pi \times 3.5 \times 0.341 = 7.5$
Pitch, ft. at the 42-in. station = 7.5 ft.

MOMENT OF INERTIA

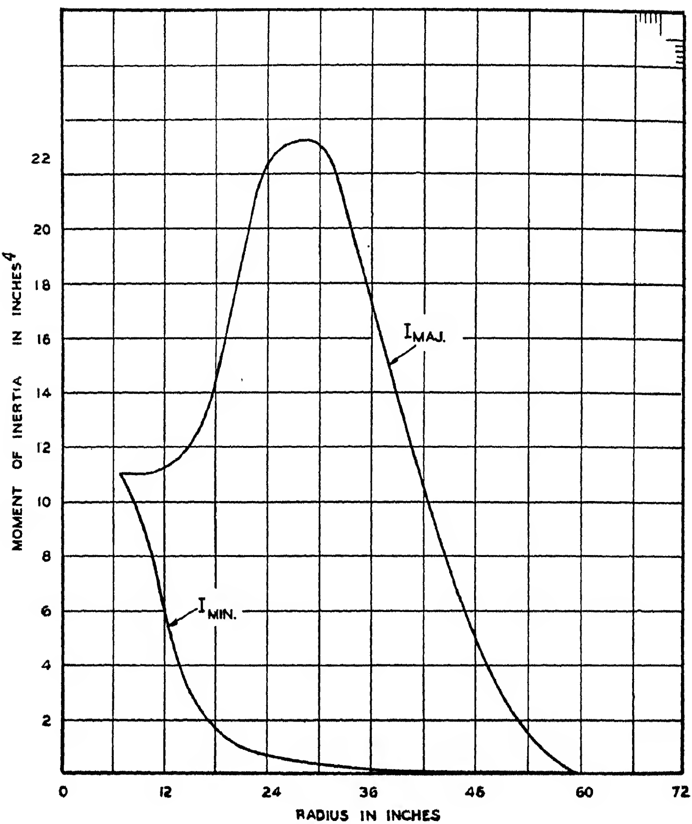

FIGURE 32

BLADE ANGLE DISTRIBUTION

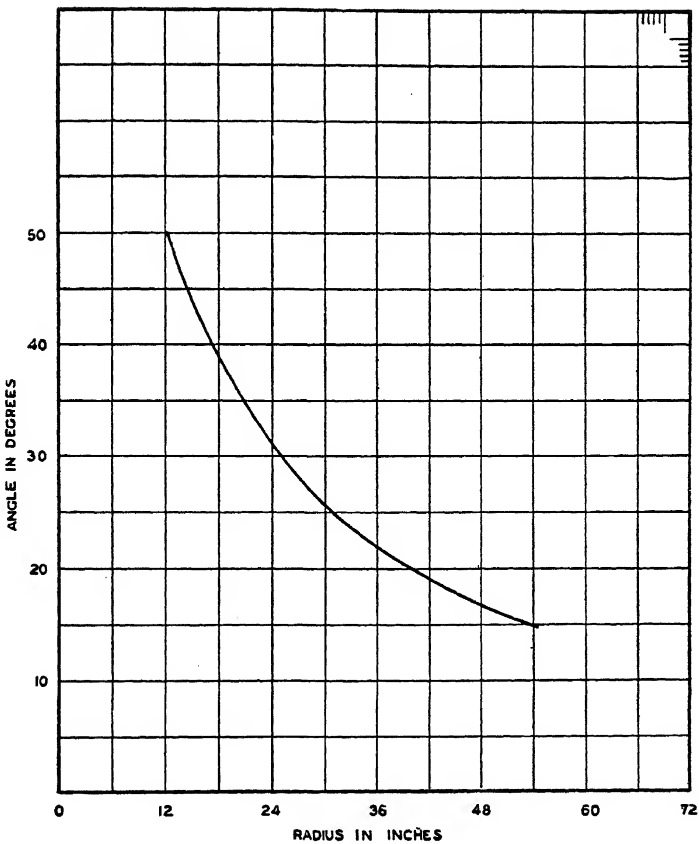

FIGURE 33

Blade Shank. Assuming the propeller may have a tip-speed of 1000 ft/sec., from Figure 13, $f = 0.31$; from Figure 31, area of section at 75% radius = 2.66 sq. in.

$$A \text{ (tip-speed)} = \frac{a}{f} = \frac{2.66}{0.31} = 8.6 \text{ sq. in.}$$

$$A \text{ (hp.)} = 11.0 \text{ sq. in. (Figure 14)}$$

The designed shank area = 11.0 sq. in.

Retaining shoulder inside of hub = 8.66 sq. in.

Blade Weight. (Figure 34)

	Stations			
	12 in.	24 in.	36 in.	48 in.
Integrated area under the area curve Figure 31 ($\int_O^R A\,dr$)............	97.2	193.0	263.0	300.0
Weight = 0.102 ($\int_O A\,dr$).........	9.90	19.7	26.8	30.6

Total calculated weight = 32 lb.

Static Moment. (Figure 35)

	Stations			
	12 in.	24 in.	36 in.	48 in.
Area........................	9.9	6.83	4.42	2.09
$A\,r$........................	118.5	164.0	159.0	100.0

Total area under the curve = 6720

Static Moment 6720 × 0.102 = 685 in-lb.

Center of Gravity of Blade.

$$L = \frac{M}{W} = \frac{685}{32} = 21.4 \text{ in.}$$

WEIGHT CURVE

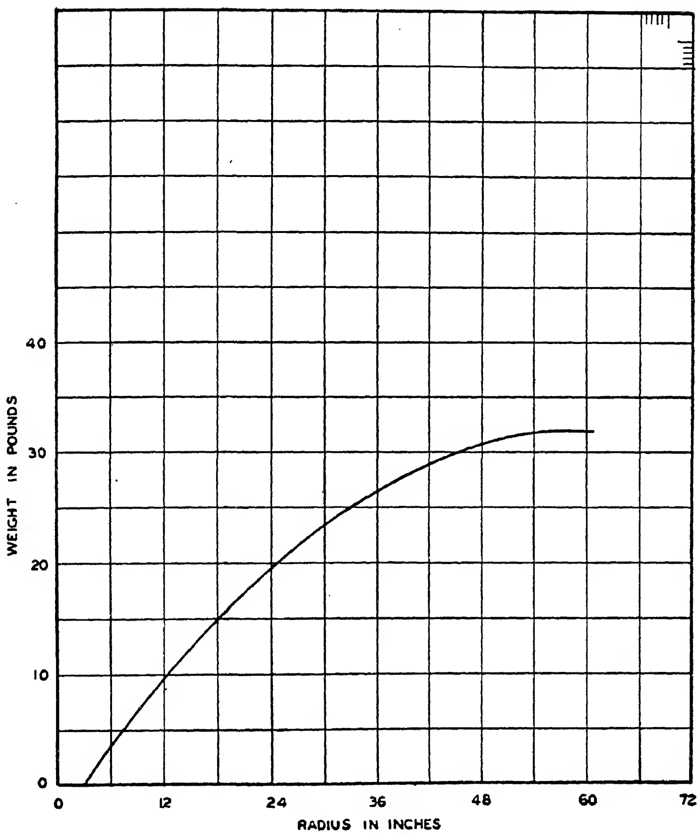

FIGURE 34

STATIC MOMENT

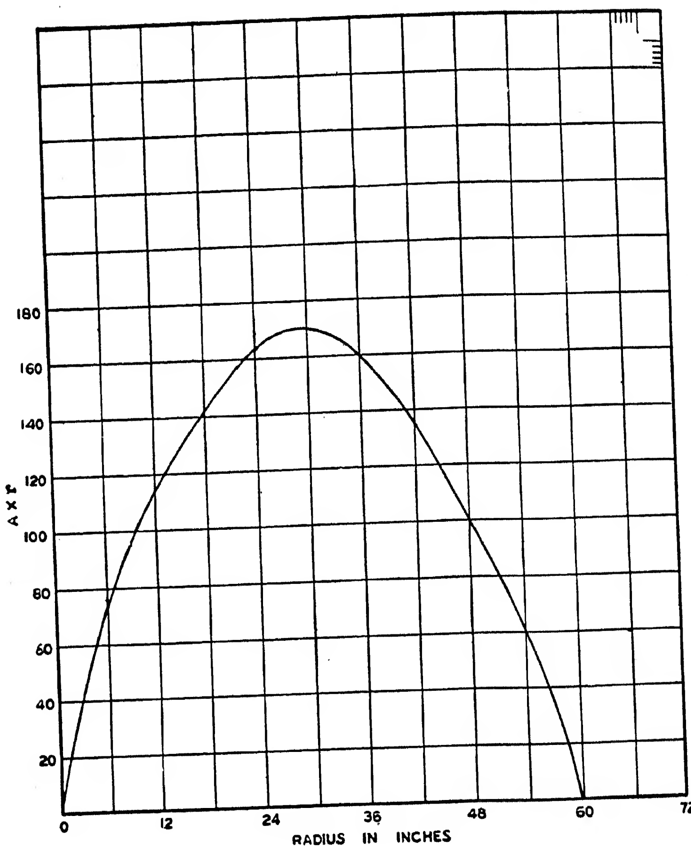

FIGURE 35

Major Polar Moment of Inertia.

	Stations			
	12 in.	24 in.	36 in.	48 in.
r (radius, ft.)	1.	2	3	4
A (Area)	9.9	6.83	4.42	2.09
Ar^2	9.9	27.3	39.8	33.4

Total area under curve = 1380, from Figure 36

$$I_{p\ (maj)} = 1380 \times 0.102 = 141 \text{ lb-ft.}^2 \text{ per blade}$$

Minor Polar Moment of Inertia.

	Stations			
	12 in.	24 in.	36 in.	48 in.
$(I_{maj} + I_{min})$	16.9	23.07	17.60	4.99

Total area under curve = 646, from Figure 36

$$I_{p\ (min)} = 646 \cdot \frac{0.102}{144} = 0.4575 \text{ lb-ft.}^2 \text{ per blade}$$

Radius of Gyration.

$$K = \sqrt{\frac{I_p}{W}} = \sqrt{\frac{141}{32}} = 2.10 \text{ ft.} = 25.2 \text{ in.}$$

Efficiency.

$$\frac{V}{N\,D} = \frac{150 \times 88}{1760 \times 10} = 0.750$$

e from Figure 18 = 80%

Thrust at Top Speed.

$$T = \frac{\text{hp.} \times e \times 375}{V} = \frac{400 \times .80 \times 375}{2 \times 150} = 400 \text{ lb. per blade}$$

Static Thrust.

Power coefficient $C_p = P_{(hp)} \cdot P_{(N)} \cdot P_{(D)} = (0.2)\ (0.19)\ (1) = 0.038$, from Figure 19

Thrust coefficient (K) and blade angle $=$ 74,000 @ 13.3°, from Figure 19a

$$T_s = \frac{K \cdot \text{hp.}}{N \cdot D} = \frac{74{,}000 \cdot 400}{1760 \cdot 10} = 1682\#/\text{propeller, or } 841\#/\text{blade}$$

POLAR MOMENT

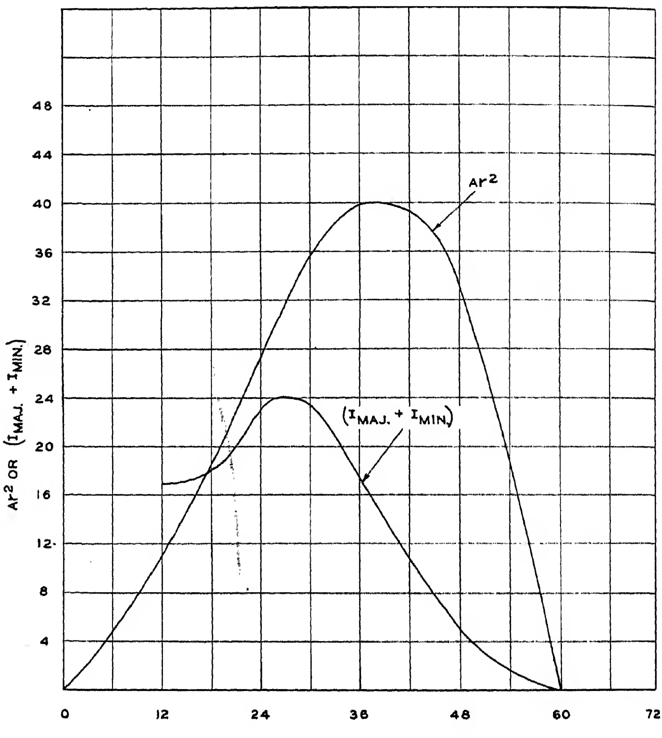

FIGURE 36

Propeller Tip-Speed. Rotational:

$$V_t = 0.0524\ ND = 0.0524 \times 1760 \times 10 = 923 \text{ ft/sec.}$$

Helical: From Figure 18: $V + N = 0.5 + 8.5 = 9.0$

$$V_r = 947 \text{ ft/sec. (Figure 18a)}$$

Torque.

$$Q = \frac{\text{hp.} \times 63{,}000}{\text{r.p.m.}} = \frac{400 \times 63{,}000}{1760} = 14{,}300 \text{ lb-in.}$$

Centrifugal Twisting Moment. (Figure 37 and 37a)

$$T_Q = 0.102\ \delta\ n^2 \int_O^R (I_{maj} - I_{min}) c_1\, dr$$

	Stations			
	12 in.	24 in.	36 in.	48 in.
Blade angle (designed)	50.08°	30.8°	21.7°	16.55°
I-major	11.2	22.4	17.45	4.96
I-minor	5.7	.667	.15	.0262
$(I_{maj} - I_{min})$	5.5	21.74	17.30	4.94
c_1 (moment coefficient Figure 23)	.492	.44	.344	.275
$(I_{maj} - I_{min})c_1$	2.71	9.55	5.95	1.36

Total integrated area under the curve = 226.5

$$T_Q = \overline{0.102}^2 \times 860 \times 226.5 = 2030 \text{ lb-in. with } 75\% \text{ radius at } \phi_1 = 17.5°$$

Determining one more point similarly,

$$T_{Q2} = 925 \text{ lb-in. with } 75\% \text{ radius at } \phi_2 = 1.0°$$

Blade angle at zero moment,

$$\phi = \tfrac{1}{2} \tan^{-1} \left(\frac{925 \sin 35° - 2030 \sin 2°}{2030 \cos 2° - 925 \cos 35°} \right) =$$

$$\tfrac{1}{2} \tan^{-1} (0.360) = \frac{19.8°}{2} = 9.9°$$

Maximum moment,

$$T_{Q\ (max)} \quad \frac{2030}{\sin 54.8°} - \frac{925}{\sin 21.8°} = 2490 \text{ lb-in.}$$

Moment at any blade angle, $\therefore T_{Q3} = 2490 \sin 2\ (\phi_3 + 9.9°)$

CENTRIFUGAL TWISTING MOMENT

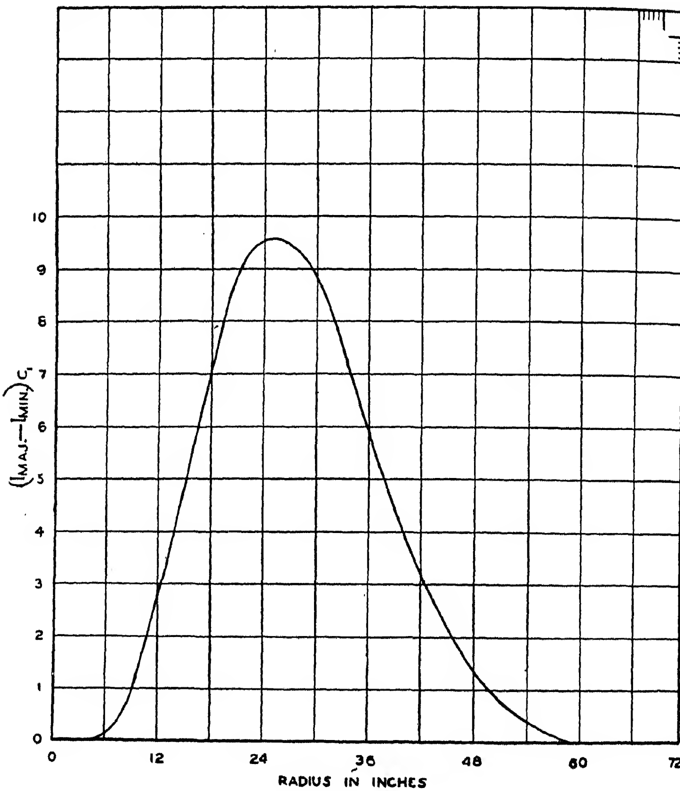

FIGURE 37

CENTRIFUGAL TWISTING MOMENT

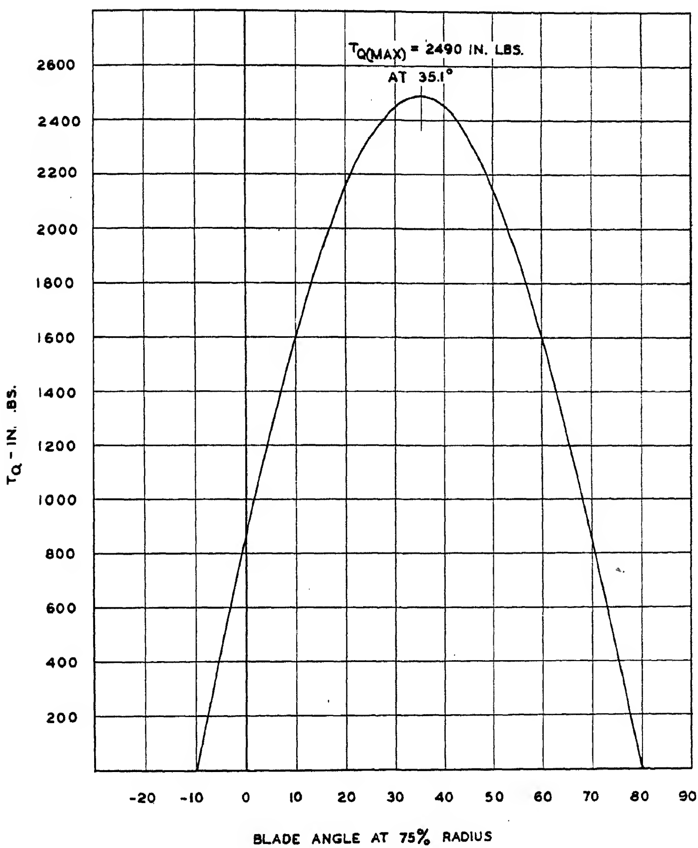

FIGURE 37a

Aerodynamic Twisting Moment. (Figure 38)

	Stations			
	12 in.	24 in.	36 in.	48 in.
b^2 (ft.)	.134	.396	.475	.286
$\sin^2\phi$	.622	.293	.16	.102
$V^2 = 48{,}400$				
$\rho/2 = 0.00118$				
$C_m\, b^2 \times \rho/2 \times W^2$	.94	5.9	12.95	12.45

Assume 2° angle of attack, and average moment coefficient of 0.05 at all stations (Figure 24).

Integrated area under the curve = 398

Aerodynamic twisting moment = 398 lb-in.

The angle of attack depends on the type of blade design and the flight requirements for the propeller. Since the rotational velocity is different at each station, the moment coefficient would likewise vary and therefore each value should be individually computed.

Centrifugal Force. (Figure 39)

$$\int_R^r 0.102\, \delta \times A\, r\, n^2\, dr$$

	Stations			
	12 in.	24 in.	36 in.	48 in.
Area	9.9	6.83	4.42	2.09
$0.0104\, A\, r\, 860$	1,060	1,460	1,420	900
Integrated area under the curve (Figure 39) from tip to the station under consideration = total load at each station =	52,500	37,500	20,000	6,000

AERODYNAMIC TWISTING MOMENT

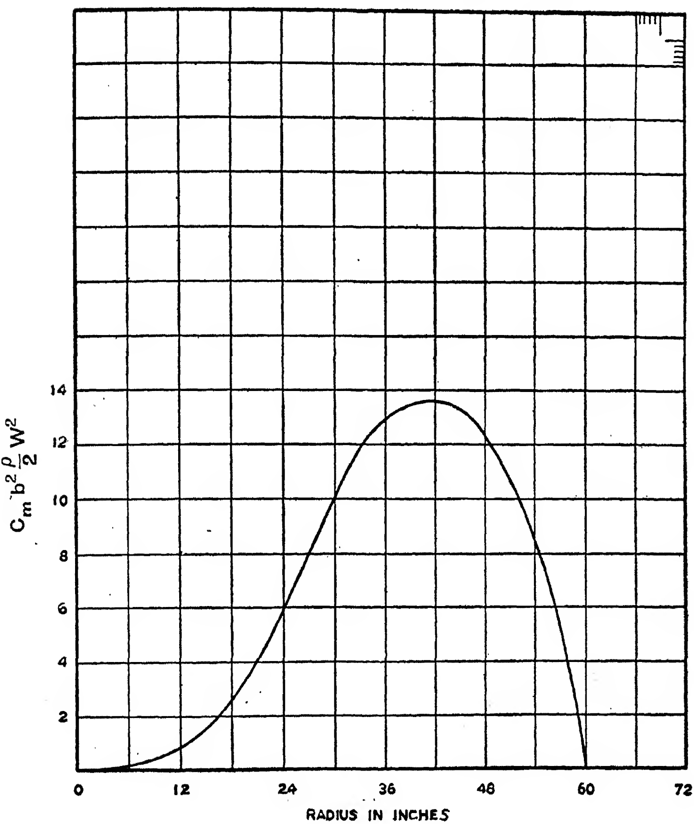

FIGURE 38

CENTRIFUGAL FORCE

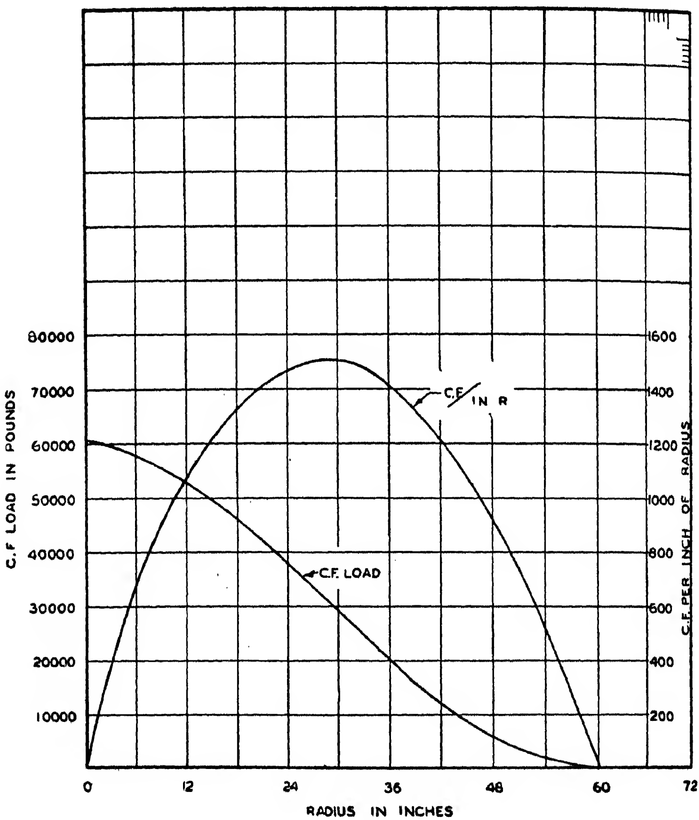

FIGURE 39

Centrifugal Stress. (Figure 40)

$$f_t = \frac{\text{C.F.}}{A}$$

	Stations			
	12 in.	24 in.	36 in.	48 in.
Centrifugal force................	52,500	37,500	20,000	6,000
Area...........................	9.9	6.83	4.42	2.09
Tensile stress (f_t)...............	5,300	5,500	4,530	2,870

Air Load. (Figure 41)

	Stations			
	12 in.	24 in.	36 in.	48 in.
b..............................	4.40	7.55	8.28	6.42
$r^2 b$............................	635	4,350	10,700	14,750

Total area under the uncorrected air load (P) curve = 425,000.

True Air Load. (Figure 42) The correction factor, $f = 1.042T_s/P$.

$$f = 1.042 \times 841/425{,}000 = 0.002063$$

	Stations			
	12 in.	24 in.	36 in.	48 in.
r^2b..............................	635	4,350	10,700	14,750
0.002063 r^2b......................	1.32	8.98	22.15	30.57

Shear. (Figure 43)

	Stations			
	12 in.	24 in.	36 in.	48 in.
Shear (integrated area under true air load curve)	859	805	622	298

TENSILE STRESS DUE TO THE CENTRIFUGAL FORCE

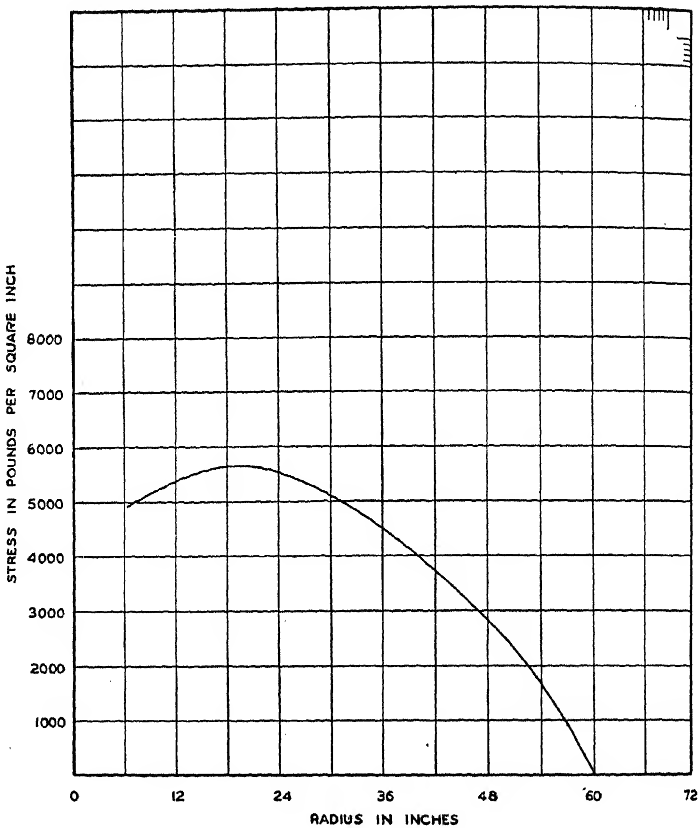

FIGURE 40

UNCORRECTED AIR LOADING - P

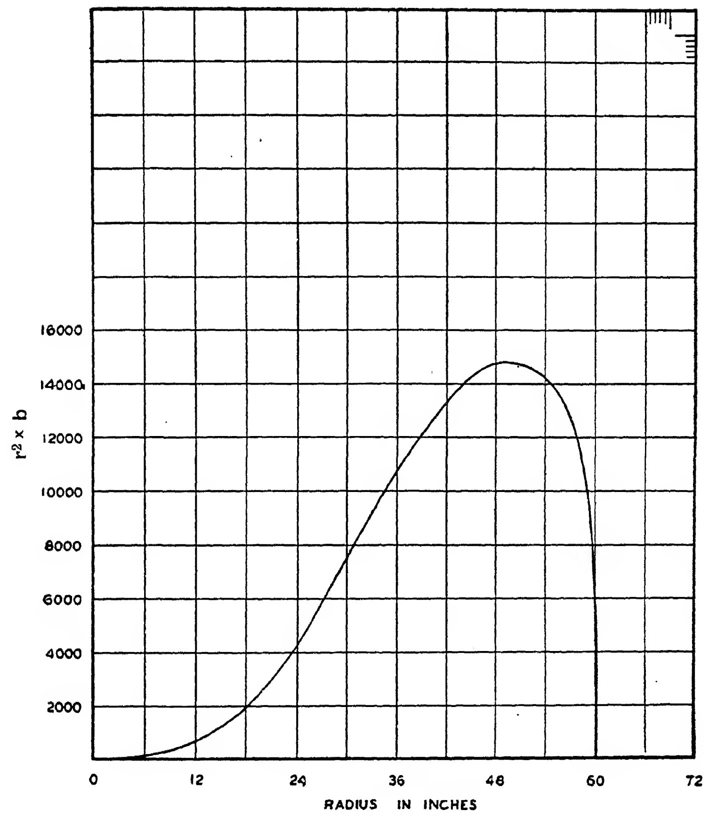

FIGURE 41

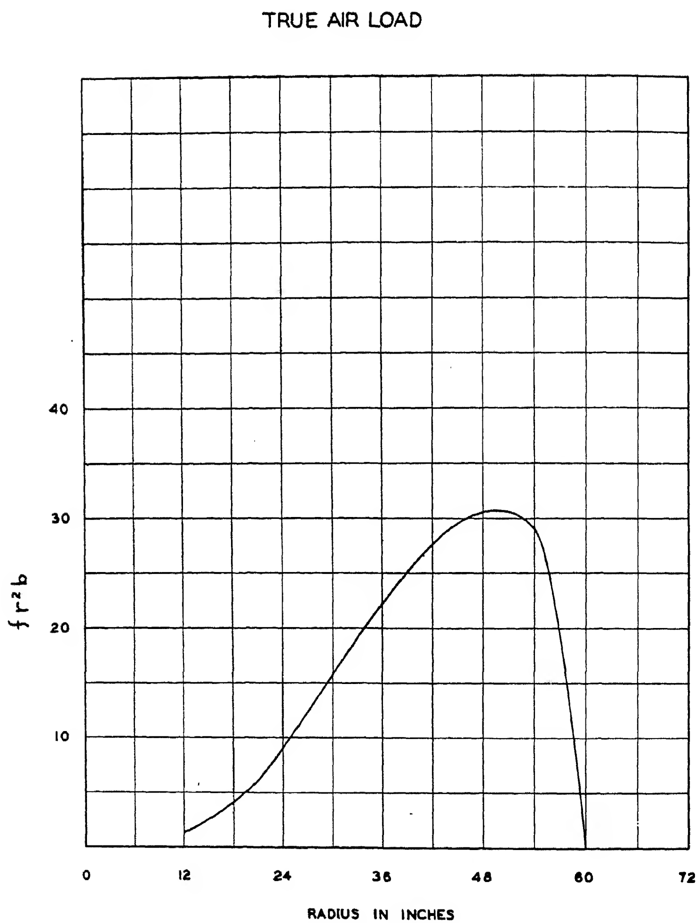
TRUE AIR LOAD
40
30
20
10
$f r^2 b$
0
12
24
36
48
60
72
RADIUS IN INCHES

FIGURE 42

SHEAR

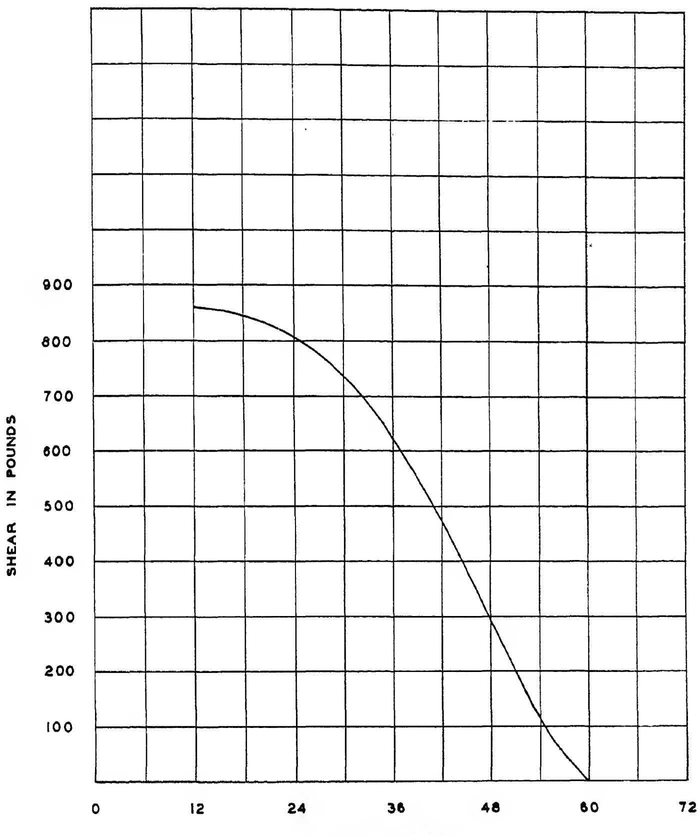

FIGURE 43

Bending Moment Due to Air Load. (Figure 44)

	Stations			
	12 in.	24 in.	36 in.	48 in.
Bending moment (integrated area under shear curve).............	26,060	15,820	7,100	1,509

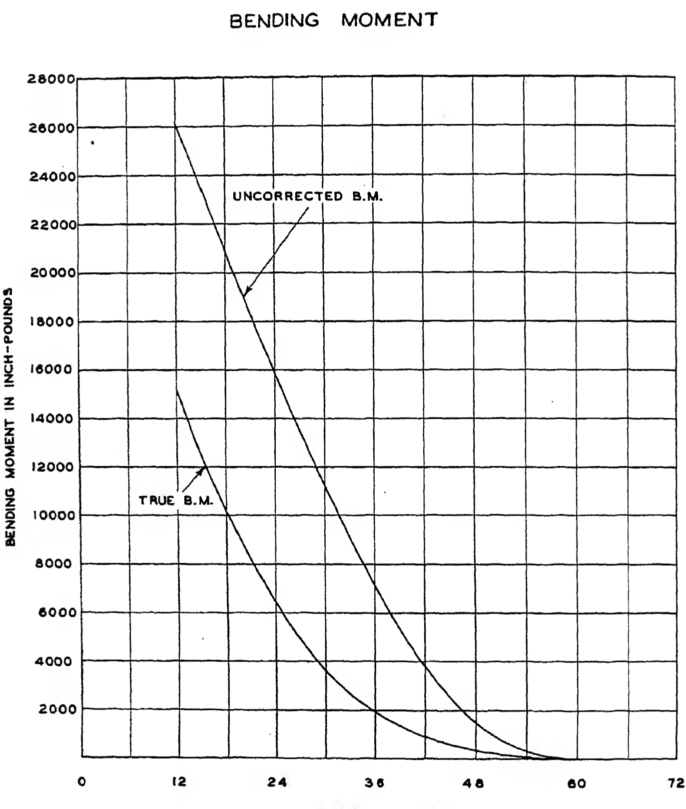

FIGURE 44

Curvature Due to Air Load. (Figure 45)

	Stations 12 in.	24 in.	36 in.	48 in.
Curvature $\left(\dfrac{B.M.}{E \cdot I_{min}}\right)$	.000457	.00237	.004735	.005845

CURVATURE

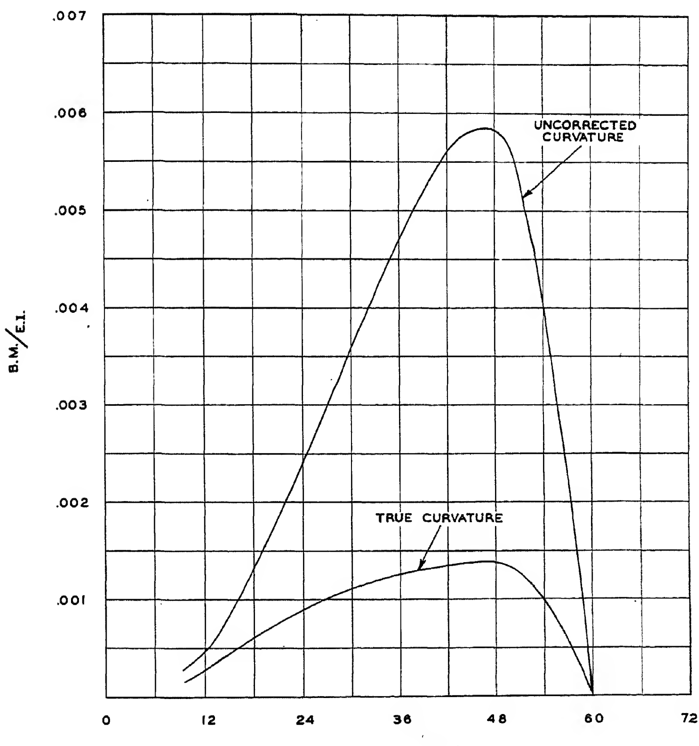

FIGURE 45

Slope Due to Air Load. (Figure 46)

	Stations			
	12 in.	24 in.	36 in.	48 in.
Slope (integrated area under curvature curve)......................	.0015	.0174	.0601	.1248

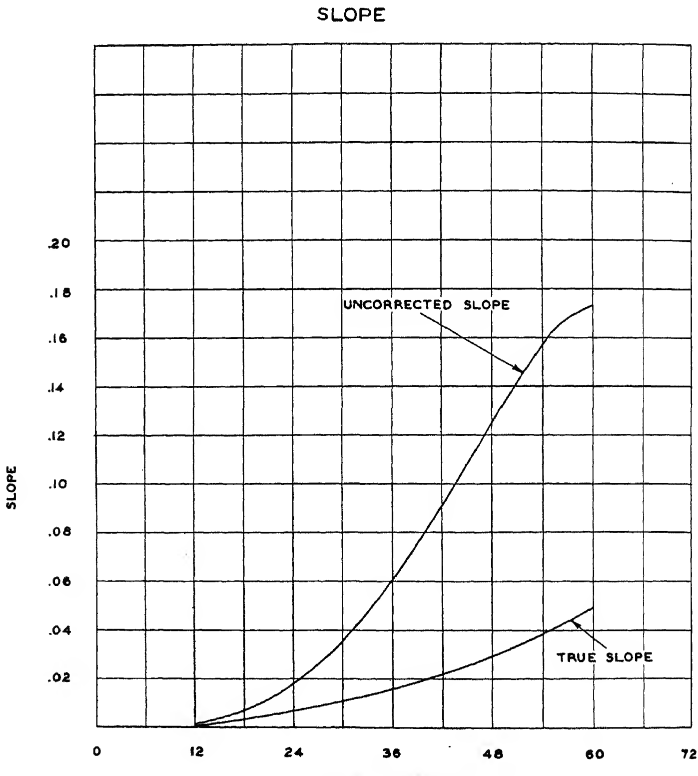

FIGURE 46

Deflection Due to Air Load. (Figure 47)

	Stations			
	12 in.	24 in.	36 in.	48 in.
Deflection (integrated area under slope curve)	.009	.107	.552	1.649

DEFLECTION

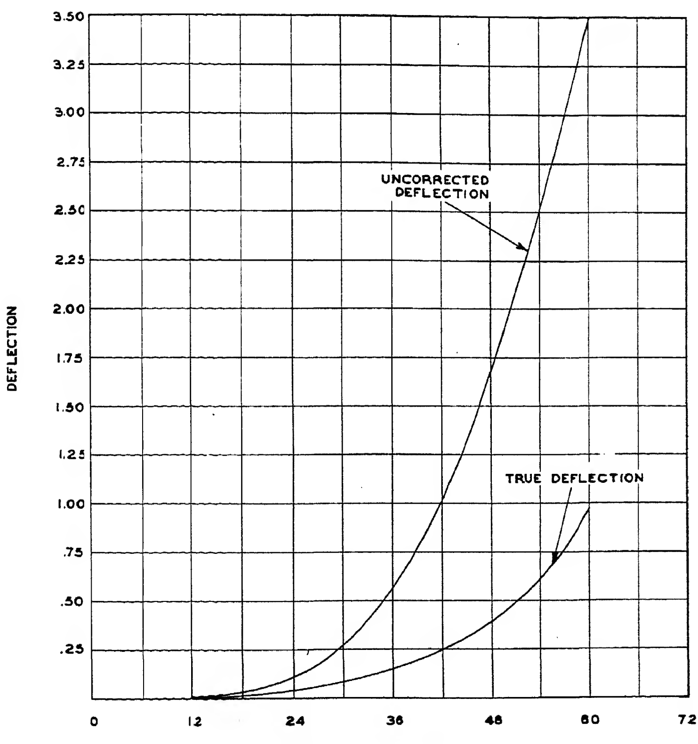

FIGURE 47

CENTRIFUGAL FORCE VERSUS
AIR LOAD DEFLECTION

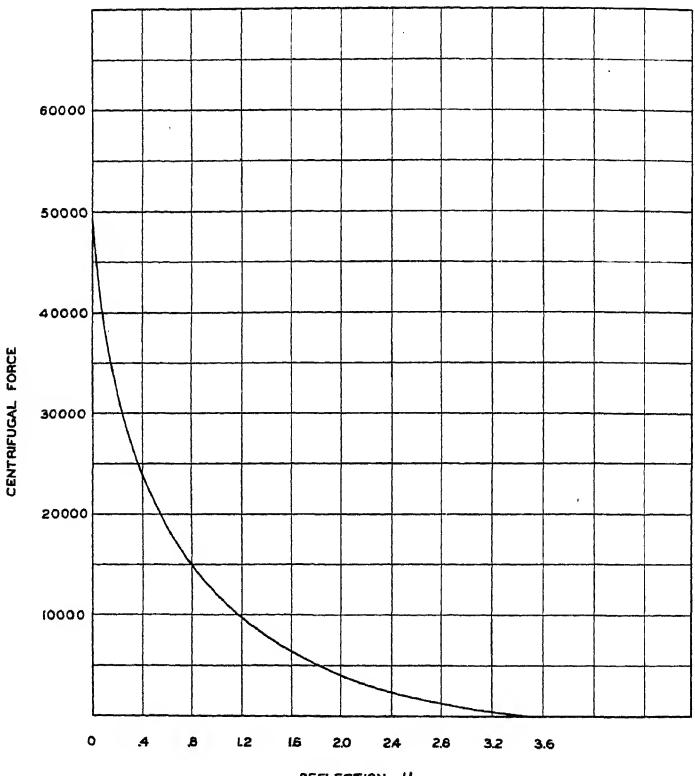

FIGURE 48

Restoring Moment. (Figure 48a)

	Stations			
	12 in.	24 in.	36 in.	48 in.
Area under curve of centrifugal force (Figure 48) versus air load deflection	32,560	28,520	16,760	3,852

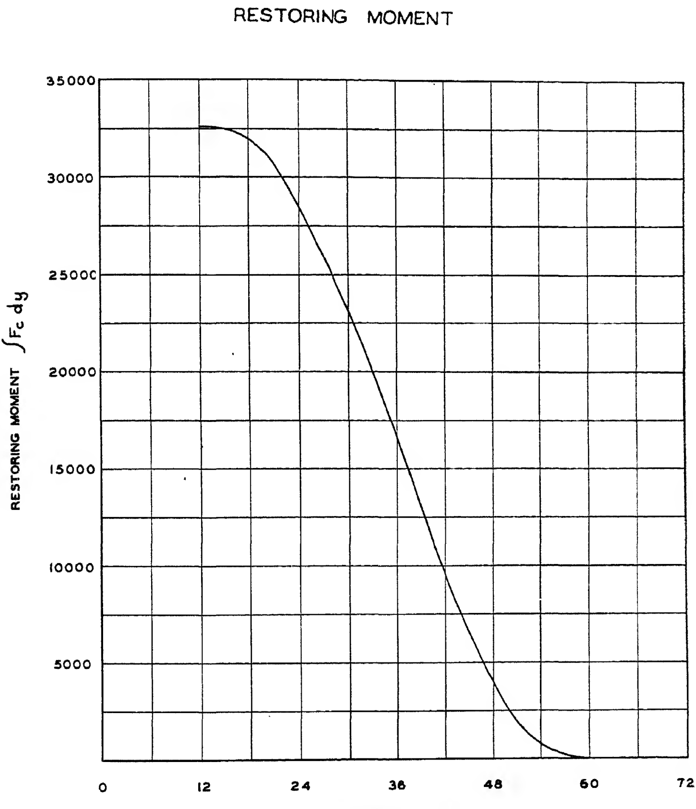

FIGURE 48a

Restoring Moment Coefficient. (Figure 48b)

	Stations 12 in.	24 in.	36 in.	48 in.
Factor $\dfrac{B.M.}{B.M. + R.M.} = Z$	.444	.357	.2975	.2812
$Z^2 = C_R$	.591	.382	.265	.237

CORRECTION FACTOR FROM RESTORING MOMENT

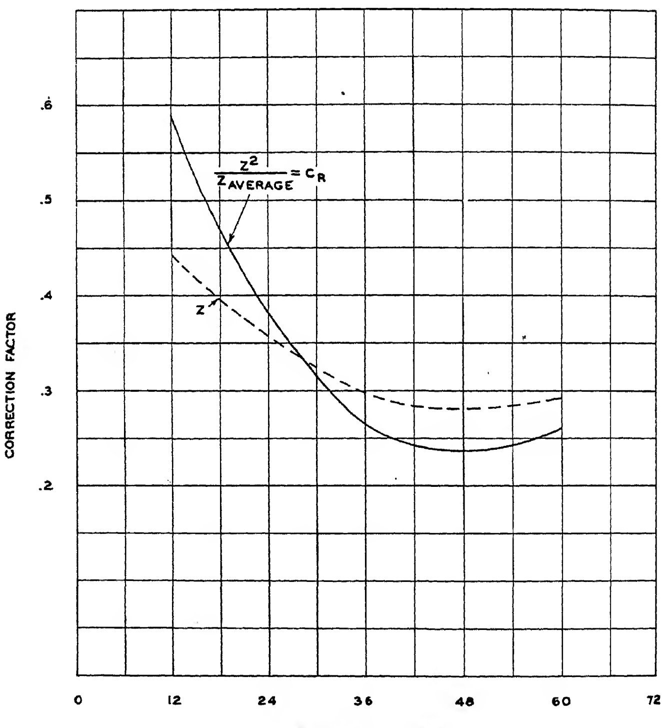

FIGURE 48b

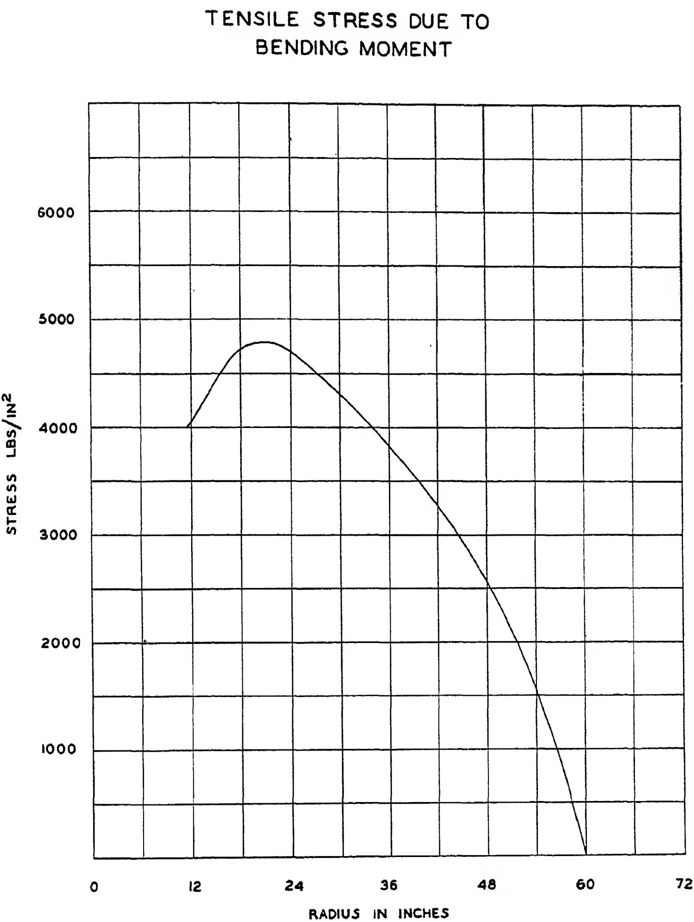
TENSILE STRESS DUE TO
BENDING MOMENT
6000
5000
4000
3000
2000
1000
STRESS LBS/IN²
0
12
24
36
48
60
72
RADIUS IN INCHES

FIGURE 48c

True Bending Moment. (Figure 44)

	Stations 12 in.	24 in.	36 in.	48 in.
$M = C_R \cdot$ B.M.	15,400	6,045	1,881	358

Bending Stress. (Figure 48c)

	Stations 12 in.	24 in.	36 in.	48 in.
$f_b = \dfrac{M \cdot h_c}{I_{min}}$	4,050	4,710	3,835	2,575

True Curvature. (Figure 45)

	Stations 12 in.	24 in.	36 in.	48 in.
Integrated area under $\dfrac{M}{E \cdot I_{min}}$ curve	.00027	.000905	.001254	.001386

True Slope. (Figure 46)

	Stations 12 in.	24 in.	36 in.	48 in.
Integrated area under true curvature curve	.000887	.00665	.01593	.02906

True Deflection. (Figure 47)

	Stations 12 in.	24 in.	36 in.	48 in.
Integrated area under true slope curve	.00532	.0409	.1463	.3907

Gyroscopic Bending Moment.

(Assuming Angular Velocity of Aircraft = 1 radian per second)

Initial Moment.

	Stations 12 in.	24 in.	36 in.	48 in.
Centrifugal Force, F_c	52,500	37,500	20,000	6,000
$\int_R^r F_c\, dr$	1,063,650	523,650	178,650	28,650
Moment, $M_{g1} = \dfrac{19.1\,\Omega}{N} \int_R^r F_c\, dr$ (Fig. 48d)	11,550	5,690	1,942	311

First Approximation.

	Stations 12 in.	24 in.	36 in.	48 in.
$\dfrac{M_{g1}}{E \cdot I_{min}}$	.0002025	.000852	.001294	.001197
$\displaystyle\int_o^r \frac{M_{g1}}{E \cdot I_{min}}\, dr$	.001398	00771	.02050	.03590
$Y_{g1} = \displaystyle\int_o^r \int_o^r \frac{M_{g1}}{E \cdot I_{min}}\, dr\, dr$	.00652	.0553	.2253	.5650
$\dfrac{Y_{g1}}{r}$	.000543	.002305	.00621	.01177
$M_{R1} = \displaystyle\int_{\left(\frac{Y_{g1}}{R}\right)}^{\left(\frac{Y_{g1}}{r}\right)} F_c\, d\left(\frac{Y_{g1}}{r}\right)$	270	192.3	82.9	14.3
$r \cdot M_{R1}$	3,240	4,615	2,985	686
$C_1 = \dfrac{M_{g1}}{M_{g1} + r \cdot M_{R1}}$	.7805	.5520	.3945	.3120
$M_{g2} = C_1 \cdot M_{g1}$	9,010	3,143	766	97

Second Approximation.

	Stations 12 in.	24 in.	36 in.	48 in.
$\dfrac{M_{g2}}{E \cdot I_{min}}$	.0001581	.000471	.000511	.000373
$\displaystyle\int_o^r \frac{M_{g2}}{E \cdot I_{min}}\, dr$	.00156	.00554	.01161	.01681
$Y_{g2} = \displaystyle\int_o^r \int_o^r \frac{M_{g2}}{E \cdot I_{min}}\, dr\, dr$	.00905	.04885	.1514	.3230
$\dfrac{Y_{g2}}{r}$	.000754	.002035	.004205	.00673
$M_{R2} = \displaystyle\int_{\left(\frac{Y_{g2}}{R}\right)}^{\left(\frac{Y_{g2}}{r}\right)} F_c\, d\left(\frac{Y_{g2}}{r}\right)$	155.8	98.9	37.35	5.755
$r \cdot M_{R2}$	1,870	2,375	1,345	276.4
$C_2 = \dfrac{M_{g1}}{M_{g2} + r \cdot M_{R2}}$	1.061	1.031	.919	.833

	Stations			
	12 in.	24 in.	36 in.	48 in.
$M_{g3} = C_2 \cdot M_{g2}$	9,555	3,240	704.5	80.8

Third Approximation.

	Stations			
	12 in.	24 in.	36 in.	48 in.
$\dfrac{M_{g3}}{E \cdot I_{min}}$	.0001677	.0004855	.0004695	.000311
$\int_0^r \dfrac{M_{g3}}{E \cdot I_{min}}\, dr$	.001629	.00576	.01166	.01621
$Y_{g3} = \int_0^r \int_0^r \dfrac{M_{g3}}{E \cdot I_{min}}\, dr\, dr$ ...	.009385	.05100	.1558	.3245
$\dfrac{Y_{g3}}{r}$	.0007815	.002125	.004325	.00676
$M_{R3} = \int_{\left(\frac{Y_{g3}}{R}\right)}^{\left(\frac{Y_{g3}}{r}\right)} F_c\, d\left(\dfrac{Y_{g3}}{r}\right)$ ..	158	98.5	35.9	5.31
$r \cdot M_{R3}$	1,896	2,365	1,293	255
$C_3 = \dfrac{M_{g1}}{M_{g3} + r \cdot M_{R3}} = C_n$	1.007	1.015	.971	.926

Since these values of C_3 are very near 1, this becomes the final approximation, and,

	Stations			
	12 in.	24 in.	36 in.	48 in.
$C_R = C_1 \cdot C_2 \cdot C_n$	.8350	.5785	.3520	.2407
$M_G = C_R \cdot M_{g1}$ (Figure 48d)....	9,600	3,290	684	74.9

Tensile Stress Due to Gyroscopic Bending Moment.

	Stations			
	12 in.	24 in.	36 in.	48 in.
I_{min}	5.7	.667	.15	.026
h_c = Dist. from c.g. to max. stressed fibre..............	1.5	.520	.306	.187
$\int G = \dfrac{M_G \cdot h_c}{I_{min}}$ = lb/in.² (Figure 48d)	2,530	2,565	1,394	539

GYROSCOPIC BENDING MOMENT AND STRESS

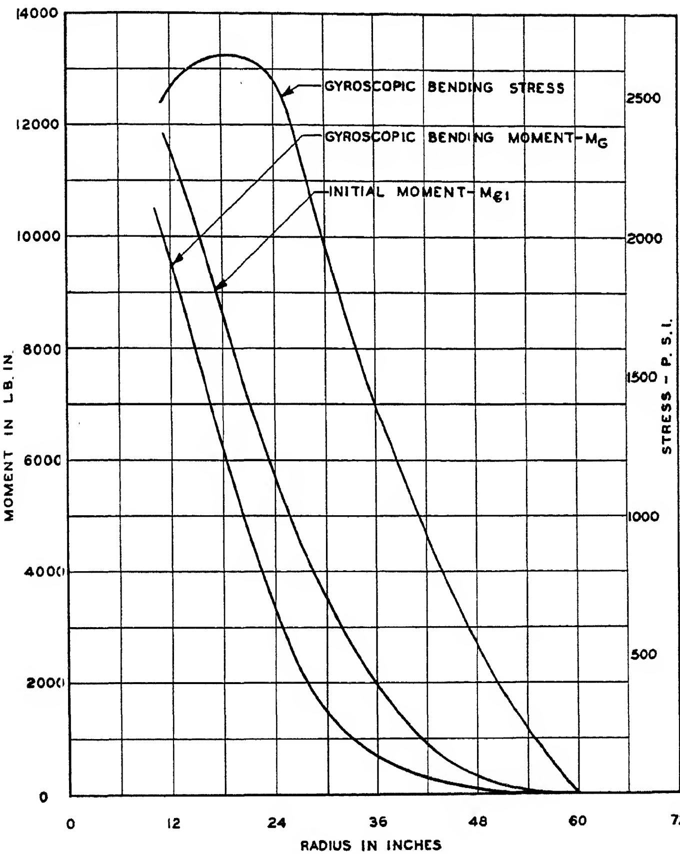

FIGURE 48d

Vibration. WEIGHT LOADING. (Figure 49)

	Stations 12 in.	24 in.	36 in.	48 in.
δA	1.009	.695	.450	.213

SHEAR. (Figure 50)

	Stations 12 in.	24 in.	36 in.	48 in.
$\int_R^r \delta A \, dr$	22	12	5.06	1.44

WEIGHT BENDING MOMENT. (Figure 51)

	Stations 12 in.	24 in.	36 in.	48 in.
$M = \int_R^r \int_R^r \delta A \, dr \, dr$	336	135	39.4	4.8

Flatwise Frequency. CURVATURE. (Figure 52)

	Stations 12 in.	24 in.	36 in.	48 in.
$\frac{M}{E \cdot I_{min}}$	.0000059	.0000202	.0000263	.000018

SLOPE. (Figure 53)

	Stations 12 in.	24 in.	36 in.	48 in.
$\int_O^r \frac{M}{E \cdot I_{min}} dr$	.0000312	.000182	.00048	.00074

DEFLECTION. (Figure 54)

	Stations 12 in.	24 in.	36 in.	48 in.
$\Delta = \int_O^r \int_O^r \frac{M}{E \cdot I_{min}} dr \, dr$	.00012	.0012	.00528	.01225

Potential energy $= \int_R^o A \cdot \Delta \, dr = 0.750$ (Figure 55)

$$\text{Kinetic energy} = \int_R^o A \cdot \Delta^2\, dr = 0.00653 \text{ (Figure 56)}$$

$$f = 187.86 \sqrt{\frac{\int A \cdot \Delta}{\int A \cdot \Delta^2}} = 187.86 \sqrt{\frac{0.750}{0.00653}} =$$

2,015 cycles per min.

Edgewise Frequency.

CURVATURE. (Figure 56a)

	Stations			
	12 in.	24 in.	36 in.	48 in.
$M/E \cdot I_{maj}$..........	.000003002	.000000602	.0000002258	.0000000968

SLOPE. (Figure 56b)

	Stations			
	12 in.	24 in.	36 in.	48 in.
$\int_O^r \frac{M}{E \cdot I_{maj}}\, dr$.......	.0000357	.0000531	.0000583	.0000599

DEFLECTION. (Figure 54)

	Stations			
	12 in.	24 in.	36 in.	48 in.
$\Delta = \int_O^r \int_O^r \frac{M \cdot}{E \cdot I_{maj}}\, dr\, dr$.	.000145	.0006976	.001371	.002081

$$\text{Potential energy} = \int_R^o A \quad \Delta\, dr = 0.208 \text{ (Figure 56c)}$$

$$\text{Kinetic energy} = \int_R^o A \quad \Delta^2\, dr = 0.000273.6 \text{ (Figure 56d)}$$

$$\phi = 47^\circ - 14^\circ = 33^\circ, \quad \cos\phi = 0.8387$$

$$f = 187.86 \cdot \cos\phi \sqrt{\frac{\int A \quad \Delta}{\int A \quad \Delta^2}} = 187.86 \cdot 0.8387 \sqrt{\frac{0.208}{.0002736}} =$$

4,340 cycles per min.

Torsional Frequency.

CURVATURE. (Figure 56a)

	Stations			
	12 in.	24 in.	36 in.	48 in.
$\frac{M}{G \cdot I_p}$*	.00000516	.000001519	.000000581	.0000002502

SLOPE. (Figure 56b)

	Stations			
	12 in.	24 in.	36 in.	48 in.
$\int_0^r \frac{M}{G \cdot I_p}\, dr$	.0000487	.0000871	.0000988	.0001036

DEFLECTION. (Figure 54)

	Stations			
	12 in.	24 in.	36 in.	48 in.
$\Delta = \int_0^r \int_0^r \frac{M}{G \cdot I_p}\, dr\, dr$ ...	.000198	.001051	.002174	.003391

$$\text{Potential energy} = \int_R^o A \quad \Delta\, dr = 0.3248 \quad \text{(Figure 56c)}$$

$$\text{Kinetic energy} = \int_R^o A \quad \Delta^2\, dr = .0006904 \text{ (Figure 56d)}$$

$$\phi = 47° - 14° = 33° \quad \cos \phi = 0.8387$$

$$f = 187.86 \frac{D}{3.636 \cos \phi} \sqrt{\frac{\int A \quad \Delta}{\int A \quad \Delta^2}} = 187.86 \frac{10}{3.636 \cdot 0.8387}$$

$$\sqrt{\frac{0.3248}{0.0006904}} = 13{,}370 \text{ cycles per min.}$$

*$G = 3{,}850{,}000$ for aluminum alloy.

WEIGHT LOADING

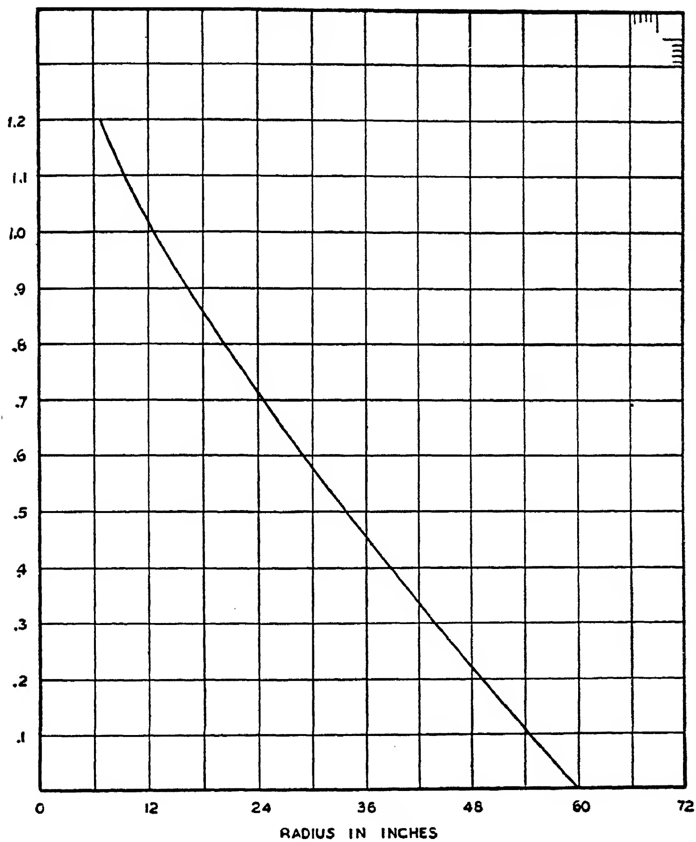

FIGURE 49

SHEAR DUE TO WEIGHT LOADING

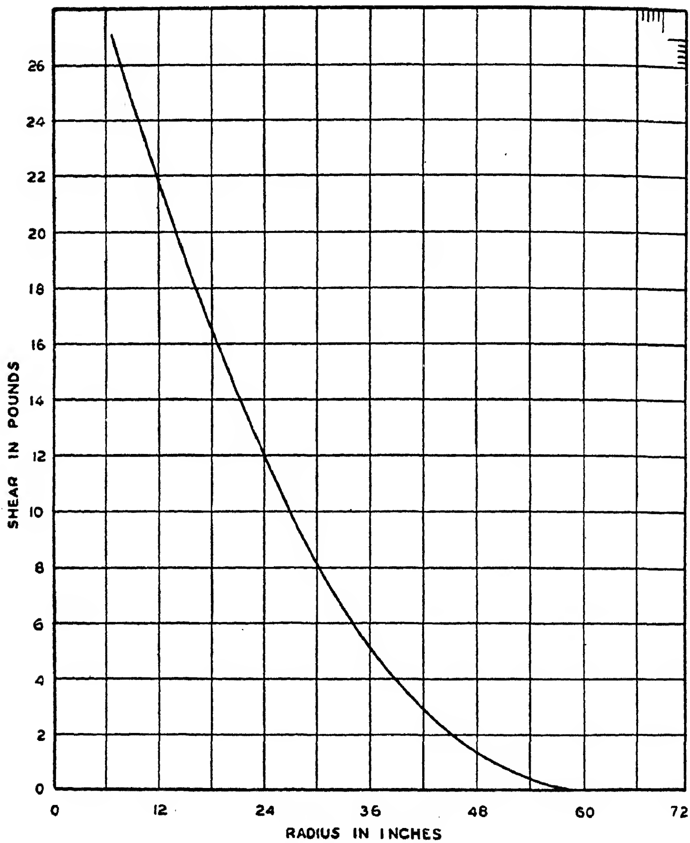

FIGURE 50

BENDING MOMENT DUE TO BLADE WEIGHT

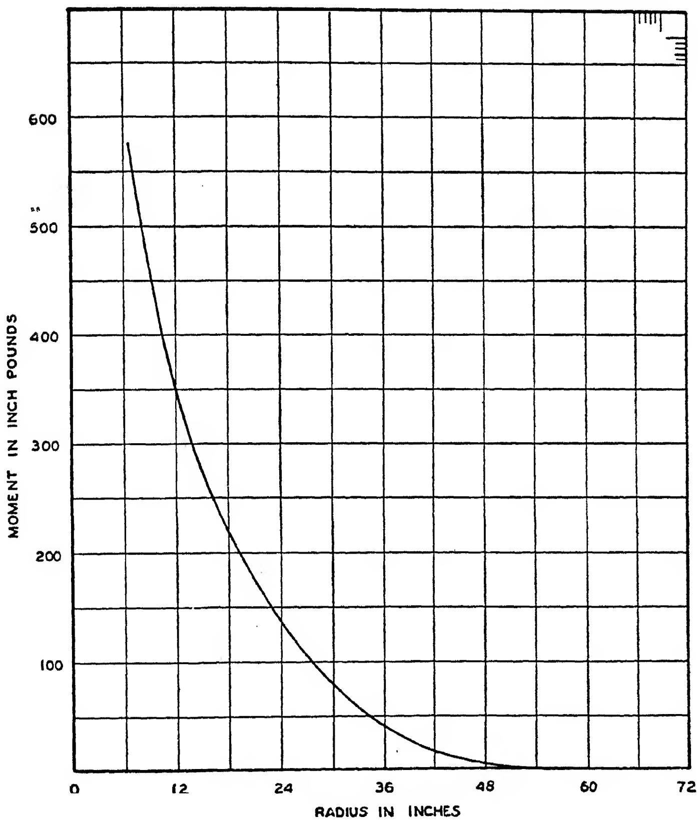

FIGURE 51

CURVATURE DUE TO WEIGHT BENDING MOMENT

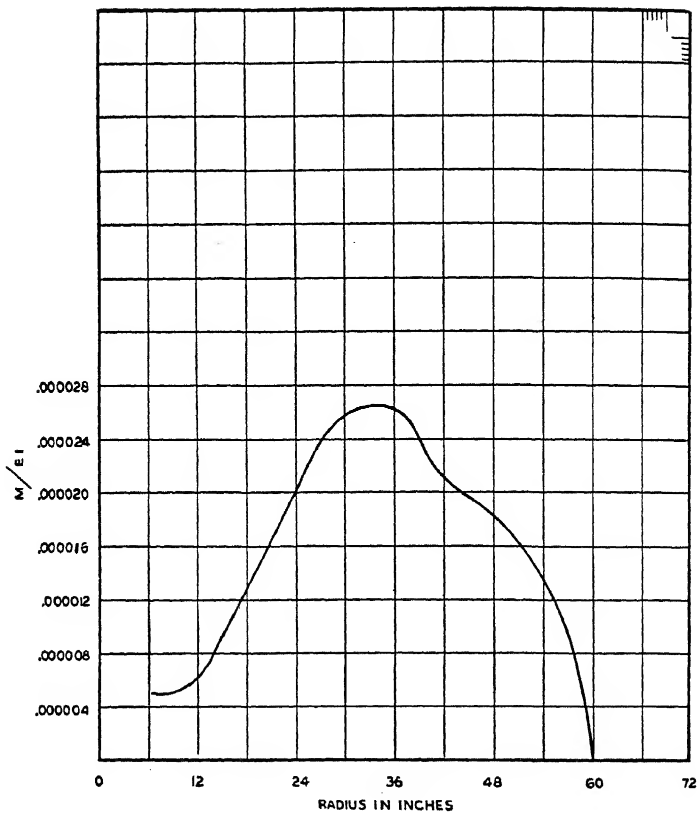

FIGURE 52

SLOPE DUE TO WEIGHT LOADING

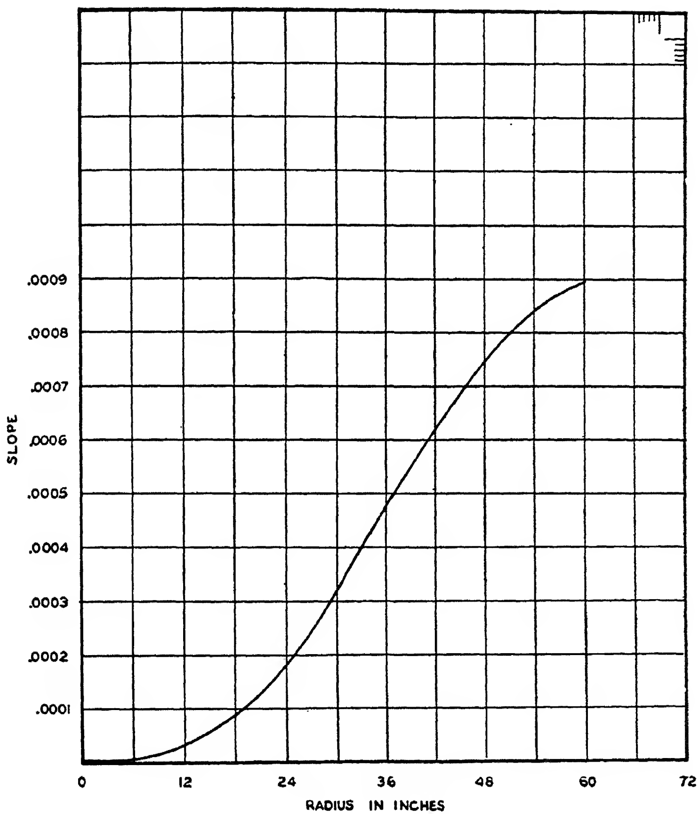

FIGURE 53

DEFLECTION DUE TO WEIGHT BENDING MOMENT

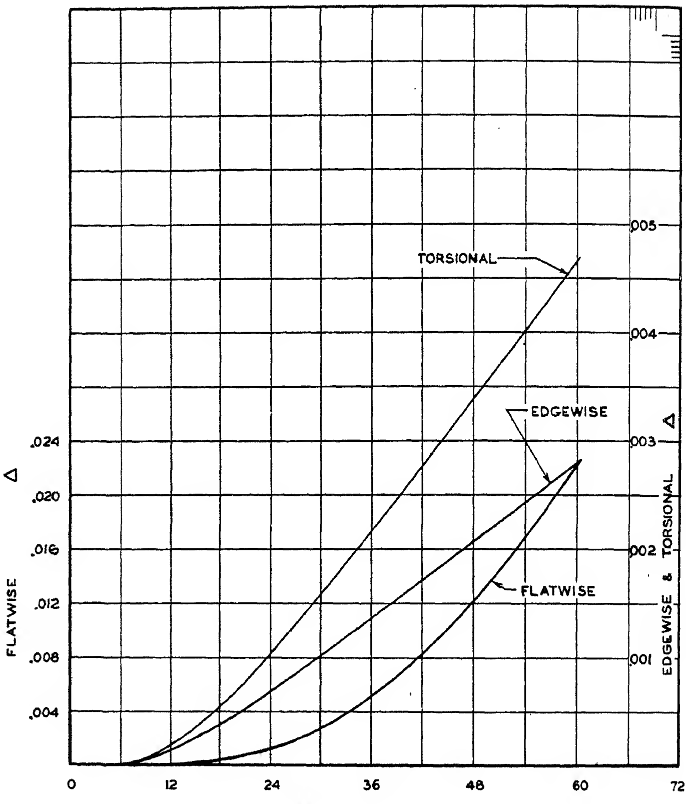

FIGURE 54

POTENTIAL ENERGY

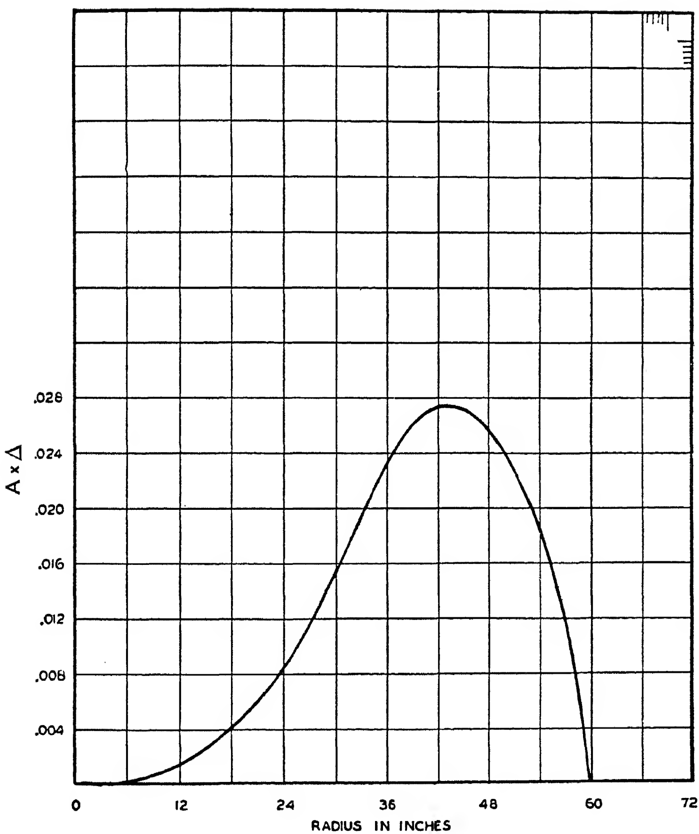

FIGURE 55

KINETIC ENERGY

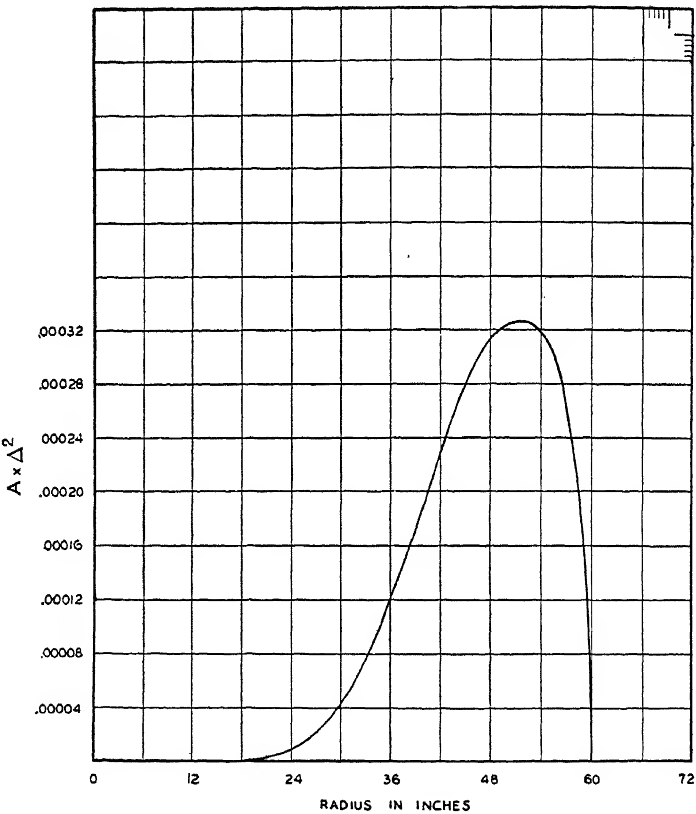

FIGURE 56

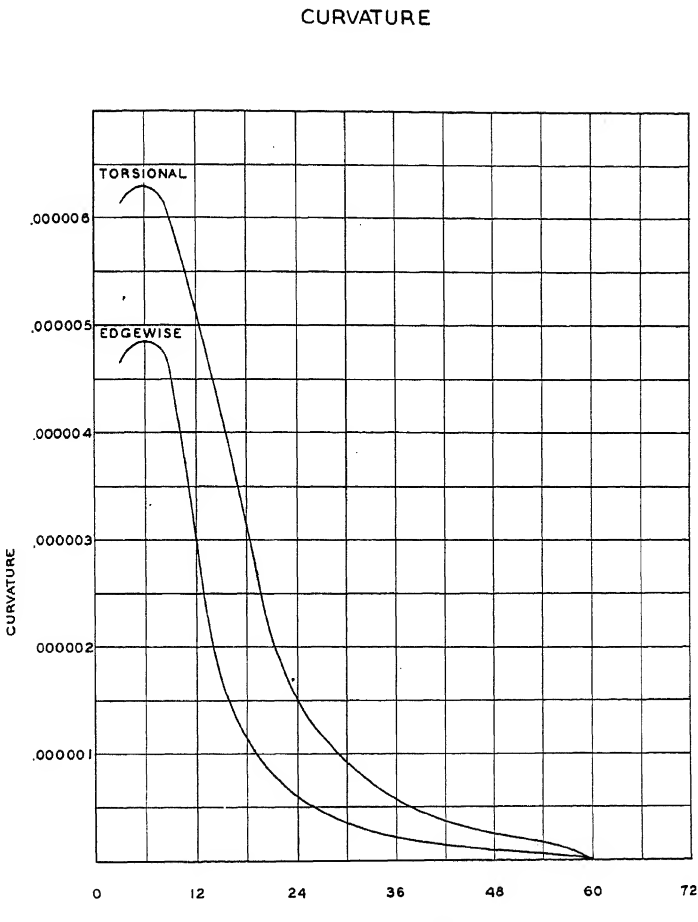
CURVATURE
TORSIONAL
EDGEWISE
.000006
.000005
.000004
.000003
000002
.000001
CURVATURE
0
12
24
36
48
60
72
RADIUS IN INCHES

FIGURE 56a

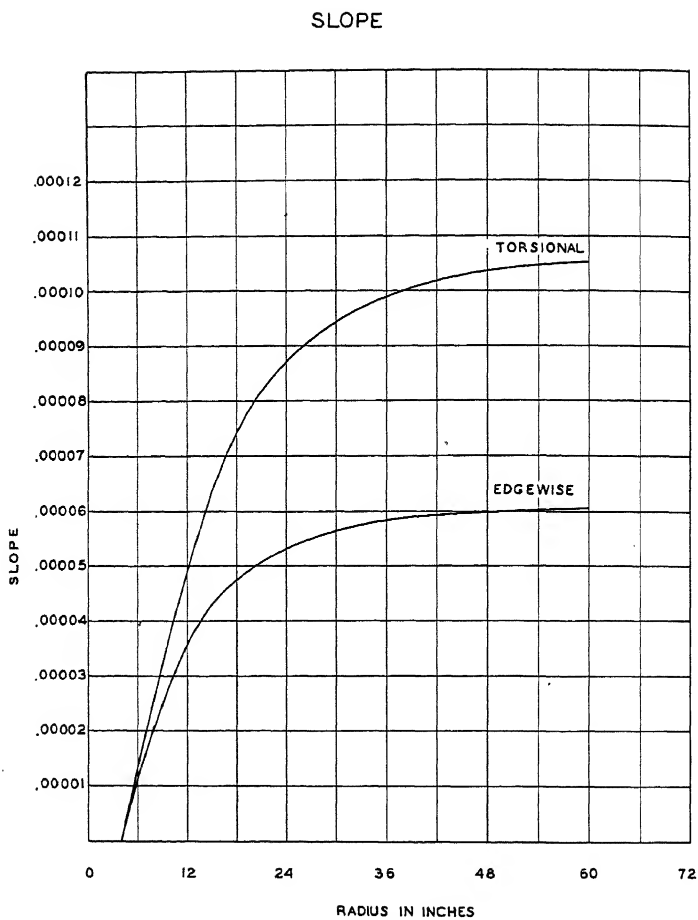
SLOPE
TORSIONAL
EDGEWISE
SLOPE
.00012
.00011
.00010
.00009
.00008
.00007
.00006
.00005
.00004
.00003
.00002
.00001
0
12
24
36
48
60
72
RADIUS IN INCHES

FIGURE 56b

POTENTIAL ENERGY

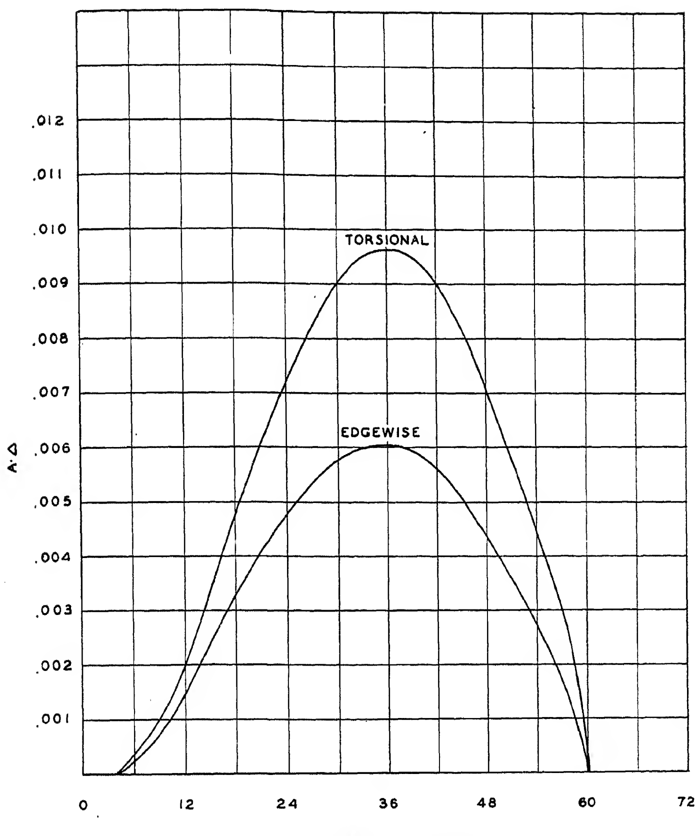

FIGURE 56c

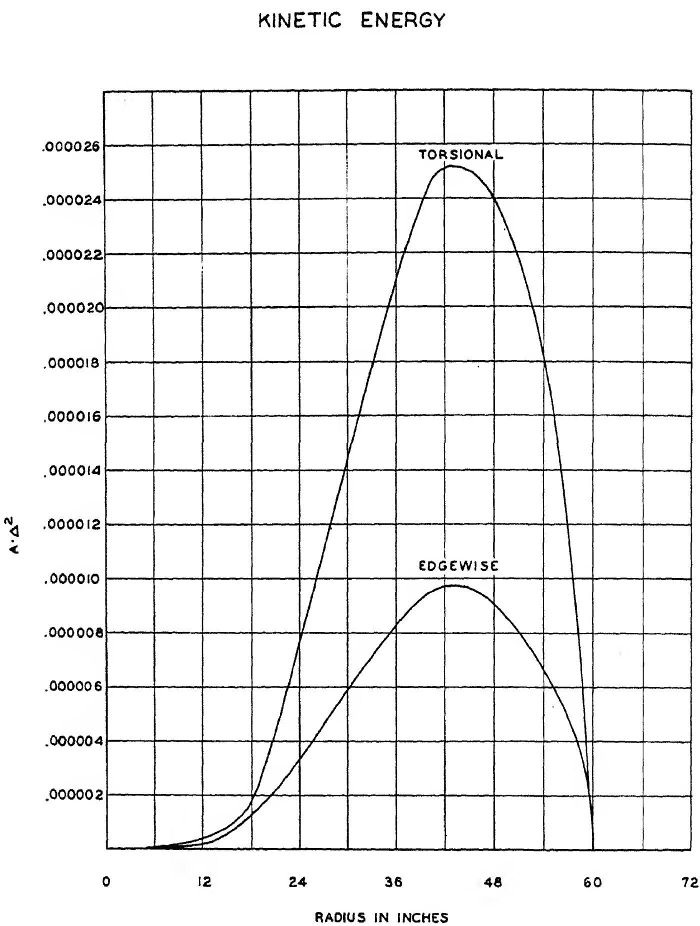
KINETIC ENERGY
TORSIONAL
EDGEWISE
.000026
.000024
.000022
.000020
.000018
.000016
.000014
.000012
.000010
.000008
.000006
.000004
.000002
$A \cdot \Delta^2$
0
12
24
36
48
60
72
RADIUS IN INCHES

FIGURE 56d

CHAPTER 8

SELECTION OF A PROPELLER

Factors to be Considered in Propeller Selection. The various propeller characteristics occurring as design problems have been discussed in detail throughout the previous chapters. The effect and result of these same variables upon the question of propeller selection for airplane performance remain to be analyzed. An accurate knowledge of the performance characteristics of propellers has become a necessity because of the continuous demand for improved airplane and engine performance, and the correct determination of the power absorption and efficiency characteristics of propellers has become increasingly important. The problem, however, is quite complicated. Although test data exist for propellers of various shapes, there is no completely accurate method for applying these data to propeller calculations. On account of the many variables, it is impossible to find data which exactly fulfill all of the requirements; therefore propeller calculations usually are made from the different test results which closely approximate the required conditions. Using test data based on a propeller quite different from the one being computed, results in the greatest error in performance calculations.

All of the propeller design characteristics have some bearing upon the blade selected for the given engine and airplane: each one must be taken into consideration before a final selection is made. The airplane requirements usually are such that one factor will have to be considered more important than the others. Consequently, the selection will be based primarily upon this one factor, making allowances

for the others and thereby arriving at a blade that represents a compromise. The operating conditions usually investigated are: (a) the determination of the propulsive efficiency; (b) the determination of the required power absorption, and blade angle setting; (c) the computation of the static thrust; and (d) the determination of the variation in propeller speed with changes in engine power, air speed, and air density.

In place of attempting to outline a method for the selection of a propeller, the following paragraphs will summarize the effect of each propeller characteristic on airplane performance. From this discussion, conclusions may be drawn regarding the preference for one propeller over another for a given airplane and engine requirement.

Diameter. The diameter of a propeller is selected from the power, propeller speed, airplane velocity, and air density which are required by the airplane, but propellers of different diameters generally have a small difference in their respective aerodynamic effects. The larger diameter propellers have higher propulsive efficiencies, provided the tip-speeds do not surpass the velocity of sound; the differences in efficiency being approximately 1 per cent for a 5 per cent change in diameter.

Tip-Speed. The tip-speed presents an important limitation to the propeller diameter: metal blades having tip-speed in excess of 1000 ft/sec. should never be used. If the tip-speed exceeds this figure, the propulsive efficiency immediately decreases and the propeller noise becomes greatly intensified. Tests show, however, that propellers with low thickness ratio can be operated at slightly higher tip-speeds than thick propellers without loss of efficiency. If the tip-speed of 1000 ft/sec. is surpassed, the efficiency relative to that at lower speeds falls off at a rate of about 10 per cent for 100 ft/sec. increase in speed. For wood pro-

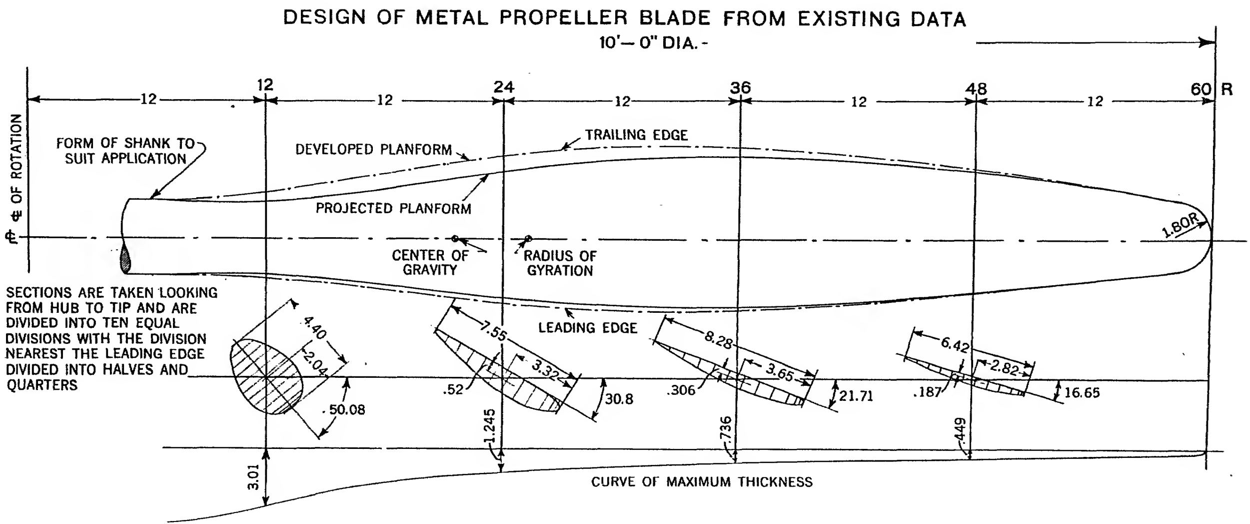
DESIGN OF METAL PROPELLER BLADE FROM EXISTING DATA
10'— 0" DIA.-
12
24
36
48
60 R
℄ OF ROTATION
FORM OF SHANK TO SUIT APPLICATION
DEVELOPED PLANFORM
PROJECTED PLANFORM
TRAILING EDGE
LEADING EDGE
CENTER OF GRAVITY
RADIUS OF GYRATION
1.80R
SECTIONS ARE TAKEN LOOKING FROM HUB TO TIP AND ARE DIVIDED INTO TEN EQUAL DIVISIONS WITH THE DIVISION NEAREST THE LEADING EDGE DIVIDED INTO HALVES AND QUARTERS
4.40
2.04
50.08
7.55
3.32
.52
30.8
8.28
3.65
.306
21.71
6.42
2.82
.187
16.65
3.01
1.245
.736
.449
CURVE OF MAXIMUM THICKNESS

FIGURE 57

pellers, the critical tip-speed is even lower than it is for the metal blades, and the efficiency drop is much greater. Figure 58 shows how the efficiency varies with the tip-speed for both wood and metal propellers.

Diameter Changed by Cutting Tips. A specially designed propeller may be adapted to another given engine and airplane by cutting off the tips. The resulting increased body interference, adverse effect of thickness and plan form of the cut-off propeller are less than the tip-speed losses of the full-length blade. Consequently, a net gain in efficiency will result if a smaller diameter is used to reduce the tip-speed. Changing the diameter of a propeller by cutting off the tips results in only a few per cent loss of maximum propulsive efficiency at the same pitch setting. This practice of cutting tips has been justified by many experimental tests and has been further substantiated by the good results obtained in actual service.

Width. The width of a propeller blade is determined from the diameter, as explained in Chapter 1. A wider blade produces more thrust than a narrower one of the same diameter, but is less efficient. The wide blades are used on airplanes requiring good take-off and climb characteristics, while the narrow blades are desirable for high-speed performance. See Figure 4 for the distinction between narrow and wide blades.

Thickness. The thickness of a propeller blade is based on the blade width (camber ratio) as referred to in Chapter 1. Thin blades, however, do have a higher efficiency than the thicker ones as shown by an N.A.C.A. test in which a blade of 0.06 thickness ratio had a 3 per cent greater efficiency than a blade with a 0.10 thickness ratio. Excessively thin blades do not possess sufficient rigidity and are subject to flutter and fatigue failures.

VARIATION OF EFFICIENCY WITH TIP-SPEED

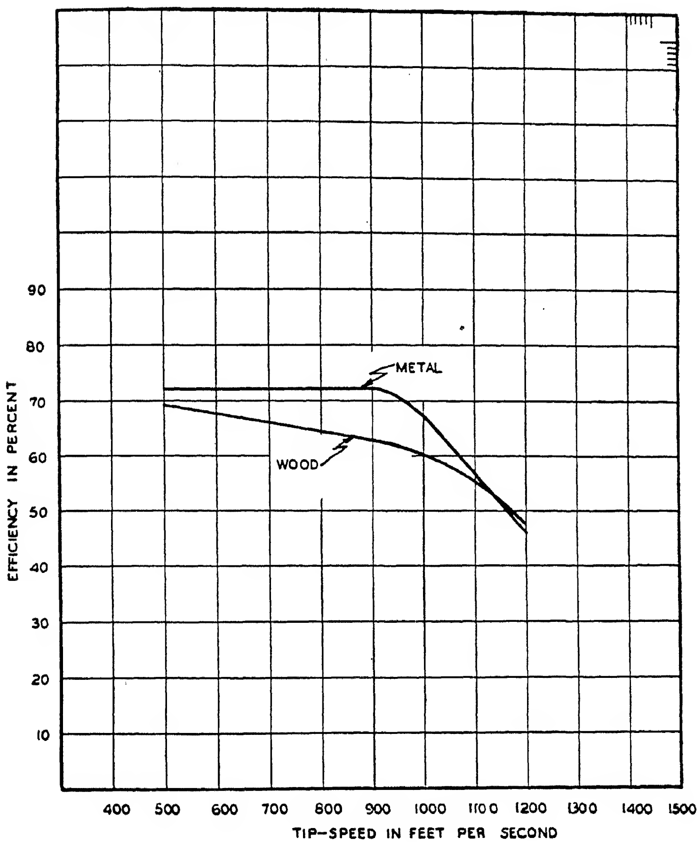

FIGURE 58

Blade Section. On low-pitch propellers, the Clark-Y sections are preferable to the R.A.F.–6 because they produce a higher maximum efficiency. On high-pitch propellers, the R.A.F.–6 sections produce about the same maximum efficiency as the Clark-Y, but they are more efficient for the conditions of climb and take-off. The maximum efficiency of low-pitch propellers having R.A.F.–6 sections decreases slightly with increasing blade thickness; but with Clark-Y sections, the efficiency increases slightly with somewhat thicker sections.

Plan Form. The actual plan form of a propeller blade has little effect upon its aerodynamic performance. It is customary to use a narrow tip when high efficiency is a requisite, but wide tips are used for conditions requiring high thrust. It is only essential that the developed plan form should possess smooth contour lines fairing evenly into the shank and tips, but from a structural viewpoint it is advantageous to taper the blade toward the tip. The sweepback often found in wood blades is for the purpose of providing a smooth flow of air past the propeller and thereby producing less disturbance.

Number of Blades. As explained in Chapter 1, the number of blades is usually determined either from clearance, tip-speed, or horsepower limitations; relatively, the efficiency is not greatly affected.

Static Thrust. When selecting a propeller, it is important at first to decide whether the efficiency or the static thrust shall be the controlling factor in its selection. Figure 59 clearly illustrates how the efficiency and static thrust increase, provided there are no tip-speed losses. In the presence of tip-speed losses, however, the static thrust continually increases while the efficiency rapidly decreases. It is more advantageous to increase the width of a blade in

EFFECT OF DIAMETER ON THE STATIC THRUST AND EFFICIENCY

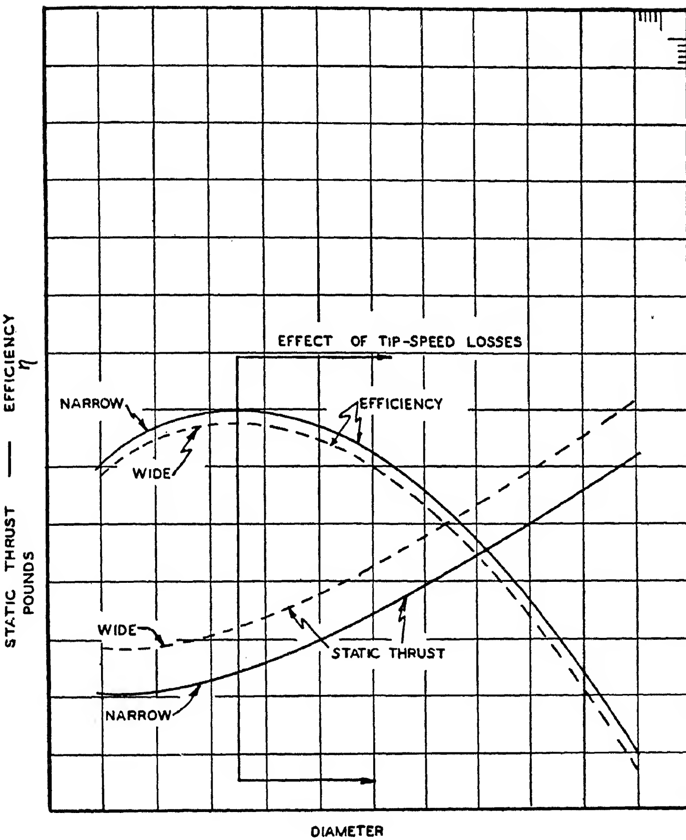

FIGURE 59

obtaining a greater static thrust than it is to enlarge the diameter, because the loss in efficiency is smaller for the same increase in thrust. In general, for propellers of the same diameter, narrow blades give a lower static thrust than the wider blades. Low-pitch settings produce higher static thrust than the high-pitch settings, and three-bladed propellers have higher thrust values than the two-bladed, although the efficiency of the three-bladed is somewhat lower.

Pitch Distribution. It may be stated generally that the efficiency of a propeller will increase with the pitch. Propellers with low-pitch angles give the best performance for a quick take-off and good climb, while propellers with high-pitch angles are more adapted to high speed and high altitude flying.

Materials. Wood, steel, and aluminum alloy are the most common materials in use today for propellers. Each has its own advantages and disadvantages from the standpoint of cost, weight, efficiency, and maintenance; consequently the purchaser usually selects the material most suitable to his requirements.

Controllable-Pitch Propellers. With the high performance required today of modern aircraft, the controllable-pitch propeller has become a real necessity. A fixed-pitch propeller ordinarily is set to obtain best performance while the airplane is cruising, consequently the take-off and climb characteristics are not at their best. The controllable propeller will permit a low-pitch setting for take-off and climb, thereby giving optimum performance. In the air the propeller can be changed to a higher pitch and thus provide the desired cruising or high-speed performance. This problem is especially important for heavy transport airplanes having large payloads which require low-pitch angles for take-off; also constantly increasing maximum speeds demand

TYPICAL CHANGE IN BLADE ANGLE
AT STATIC AND TOP SPEED CONDITIONS

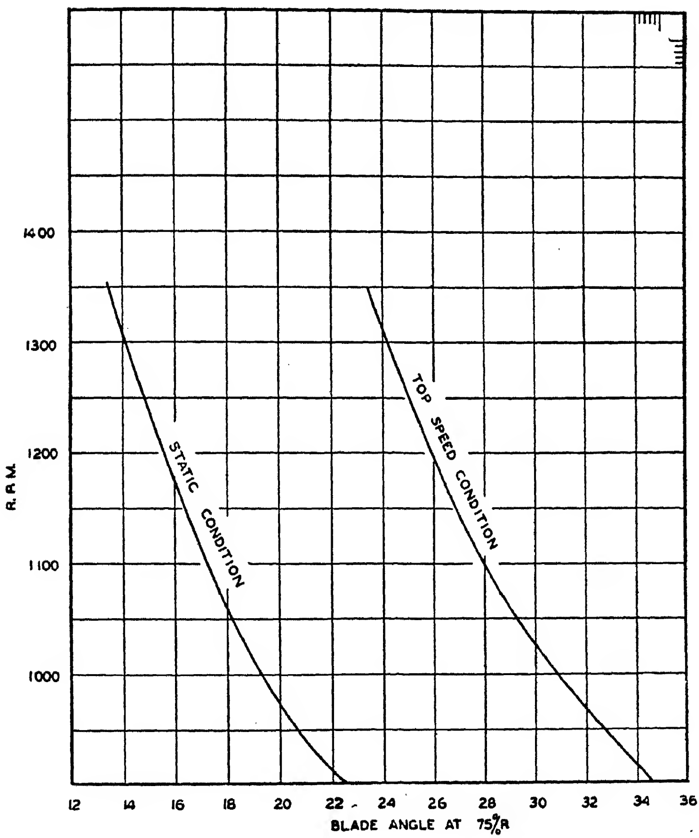

FIGURE 60

TYPICAL THRUST AVAILABLE WITH CHANGE IN BLADE ANGLE SETTING

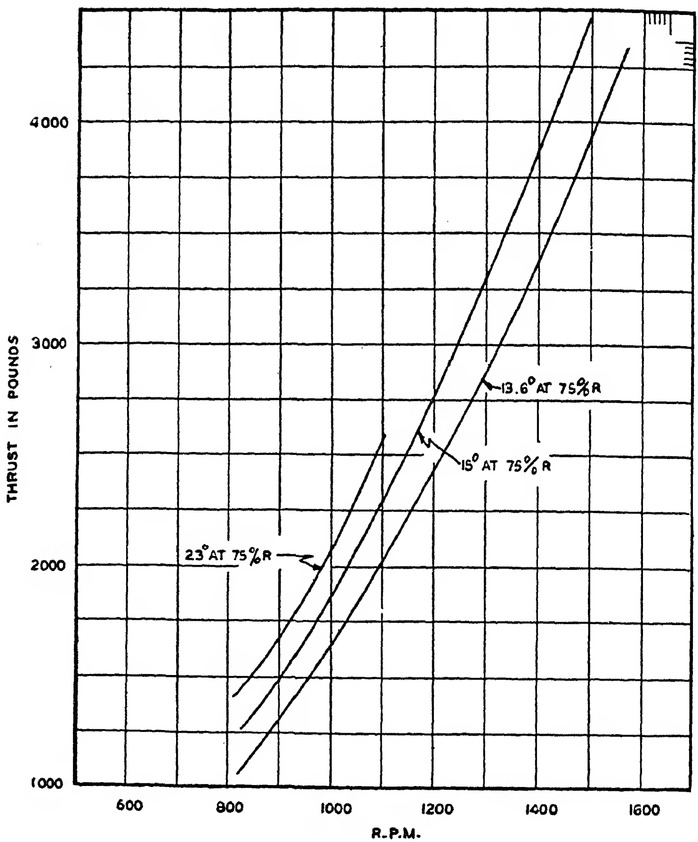

FIGURE 61

TYPICAL HP. AVAILABLE WITH CHANGE
IN BLADE ANGLE SETTING

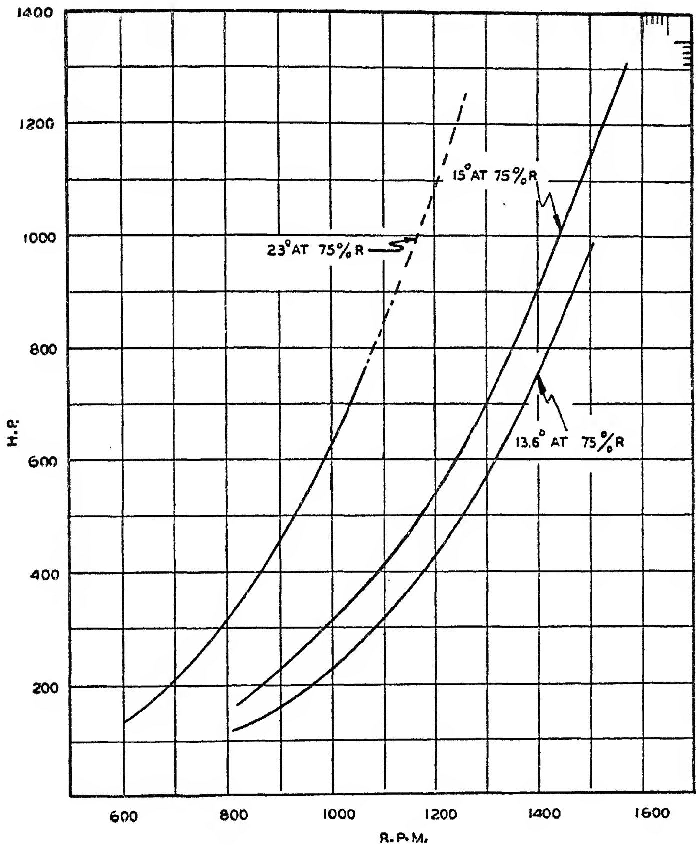

FIGURE 62

larger pitch angles. Figure 60 illustrates the change in angle setting required from the static to the top-speed condition, and Figures 61 and 62 show the additional thrust and horsepower available with the change in angle setting. A controllable-pitch propeller could be set to produce the required change and the airplane would have maximum performance at take-off, during climb, and while cruising.

TABLES

PROPELLER DIAMETERS

The diameters in the following tables are dimensioned in feet, based on three-bladed propellers with Clark-Y sections and a thickness ratio of 0.075 at the 75% radius.

It applies to propellers of v/nD from 0.4 to 3.2 and blades which are fairly wide and of normal planform.

For. R.A.F.-6 sections multiply these diameters by 0.95.

For two-bladed propellers multiply these diameters by 1.102 and for four-bladed propellers multiply by 0.9375 (see also Figure 63 for conversion from three-bladed to multi-blade propellers).

If the engine is rated at altitude multiply the B.hp. with air density factor, Figure 3.

DIAMETER										50 H.P.
M.P.H.	R.P.M.									
	1600	1700	1800	1900	2000	2100	2200	2300	2400	2500
100	6.50	6.32	6.16	6.03	5.90	5.77	5.65	5.53	5.44	5.34
110	6.26	6.08	5.93	5.79	5.68	5.56	5.45	5.33	5.22	5.14
120	6.05	5.88	5.74	5.61	5.49	5.37	5.25	5.14	5.05	4.98
130	5.85	5.62	5.55	5.43	5.31	5.20	5.08	4.98	4.89	4.80
140	5.68	5.53	5.33	5.25	5.15	5.04	4.94	4.83	4.74	4.66
150	5.53	5.34	5.24	5.13	5.01	4.91	4.80	471	4.62	4.53
160	5.38	5.24	5.10	5.00	4.88	4.78	4.67	4.59	4.49	4.42
170	5.26	5.11	4.99	4.87	4.76	4.67	4.57	4.47	4.39	4.32
180	5.14	5.00	4.87	4.76	4.66	4.56	4.46	4.37	4.29	4.22
190	5.03	4.88	4.77	4.67	4.56	4.46	4.36	4.28	4.21	4.17
200	4.93	4.75	4.67	4.58	4.47	4.37	4.29	4.20	4.12	4.05
210	4.84	4.71	4.58	4.47	4.38	4.30	4.21	4.12	4.03	3.97
220	4.75	4.61	4.50	4.40	4.31	4.21	4.13	4.04	3.96	3.91
230	4.66	4.53	4.42	4.31	4.23	4.13	4.05	3.96	3.88	3.83
240	4.58	4.44	4.34	4.25	4.16	4.06	3.79	3.89	3.83	3.77
250	4.51	4.38	4.27	4.17	4.08	4.00	3.92	3.84	3.77	3.71
260	4.43	4.30	4.20	4.11	4.02	3.94	3.84	3.77	3.70	3.64
270	4.38	4.26	4.15	4.06	3.97	3.88	3.80	3.72	3.65	3.59
280	4.31	4.18	4.08	3.99	3.91	3.83	3.75	3.67	3.61	3.53
290	4.25	4.13	4.02	3.93	3.85	3.77	3.69	3.61	3.56	3.48
300	4.19	4.08	3.97	3.87	3.79	3.71	3.64	3.56	3.51	3.44

DIAMETER										60 H.P.
M.P.H.	R.P.M.									
	1600	1700	1800	1900	2000	2100	2200	2300	2400	2500
100	6.85	6.66	6.49	6.35	6.21	6.08	5.95	5.82	5.72	5.62
110	6.59	6.40	6.24	6.10	5.98	5.85	5.74	5.61	5.50	5.42
120	6.37	6.20	6.04	5.91	5.78	5.66	5.54	5.42	5.32	5.24
130	6.16	5.91	5.84	5.72	5.59	5.47	5.36	5.24	5.15	5.06
140	5.98	5.83	5.66	5.54	5.43	5.31	5.20	5.09	5.00	4.91
150	5.83	5.65	5.52	5.40	5.27	5.16	5.05	4.96	4.87	4.77
160	5.66	5.52	5.37	5.25	5.13	5.03	4.92	4.83	4.74	4.66
170	5.49	5.38	5.24	5.12	5.01	4.91	4.81	4.71	4.63	4.55
180	5.42	5.25	5.12	5.00	4.90	4.80	4.70	4.61	4.51	4.44
190	5.30	5.14	5.02	4.92	4.80	4.70	4.60	4.51	4.43	4.39
200	5.19	5.05	4.93	4.83	4.72	4.61	4.52	4.42	4.33	4.27
210	5.09	4.97	4.84	4.72	4.62	4.53	4.43	4.33	4.25	4.18
220	5.01	4.86	4.74	4.63	4.54	4.43	4.35	4.26	4.18	4.14
230	4.91	4.77	4.65	4.55	4.45	4.35	4.27	4.18	4.09	4.03
240	4.83	4.69	4.59	4.48	4.38	4.29	4.19	4.10	4.03	3.97
250	4.75	4.63	4.51	4.40	4.31	4.22	4.13	4.04	3.96	3.90
260	4.67	4.54	4.42	4.33	4.23	4.15	4.05	3.97	3.89	3.83
270	4.63	4.48	4.37	4.28	4.18	4.09	4.01	3.92	3.84	3.78
280	4.55	4.41	4.30	4.21	4.12	4.03	3.95	3.87	3.80	3.72
290	4.48	4.35	4.24	4.14	4.06	3.97	3.89	3.81	3.75	3.67
300	4.41	4.29	4.18	4.08	4.00	3.91	3.84	3.76	3.70	3.63

DIAMETER										70 H.P.
M.P.H.	R.P.M.									
	1600	1700	1800	1900	2000	2100	2200	2300	2400	2500
100	7.15	6.95	6.77	6.62	6.49	6.35	6.21	6.08	5.97	5.86
110	6.88	6.68	6.51	6.36	6.24	6.11	5.99	5.86	5.75	5.65
120	6.65	6.47	6.31	6.16	6.04	5.90	5.78	5.65	5.55	5.47
130	6.44	6.17	6.10	5.97	5.84	5.72	5.59	5.47	5.37	5.27
140	6.25	6.08	5.92	5.78	5.66	5.55	5.43	5.31	5.22	5.12
150	6.08	5.91	5.76	5.63	5.51	5.40	5.28	5.17	5.08	4.99
160	5.92	5.76	5.61	5.49	5.37	5.26	5.14	5.04	4.94	4.86
170	5.78	5.62	5.48	5.36	5.24	5.13	5.03	4.92	4.83	4.75
180	5.66	5.50	5.36	5.23	5.12	5.02	4.91	4.81	4.72	4.64
190	5.54	5.37	5.24	5.13	5.02	4.91	4.80	4.71	4.63	4.58
200	5.42	5.27	5.14	5.04	4.93	4.81	4.72	4.62	4.52	4.45
210	5.33	5.17	5.05	4.93	4.82	4.73	4.63	4.52	4.43	4.36
220	5.22	5.07	4.95	4.83	4.74	4.63	4.54	4.44	4.36	4.32
230	5.12	4.98	4.85	4.75	4.65	4.54	4.45	4.36	4.27	4.21
240	5.04	4.88	4.78	4.67	4.57	4.47	4.37	4.28	4.21	4.14
250	4.96	4.82	4.70	4.59	4.49	4.40	4.31	4.22	4.13	4.07
260	4.88	4.73	4.62	4.52	4.42	4.33	4.23	4.14	4.06	4.00
270	4.82	4.68	4.56	4.46	4.36	4.27	4.17	4.08	4.01	3.95
280	4.74	4.60	4.49	4.39	4.30	4.21	4.12	4.03	3.96	3.88
290	4.66	4.54	4.43	4.33	4.23	4.14	4.06	3.97	3.91	3.83
300	4.60	4.48	4.36	4.26	4.16	4.08	4.01	3.92	3.85	3.78

DIAMETER										80 H.P.
M.P.H.	R.P.M.									
	1600	1700	1800	1900	2000	2100	2200	2300	2400	2500
100	7.42	7.21	7.03	6.88	6.73	6.59	6.45	6.31	6.20	6.08
110	7.14	6.94	6.76	6.61	6.48	6.34	6.22	6.08	5.96	5.87
120	6.90	6.71	6.55	6.40	6.26	6.13	5.99	5.86	5.76	5.68
130	6.69	6.41	6.33	6.20	6.06	5.94	5.80	5.68	5.58	5.48
140	6.48	6.31	6.14	6.00	5.88	5.75	5.63	5.51	5.40	5.32
150	6.31	6.13	5.98	5.85	5.71	5.59	5.47	5.36	5.28	5.17
160	6.14	5.97	5.82	5.69	5.56	5.45	5.32	5.23	5.12	5.05
170	6.00	5.83	5.68	5.56	5.43	5.31	5.21	5.09	5.02	4.93
180	5.87	5.70	5.56	5.43	5.32	5.20	5.08	5.00	4.89	4.81
190	5.74	5.57	5.44	5.33	5.20	5.08	4.99	4.88	4.80	4.75
200	5.63	5.48	5.34	5.22	5.10	5.00	4.89	4.79	4.69	4.62
210	5.52	5.38	5.24	5.10	5.01	4.90	4.80	4.69	4.60	4.53
220	5.43	5.27	5.12	5.02	4.91	4.80	4.71	4.61	4.53	4.48
230	5.32	5.16	5.04	4.92	4.82	4.72	4.62	4.52	4.43	4.37
240	5.23	5.07	4.96	4.85	4.75	4.64	4.53	4.44	4.37	4.30
250	5.15	5.00	4.88	4.77	4.66	4.56	4.47	4.38	4.29	4.22
260	5.06	4.92	4.80	4.69	4.58	4.49	4.39	4.30	4.21	4.14
270	5.00	4.86	4.73	4.63	4.52	4.43	4.34	4.25	4.16	4.10
280	4.92	4.78	4.66	4.56	4.46	4.37	4.27	4.19	4.12	4.03
290	4.85	4.72	4.59	4.49	4.39	4.30	4.22	4.12	4.06	3.97
300	4.78	4.65	4.53	4.41	4.33	4.24	4.16	4.07	4.00	3.93

DIAMETER										90 H.P.
M.P.H.	R.P.M.									
	1600	1700	1800	1900	2000	2100	2200	2300	2400	2500
100	7.67	7.46	7.27	7.12	6.95	6.80	6.66	6.53	6.41	6.29
110	7.38	7.18	6.99	6.84	6.70	6.55	6.43	6.28	6.16	6.07
120	7.14	6.94	6.77	6.61	6.48	6.34	6.19	6.07	5.96	5.87
130	6.90	6.72	6.54	6.41	6.26	6.14	6.00	5.87	5.77	5.67
140	6.70	6.52	6.35	6.20	6.07	5.95	5.82	5.70	5.59	5.49
150	6.53	6.34	6.16	6.05	5.92	5.78	5.66	5.56	5.44	5.35
160	6.35	6.17	6.02	5.90	5.76	5.64	5.51	5.41	5.30	5.22
170	6.20	6.03	5.88	5.75	5.62	5.51	5.39	5.27	5.19	5.10
180	6.07	5.90	5.75	5.61	5.49	5.38	5.27	5.17	5.06	4.97
190	5.93	5.75	5.62	5.51	5.38	5.27	5.15	5.05	4.96	4.91
200	5.82	5.66	5.51	5.40	5.28	5.17	5.06	4.95	4.85	4.78
210	5.71	5.56	5.41	5.28	5.18	5.07	4.96	4.85	4.76	4.68
220	5.60	5.44	5.30	5.18	5.08	4.96	4.88	4.76	4.68	4.63
230	5.49	5.34	5.20	5.09	4.98	4.87	4.78	4.68	4.58	4.52
240	5.41	5.24	5.13	5.01	4.90	4.80	4.69	4.59	4.51	4.44
250	5.32	5.16	5.04	4.92	4.81	4.72	4.62	4.52	4.44	4.37
260	5.24	5.08	4.95	4.84	4.73	4.64	4.53	4.44	4.36	4.29
270	5.17	5.02	4.90	4.78	4.68	4.58	4.48	4.39	4.30	4.23
280	5.09	4.95	4.82	4.71	4.61	4.51	4.42	4.33	4.25	4.17
290	5.01	4.88	4.75	4.64	4.54	4.44	4.36	4.27	4.20	4.11
300	4.94	4.81	4.68	4.57	4.47	4.37	4.30	4.20	4.13	4.06

DIAMETER										100 H.P.
M.P.H.	R.P.M.									
	1600	1700	1800	1900	2000	2100	2200	2300	2400	2500
100	7.90	7.68	7.49	7.32	7.16	7.01	6.86	6.72	6.60	6.48
110	7.60	7.39	7.20	7.04	6.90	6.75	6.62	6.47	6.35	6.25
120	7.35	7.15	6.97	6.81	6.67	6.53	6.38	6.25	6.14	6.05
130	7.11	6.92	6.74	6.60	6.45	6.32	6.18	6.05	5.94	5.84
140	6.90	6.72	6.54	6.39	6.26	6.13	6.00	5.87	5.76	5.66
150	6.72	6.53	6.37	6.23	6.09	5.96	5.83	5.72	5.62	5.51
160	6.54	6.36	6.20	6.07	5.93	5.81	5.68	5.57	5.46	5.37
170	6.39	6.21	6.06	5.92	5.79	5.67	5.55	5.43	5.34	5.25
180	6.25	6.07	5.92	5.78	5.66	5.54	5.42	5.32	5.21	5.12
190	6.11	5.93	5.79	5.67	5.54	5.42	5.31	5.20	5.11	5.06
200	5.99	5.83	5.68	5.56	5.44	5.32	5.21	5.10	5.00	4.92
210	5.88	5.72	5.57	5.44	5.33	5.22	5.11	5.00	4.90	4.82
220	5.77	5.60	5.46	5.34	5.23	5.11	5.02	4.91	4.82	4.77
230	5.66	5.50	5.36	5.24	5.13	5.02	4.92	4.82	4.72	4.65
240	5.57	5.40	5.28	5.16	5.05	4.94	4.83	4.73	4.65	4.56
250	5.48	5.32	5.19	5.07	4.96	4.86	4.76	4.66	4.57	4.50
260	5.39	5.23	5.10	4.99	4.88	4.78	4.67	4.58	4.49	4.42
270	5.32	5.17	5.04	4.93	4.82	4.72	4.62	4.52	4.43	4.36
280	5.24	5.09	4.96	4.85	4.75	4.65	4.55	4.46	4.38	4.29
290	5.16	5.02	4.89	4.78	4.68	4.58	4.49	4.39	4.32	4.23
300	5.09	4.95	4.82	4.71	4.61	4.51	4.43	4.33	4.26	4.18

DIAMETER										125 H.P.
M.P.H.	R.P.M.									
	1600	1700	1800	1900	2000	2100	2200	2300	2400	2500
100	8.42	8.18	7.97	7.80	7.63	7.47	7.30	7.15	7.03	6.90
110	8.10	7.87	7.67	7.50	7.35	7.19	7.04	6.89	6.76	6.66
120	7.82	7.61	7.42	7.25	7.10	6.95	6.78	6.65	6.53	6.43
130	7.56	7.25	7.17	7.02	6.86	6.72	6.57	6.43	6.32	6.21
140	7.35	7.15	6.95	6.80	6.66	6.52	6.36	6.24	6.13	6.03
150	7.15	6.95	6.77	6.63	6.48	6.34	6.21	6.08	5.89	5.86
160	6.95	6.76	6.60	6.45	6.31	6.18	6.04	5.92	5.81	5.72
170	6.80	6.61	6.45	6.30	6.16	6.04	5.91	5.77	5.68	5.58
180	6.65	6.46	6.30	6.15	6.02	5.89	5.76	5.66	5.54	5.45
190	6.50	6.31	6.15	6.03	5.89	5.77	5.65	5.53	5.43	5.38
200	6.36	6.20	6.04	5.91	5.78	5.66	5.54	5.42	5.33	5.22
210	6.25	6.09	5.93	5.79	5.67	5.55	5.42	5.32	5.22	5.13
220	6.13	5.96	5.81	5.68	5.56	5.43	5.33	5.22	5.12	5.07
230	6.02	5.85	5.70	5.57	5.46	5.34	5.22	5.13	5.02	4.94
240	5.92	5.75	5.62	5.49	5.37	5.25	5.13	5.03	4.94	4.88
250	5.83	5.65	5.52	5.38	5.27	5.17	5.06	4.96	4.86	4.78
260	5.73	5.56	5.42	5.31	5.18	5.08	4.98	4.87	4.78	4.69
270	5.66	5.50	5.36	5.25	5.13	5.02	4.91	4.80	4.72	4.64
280	5.57	5.41	5.27	5.16	5.05	4.95	4.85	4.75	4.66	4.56
290	5.49	5.34	5.20	5.08	4.98	4.87	4.78	4.67	4.59	4.50
300	5.42	5.27	5.12	5.01	4.90	4.80	4.71	4.61	4.53	4.44

DIAMETER										150 HP.
M.P.H.	R.P.M.									
	1600	1700	1800	1900	2000	2100	2200	2300	2400	2500
100	8.85	8.60	8.39	8.20	8.02	7.85	7.68	7.52	7.39	7.26
110	8.50	8.27	8.06	7.87	7.72	7.55	7.40	7.24	7.11	7.00
120	8.24	8.01	7.81	7.62	7.47	7.32	7.14	7.00	6.88	6.77
130	7.96	7.63	7.54	7.39	7.22	7.07	6.91	6.77	6.65	6.53
140	7.72	7.52	7.32	7.15	7.00	6.85	6.71	6.57	6.45	6.34
150	7.52	7.31	7.13	6.97	6.80	6.68	6.52	6.40	6.29	6.17
160	7.32	7.12	6.94	6.78	6.65	6.50	6.35	6.23	6.11	6.02
170	7.15	6.95	6.77	6.64	6.48	6.34	6.22	6.08	5.99	5.89
180	7.00	6.78	6.64	6.47	6.33	6.21	6.07	5.97	5.84	5.74
190	6.83	6.65	6.48	6.34	6.21	6.08	5.94	5.83	5.73	5.67
200	6.72	6.53	6.35	6.23	6.10	5.96	5.83	5.72	5.60	5.51
210	6.59	6.40	6.24	6.10	5.97	5.85	5.71	5.60	5.49	5.40
220	6.46	6.27	6.12	5.98	5.86	5.72	5.61	5.50	5.40	5.34
230	6.34	6.17	6.00	5.87	5.75	5.62	5.50	5.40	5.28	5.21
240	6.25	6.05	5.92	5.78	5.65	5.53	5.39	5.29	5.21	5.13
250	6.14	5.97	5.81	5.69	5.55	5.43	5.32	5.22	5.12	5.04
260	6.04	5.86	5.71	5.59	5.46	5.36	5.23	5.13	5.03	4.95
270	5.96	5.78	5.65	5.52	5.41	5.28	5.17	5.06	4.96	4.88
280	5.87	5.70	5.55	5.43	5.32	5.21	5.09	5.00	4.91	4.80
290	5.77	5.62	5.47	5.36	5.25	5.14	5.02	4.91	4.84	4.74
300	5.70	5.54	5.40	5.28	5.11	5.05	4.95	4.85	4.77	4.68

DIAMETER										175 H.P.
M.P.H.	R.P.M.									
	1600	1700	1800	1900	2000	2100	2200	2300	2400	2500
100	9.25	8.98	8.75	8.55	8.38	8.20	8.02	7.86	7.72	7.58
110	8.90	8.64	8.42	8.23	8.07	7.89	7.73	7.56	7.43	7.30
120	8.60	8.35	8.15	7.97	7.80	7.64	7.45	7.30	7.18	7.08
130	8.32	7.98	7.88	7.72	7.54	7.40	7.22	7.08	6.95	6.83
140	8.07	7.86	7.65	7.47	7.32	7.16	7.01	6.87	6.74	6.62
150	7.86	7.64	7.45	7.29	7.11	6.97	6.81	6.70	6.57	6.45
160	7.65	7.45	7.25	7.10	6.93	6.80	6.64	6.51	6.39	6.28
170	7.48	7.26	7.09	6.93	6.77	6.68	6.49	6.35	6.24	6.14
180	7.31	7.10	6.92	6.76	6.62	6.47	6.33	6.22	6.10	5.99
190	7.15	6.94	6.77	6.64	6.48	6.34	6.20	6.08	5.97	5.91
200	7.00	6.82	6.64	6.50	6.36	6.22	6.08	5.96	5.85	5.75
210	6.88	6.69	6.51	6.35	6.23	6.10	5.96	5.85	5.73	5.64
220	6.74	6.55	6.39	6.23	6.12	5.98	5.86	5.74	5.64	5.57
230	6.62	6.43	6.27	6.13	6.00	5.87	5.74	5.64	5.52	5.44
240	6.51	6.32	6.18	6.03	5.91	5.78	5.64	5.53	5.44	5.36
250	6.41	6.22	6.07	5.93	5.80	5.69	5.56	5.45	5.35	5.26
260	6.30	6.12	5.97	5.84	5.70	5.60	5.46	5.35	5.25	5.16
270	6.22	6.04	5.89	5.77	5.64	5.52	5.39	5.28	5.18	5.10
280	6.13	5.95	5.80	5.67	5.55	5.44	5.31	5.22	5.12	5.02
290	6.04	5.82	5.71	5.59	5.48	5.35	5.23	5.13	5.05	4.94
300	5.95	5.78	5.64	5.51	5.39	5.27	5.17	5.06	4.98	4.89

DIAMETER										200 HP.
M.P.H.	R.P.M.									
	1600	1700	1800	1900	2000	2100	2200	2300	2400	2500
100	9.59	9.33	9.09	8.89	8.70	8.51	8.31	8.15	8.00	7.85
110	9.22	8.96	8.75	8.54	8.37	8.20	8.02	7.85	7.70	7.58
120	8.92	8.69	8.46	8.27	8.10	7.93	7.75	7.60	7.44	7.33
130	8.64	8.39	8.18	8.01	7.85	7.68	7.50	7.35	7.21	7.09
140	8.39	8.15	7.94	7.75	7.60	7.45	7.28	7.13	6.99	6.87
150	8.16	7.94	7.74	7.56	7.39	7.24	7.08	6.94	6.72	6.69
160	7.84	7.73	7.52	7.37	7.20	7.06	6.89	6.76	6.63	6.50
170	7.75	7.55	7.36	7.19	7.03	6.88	6.73	6.59	6.47	6.37
180	7.58	7.38	7.18	7.02	6.87	6.73	6.56	6.45	6.32	6.22
190	7.42	7.20	7.03	6.89	6.72	6.58	6.44	6.31	6.21	6.14
200	7.27	7.08	6.90	6.75	6.60	6.45	6.33	6.20	6.07	5.97
210	7.13	6.95	6.76	6.60	6.47	6.34	6.20	6.07	5.95	5.86
220	7.00	6.80	6.63	6.48	6.35	6.20	6.08	5.96	5.86	5.80
230	6.87	6.68	6.51	6.36	6.23	6.10	5.96	5.86	5.74	5.66
240	6.76	6.56	6.41	6.26	6.13	5.99	5.86	5.75	5.66	5.54
250	6.66	6.46	6.30	6.15	6.03	5.90	5.78	5.67	5.53	5.45
260	6.54	6.35	6.19	6.06	5.93	5.80	5.68	5.54	5.44	5.37
270	6.45	6.28	6.12	5.98	5.85	5.73	5.60	5.48	5.38	5.30
280	6.35	6.18	6.02	5.89	5.76	5.64	5.52	5.42	5.32	5.21
290	6.25	6.09	5.94	5.80	5.68	5.55	5.44	5.32	5.24	5.13
300	6.16	6.00	5.85	5.72	5.60	5.47	5.37	5.29	5.17	5.07

DIAMETER										225 H.P.
M.P.H.	R.P.M.									
	1600	1700	1800	1900	2000	2100	2200	2300	2400	2500
100	9.92	9.64	9.40	9.19	8.98	8.80	8.61	8.44	8.28	8.13
110	9.54	9.28	9.04	8.84	8.66	8.47	8.31	8.13	7.97	7.84
120	9.22	8.98	8.75	8.55	8.38	8.20	8.01	7.85	7.72	7.59
130	8.92	8.69	8.47	8.28	8.10	7.93	7.76	7.59	7.46	7.33
140	8.67	8.43	8.21	8.02	7.86	7.69	7.53	7.47	7.23	7.10
150	8.44	8.20	8.00	7.82	7.65	7.48	7.32	7.18	7.06	6.91
160	8.22	7.98	7.78	7.62	7.44	7.29	7.13	6.99	6.85	6.74
170	8.02	7.79	7.60	7.43	7.27	7.12	6.97	6.82	6.71	6.59
180	7.84	7.62	7.43	7.25	7.10	6.96	6.81	6.68	6.54	6.43
190	7.67	7.44	7.27	7.12	6.96	6.81	6.66	6.53	6.41	6.30
200	7.52	7.32	7.13	6.98	6.83	6.68	6.54	6.40	6.27	6.16
210	7.38	7.18	7.00	6.83	6.69	6.55	6.41	6.27	6.15	6.05
220	7.25	7.03	6.85	6.71	6.57	6.42	6.30	6.16	6.05	5.93
230	7.10	6.90	6.72	6.58	6.43	6.30	6.17	6.05	5.93	5.83
240	7.00	6.78	6.62	6.47	6.33	6.20	6.06	5.94	5.83	5.75
250	6.88	6.68	6.52	6.37	6.22	6.10	5.96	5.85	5.73	5.65
260	6.77	6.57	6.40	6.27	6.13	6.00	5.87	5.75	5.65	5.55
270	6.68	6.49	6.33	6.18	6.05	5.93	5.80	5.68	5.57	5.47
280	6.58	6.39	6.22	6.09	5.96	5.83	5.71	5.59	5.50	5.39
290	6.47	6.30	6.14	6.00	5.88	5.75	5.63	5.51	5.42	5.31
300	6.39	6.21	6.06	5.91	5.78	5.66	5.56	5.43	5.34	5.24

DIAMETER										250 H.P.
M.P.H	R.P.M.									
	1600	1700	1800	1900	2000	2100	2200	2300	2400	2500
100	10.21	9.93	9.69	9.47	9.25	9.06	8.87	8.69	8.53	8.38
110	9.83	9.56	9.31	9.10	8.92	8.73	8.56	8.37	8.21	8.08
120	9.50	9.25	9.02	8.80	8.63	8.45	8.25	8.08	7.94	7.82
130	9.19	8.95	8.72	8.53	8.34	8.18	7.99	7.82	7.68	7.55
140	8.92	8.69	8.46	8.26	8.09	7.93	7.76	7.59	7.44	7.32
150	8.69	8.44	8.23	8.06	7.88	7.70	7.54	7.40	7.27	7.12
160	8.46	8.22	8.02	7.85	7.67	7.51	7.35	7.21	7.06	6.94
170	8.27	8.03	7.83	7.66	7.49	7.33	7.18	7.02	6.91	6.79
180	8.08	7.85	7.66	7.47	7.32	7.17	7.01	6.88	6.73	6.63
190	7.90	7.69	7.49	7.34	7.17	7.01	6.86	6.72	6.60	6.49
200	7.75	7.54	7.34	7.18	7.04	6.88	6.73	6.60	6.47	6.36
210	7.60	7.40	7.21	7.04	6.89	6.75	6.60	6.46	6.33	6.23
220	7.47	7.24	7.05	6.91	6.76	6.60	6.49	6.34	6.23	6.12
230	7.32	7.11	6.93	6.78	6.63	6.49	6.36	6.23	6.11	6.02
240	7.21	6.98	6.83	6.67	6.53	6.39	6.25	6.12	6.02	5.92
250	7.08	6.88	6.71	6.56	6.41	6.28	6.15	6.02	5.91	5.82
260	6.98	6.76	6.59	6.45	6.31	6.18	6.04	5.92	5.81	5.72
270	6.88	6.69	6.52	6.37	6.23	6.11	5.98	5.85	5.73	5.63
280	6.78	6.58	6.41	6.27	6.14	6.01	5.88	5.76	5.67	5.55
290	6.67	6.49	6.33	6.18	6.05	5.92	5.81	5.68	5.59	5.47
300	6.59	6.40	6.23	6.08	5.95	5.83	5.73	5.60	5.50	5.40

DIAMETER										275 H.P.
M.P.H.	R.P.M.									
	1600	1700	1800	1900	2000	2100	2200	2300	2400	2500
100	10.51	10.22	9.97	9.74	9.52	9.32	9.12	8.94	8.78	8.62
110	10.11	9.83	9.58	9.36	9.18	8.98	8.81	8.61	8.45	8.32
120	9.77	9.51	9.27	9.05	8.87	8.68	8.48	8.32	8.17	8.05
130	9.45	9.21	8.97	8.78	8.58	8.41	8.22	8.05	7.91	7.77
140	9.18	8.94	8.70	8.50	8.32	8.15	7.98	7.81	7.66	7.52
150	8.94	8.68	8.47	8.28	8.10	7.92	7.76	7.61	7.48	7.32
160	8.70	8.45	8.25	8.08	7.88	7.72	7.55	7.41	7.26	7.15
170	8.50	8.26	8.07	7.88	7.70	7.55	7.38	7.22	7.11	6.98
180	8.31	8.08	7.88	7.69	7.52	7.37	7.21	7.08	6.93	6.81
190	8.12	7.88	7.70	7.54	7.37	7.21	7.06	6.91	6.79	6.68
200	7.97	7.76	7.56	7.39	7.24	7.08	6.93	6.78	6.65	6.54
210	7.82	7.61	7.41	7.24	7.09	6.94	6.79	6.65	6.52	6.41
220	7.68	7.45	7.26	7.11	6.96	6.79	6.68	6.52	6.41	6.28
230	7.52	7.32	7.13	6.98	6.83	6.68	6.55	6.42	6.28	6.18
240	7.41	7.18	7.02	6.86	6.72	6.58	6.43	6.29	6.18	6.09
250	7.29	7.08	6.91	6.75	6.59	6.46	6.32	6.19	6.08	5.98
260	7.18	6.96	6.78	6.64	6.49	6.36	6.22	6.09	5.98	5.88
270	7.08	6.88	6.71	6.56	6.42	6.28	6.14	6.01	5.89	5.79
280	6.97	6.77	6.59	6.45	6.32	6.18	6.05	5.93	5.82	5.71
290	6.86	6.68	6.51	6.36	6.23	6.09	5.98	5.84	5.75	5.62
300	6.77	6.58	6.42	6.26	6.12	5.99	5.88	5.76	5.66	5.56

DIAMETER										300 H.P.
M.P.H.	R.P.M.									
	1600	1700	1800	1900	2000	2100	2200	2300	2400	2500
100	10.73	10.44	10.19	9.96	9.73	9.53	9.32	9.15	8.97	8.82
110	10.33	10.05	9.80	9.57	9.38	9.18	8.99	8.80	8.64	8.50
120	10.00	9.72	9.47	9.26	9.07	8.88	8.68	8.50	8.34	8.24
130	9.66	9.29	9.16	8.97	8.77	8.60	8.41	8.22	8.08	7.94
140	9.38	9.14	8.89	8.69	8.52	8.34	8.14	7.98	7.83	7.70
150	9.13	8.88	8.66	8.48	8.29	8.10	7.94	7.78	7.64	7.50
160	8.88	8.65	8.44	8.26	8.06	7.91	7.72	7.58	7.42	7.30
170	8.68	8.45	8.25	8.05	7.88	7.71	7.53	7.37	7.25	7.14
180	8.49	8.25	8.05	7.87	7.70	7.53	7.39	7.24	7.08	6.96
190	8.31	8.06	7.88	7.71	7.53	7.37	7.24	7.07	6.93	6.87
200	8.14	7.93	7.72	7.56	7.40	7.23	7.08	6.92	6.80	6.69
210	7.98	7.77	7.57	7.40	7.24	6.98	6.95	6.80	6.67	6.57
220	7.84	7.60	7.43	7.25	6.99	6.96	6.83	6.68	6.55	6.48
230	7.69	7.47	7.28	7.00	6.97	6.83	6.69	6.55	6.44	6.33
240	7.57	7.34	7.18	7.01	6.87	6.71	6.58	6.43	6.32	6.24
250	7.45	7.22	7.05	6.90	6.74	6.60	6.48	6.33	6.22	6.12
260	7.32	7.10	6.94	6.78	6.63	6.49	6.37	6.23	6.10	6.00
270	7.23	7.03	6.85	6.70	6.54	6.42	6.29	6.14	6.03	5.93
280	7.12	6.92	6.74	6.60	6.46	6.30	6.19	6.07	5.96	5.84
290	7.04	6.82	6.64	6.49	6.35	6.24	6.07	5.97	5.87	5.76
300	6.94	6.72	6.53	6.38	6.25	6.13	5.99	5.89	5.78	5.68

DIAMETER										325 H.P.
M.P.H.	R.P.M.									
	1600	1700	1800	1900	2000	2100	2200	2300	2400	2500
100	10.98	10.68	10.42	10.18	9.96	9.75	9.54	9.35	9.18	9.01
110	10.57	10.28	10.01	9.80	9.60	9.39	9.21	9.00	8.83	8.69
120	10.22	9.95	9.70	9.47	9.28	9.08	8.87	8.70	8.55	8.42
130	9.89	9.63	9.38	9.18	8.97	8.79	8.60	8.42	8.27	8.13
140	9.60	9.35	9.10	8.90	8.70	8.53	8.35	8.17	8.01	7.87
150	9.35	9.08	8.87	8.67	8.48	8.29	8.11	7.96	7.82	7.66
160	9.10	8.85	8.62	8.45	8.25	8.08	7.90	7.75	7.59	7.48
170	8.89	8.64	8.43	8.24	8.06	7.89	7.72	7.56	7.43	7.30
180	8.69	8.45	8.24	8.04	7.87	7.71	7.54	7.41	7.24	7.12
190	8.50	8.25	8.06	7.89	7.71	7.55	7.38	7.23	7.10	6.98
200	8.32	8.11	7.90	7.73	7.57	7.40	7.24	7.09	6.95	6.84
210	8.18	7.96	7.75	7.57	7.42	7.26	7.10	6.96	6.82	6.71
220	8.03	7.79	7.59	7.44	7.27	7.10	6.98	6.82	6.71	6.57
230	7.87	7.65	7.46	7.29	7.13	6.98	6.85	6.71	6.57	6.47
240	7.75	7.51	7.34	7.17	7.03	6.88	6.72	6.58	6.47	6.37
250	7.62	7.41	7.22	7.06	6.89	6.75	6.61	6.48	6.37	6.26
260	7.50	7.29	7.09	6.95	6.79	6.65	6.50	6.37	6.25	6.15
270	7.41	7.20	7.01	6.86	6.71	6.57	6.43	6.29	6.16	6.06
280	7.30	7.08	6.89	6.75	6.61	6.47	6.33	6.20	6.09	5.97
290	7.18	6.98	6.80	6.65	6.51	6.37	6.25	6.11	6.01	5.88
300	7.08	6.88	6.71	6.55	6.41	6.27	6.16	6.02	5.91	5.82

DIAMETER										350 H.P.
M.P.H.	R.P.M.									
	1600	1700	1800	1900	2000	2100	2200	2300	2400	2500
100	11.22	10.90	10.64	10.39	10.16	9.95	9.74	9.55	9.37	9.20
110	10.79	10.49	10.22	10.00	9.80	9.58	9.40	9.19	9.02	8.88
120	10.43	10.15	9.90	9.67	9.47	9.27	9.06	8.88	8.72	8.59
130	10.09	9.83	9.57	9.37	9.16	8.98	8.77	8.59	8.44	8.30
140	9.80	9.55	9.29	9.07	8.88	8.70	8.52	8.34	8.18	8.03
150	9.55	9.27	9.05	8.85	8.65	8.46	8.28	8.13	7.98	7.82
160	9.29	9.03	8.81	8.62	8.42	8.25	8.07	7.92	7.75	7.63
170	9.08	8.81	8.60	8.41	8.23	8.05	7.88	7.71	7.58	7.46
180	8.87	8.62	8.41	8.20	8.03	7.87	7.70	7.56	7.41	7.28
190	8.67	8.42	8.23	8.06	7.87	7.70	7.54	7.38	7.25	7.13
200	8.48	8.28	8.06	7.89	7.73	7.56	7.39	7.24	7.10	6.99
210	8.35	8.13	7.91	7.73	7.57	7.41	7.25	7.10	6.96	6.85
220	8.20	7.95	7.75	7.59	7.43	7.27	7.13	6.97	6.85	6.71
230	8.03	7.81	7.60	7.45	7.28	7.13	6.99	6.85	6.71	6.60
240	7.91	7.67	7.50	7.32	7.17	7.02	6.86	6.72	6.60	6.50
250	7.78	7.56	7.37	7.20	7.04	6.89	6.75	6.61	6.49	6.39
260	7.66	7.45	7.24	7.09	6.93	6.78	6.63	6.50	6.38	6.27
270	7.56	7.34	7.16	7.00	6.85	6.71	6.56	6.42	6.29	6.18
280	7.45	7.23	7.04	6.88	6.74	6.60	6.46	6.33	6.22	6.10
290	7.32	7.13	6.95	6.79	6.65	6.50	6.38	6.24	6.13	6.01
300	7.23	7.03	6.85	6.68	6.54	6.40	6.28	6.15	6.04	5.93

DIAMETER										375 H.P.
M.P.H.	R.P.M.									
	1600	1700	1800	1900	2000	2100	2200	2300	2400	2500
100	11.44	11.13	10.84	10.60	10.36	10.14	9.93	9.73	9.56	9.38
110	11.00	10.70	10.43	10.20	9.99	9.77	9.59	9.37	9.19	9.05
120	10.64	10.35	10.10	9.86	9.66	9.45	9.24	9.05	8.90	8.76
130	10.30	10.03	9.76	9.55	9.34	9.16	8.95	8.76	8.60	8.46
140	9.99	9.73	9.47	9.25	9.06	8.87	8.69	8.50	8.33	8.19
150	9.73	9.45	9.22	9.02	8.82	8.63	8.45	8.29	8.14	7.97
160	9.47	9.20	8.98	8.78	8.59	8.41	8.23	8.07	7.90	7.78
170	9.26	8.99	8.77	8.57	8.39	8.22	8.03	7.86	7.73	7.60
180	9.05	8.79	8.58	8.37	8.19	8.02	7.85	7.71	7.54	7.42
190	8.85	8.59	8.39	8.21	8.02	7.85	7.68	7.53	7.40	7.27
200	8.65	8.45	8.23	8.05	7.88	7.71	7.54	7.38	7.24	7.13
210	8.52	8.28	8.07	7.88	7.72	7.56	7.40	7.24	7.09	6.98
220	8.36	8.11	7.90	7.74	7.57	7.42	7.27	7.10	6.98	6.84
230	8.19	7.97	7.75	7.59	7.43	7.27	7.13	6.98	6.84	6.73
240	8.06	7.82	7.64	7.46	7.31	7.16	7.00	6.85	6.73	6.63
250	7.94	7.71	7.52	7.35	7.17	7.03	6.88	6.74	6.62	6.52
260	7.81	7.60	7.38	7.23	7.06	6.92	6.76	6.63	6.50	6.40
270	7.71	7.48	7.30	7.14	6.98	6.83	6.70	6.55	6.42	6.31
280	7.59	7.38	7.18	7.02	6.88	6.73	6.58	6.45	6.33	6.22
290	7.47	7.27	7.08	6.92	6.78	6.63	6.50	6.37	6.26	6.12
300	7.38	7.16	6.98	6.82	6.67	6.52	6.41	6.28	6.16	6.05

DIAMETER										400 H.P.
M.P.H.	R.P.M.									
	1600	1700	1800	1900	2000	2100	2200	2300	2400	2500
100	11.6.5	11.32	11.03	10.80	10.56	10.33	10.11	9.90	9.71	9.55
110	11.20	10.89	10.61	10.38	10.18	9.95	9.73	9.53	9.35	9.20
120	10.82	10.53	10.28	10.04	9.84	9.61	9.42	9.21	9.03	8.90
130	10.50	10.22	9.92	9.71	9.50	9.31	9.11	8.91	8.75	8.60
140	10.18	9.90	9.63	9.40	9.22	9.02	8.82	8.65	8.49	8.34
150	9.90	9.61	9.40	9.18	8.96	8.79	8.58	8.42	8.26	8.12
160	9.62	9.38	9.14	8.95	8.74	8.55	8.37	8.20	8.05	7.91
170	9.40	9.15	8.94	8.74	8.52	8.35	8.17	8.00	7.86	7.73
180	9.20	8.95	8.72	8.51	8.34	8.16	7.97	7.84	7.67	7.55
190	9.00	8.74	8.52	8.35	8.17	7.99	7.82	7.66	7.52	7.40
200	8.83	8.59	8.36	8.19	8.01	7.84	7.67	7.51	7.36	7.25
210	8.66	8.42	8.21	8.03	7.85	7.68	7.51	7.37	7.24	7.10
220	8.50	8.25	8.05	7.86	7.72	7.52	7.37	7.24	7.10	7.02
230	8.34	8.10	7.90	7.74	7.56	7.39	7.23	7.10	6.95	6.87
240	8.21	7.95	7.78	7.61	7.43	7.27	7.11	6.96	6.85	6.75
250	8.06	7.84	7.65	7.48	7.31	7.15	7.01	6.86	6.72	6.63
260	7.94	7.73	7.52	7.35	7.20	7.04	6.88	6.75	6.63	6.51
270	7.83	7.62	7.43	7.25	7.10	6.95	6.79	6.65	6.53	6.42
280	7.73	7.52	7.33	7.15	7.00	6.85	6.69	6.57	6.46	6.33
290	7.62	7.42	7.23	7.07	6.91	6.75	6.59	6.48	6.36	6.24
300	7.52	7.31	7.12	6.96	6.80	6.64	6.51	6.38	6.27	6.15

DIAMETER										425 H.P.
M.P.H.	R.P.M.									
	1600	1700	1800	1900	2000	2100	2200	2300	2400	2500
100	11.84	11.51	11.23	10.98	10.73	10.50	10.27	10.07	9.89	9.72
110	11.39	11.08	10.79	10.56	10.34	10.12	9.93	9.70	9.52	9.37
120	11.03	10.72	10.44	10.20	10.00	9.78	9.57	9.37	9.21	9.07
130	10.65	10.38	10.11	9.89	9.67	9.48	9.27	9.07	8.91	8.75
140	10.34	10.07	9.81	9.58	9.38	9.19	8.99	8.80	8.63	8.48
150	10.07	9.78	9.55	9.34	9.14	8.93	8.73	8.57	8.43	8.25
160	9.80	9.53	9.30	9.10	8.89	8.70	8.52	8.35	8.18	8.06
170	9.58	9.30	9.08	8.88	8.68	8.50	8.32	8.14	8.01	7.87
180	9.37	9.10	8.88	8.66	8.48	8.31	8.13	7.98	7.81	7.68
190	9.15	8.89	8.68	8.51	8.31	8.13	7.95	7.79	7.65	7.53
200	8.95	8.74	8.52	8.33	8.16	7.98	7.80	7.64	7.50	7.38
210	8.81	8.58	8.35	8.16	7.99	7.83	7.65	7.50	7.35	7.23
220	8.65	8.40	8.18	8.01	7.84	7.68	7.53	7.36	7.23	7.08
230	8.48	8.24	8.03	7.86	7.69	7.53	7.38	7.23	7.08	6.97
240	8.35	8.10	7.92	7.73	7.57	7.41	7.24	7.09	6.97	6.86
250	8.22	7.98	7.78	7.61	7.43	7.28	7.13	6.98	6.86	6.74
260	8.08	7.87	7.65	7.48	7.32	7.16	7.02	6.87	6.74	6.63
270	7.98	7.75	7.56	7.39	7.23	7.08	6.93	6.78	6.64	6.53
280	7.86	7.63	7.43	7.27	7.12	6.97	6.82	6.68	6.56	6.43
290	7.73	7.53	7.33	7.17	7.02	6.87	6.73	6.59	6.48	6.34
300	7.63	7.42	7.23	7.05	6.90	6.75	6.63	6.49	6.38	6.27

DIAMETER										450 H.P.
M.P.H.	R.P.M.									
	1600	1700	1800	1900	2000	2100	2200	2300	2400	2500
100	12.05	11.71	11.42	11.16	10.91	10.69	10.45	10.25	10.06	9.88
110	11.58	11.27	10.97	10.74	10.53	10.29	10.10	9.87	9.68	9.53
120	11.20	10.90	10.63	10.38	10.17	9.96	9.73	9.53	9.37	9.23
130	10.83	10.55	10.28	10.06	9.83	9.65	9.43	9.23	9.06	8.91
140	10.52	10.25	9.98	9.75	9.54	9.35	9.15	8.96	8.78	8.63
150	10.25	9.96	9.72	9.50	9.29	9.08	8.90	8.73	8.58	8.40
160	9.98	9.70	9.45	9.26	9.05	8.86	8.67	8.50	8.32	8.19
170	9.75	9.47	9.24	9.03	8.83	8.65	8.46	8.28	8.15	8.01
180	9.53	9.26	9.03	8.82	8.63	8.45	8.27	8.12	7.94	7.81
190	9.32	9.04	8.83	8.65	8.45	8.27	8.10	7.93	7.79	7.66
200	9.11	8.89	8.66	8.47	8.30	8.12	7.94	7.78	7.62	7.50
210	8.97	8.73	8.50	8.30	8.13	7.96	7.79	7.63	7.47	7.35
220	8.80	8.54	8.32	8.15	7.98	7.81	7.65	7.49	7.35	7.20
230	8.63	8.39	8.17	8.00	7.82	7.66	7.51	7.35	7.21	7.09
240	8.50	8.24	8.05	7.86	7.70	7.54	7.37	7.22	7.09	6.98
250	8.36	8.12	7.92	7.73	7.56	7.40	7.25	7.10	6.97	6.86
260	8.23	7.97	7.78	7.62	7.45	7.29	7.13	6.98	6.85	6.75
270	8.12	7.89	7.69	7.52	7.36	7.20	7.05	6.90	6.76	6.64
280	8.00	7.77	7.56	7.40	7.25	7.09	6.93	6.79	6.68	6.55
290	7.86	7.66	7.46	7.29	7.14	6.98	6.85	6.70	6.58	6.45
300	7.77	7.55	7.36	7.18	7.02	6.87	6.75	6.60	6.48	6.38

DIAMETER										475 H.P.
M.P.H.	R.P.M.									
	1600	1700	1800	1900	2000	2100	2200	2300	2400	2500
100	12.23	11.88	11.59	11.33	11.07	10.84	10.61	10.40	10.21	10.03
110	11.76	11.44	11.14	10.90	10.68	10.44	10.25	10.02	9.83	9.67
120	11.37	11.06	10.78	10.53	10.33	10.10	9.88	9.67	9.51	9.37
130	11.00	10.72	10.44	10.22	9.98	9.78	9.57	9.37	9.20	9.05
140	10.68	10.40	10.13	9.90	9.68	9.48	9.28	9.09	8.91	8.75
150	10.40	10.10	9.86	9.65	9.43	9.22	9.03	8.86	8.70	8.52
160	10.12	9.84	9.60	9.40	9.18	8.99	8.79	8.63	8.44	8.32
170	9.90	9.61	9.37	9.17	8.97	8.78	8.59	8.41	8.27	8.12
180	9.67	9.40	9.17	8.94	8.75	8.58	8.40	8.24	8.06	7.93
190	9.45	9.18	8.92	8.78	8.58	8.40	8.22	8.05	7.90	7.77
200	9.25	9.02	8.79	8.60	8.42	8.24	8.06	7.89	7.74	7.62
210	9.10	8.86	8.63	8.43	8.25	8.08	7.90	7.74	7.58	7.47
220	8.93	8.67	8.45	8.27	8.10	7.93	7.78	7.59	7.46	7.31
230	8.75	8.52	8.29	8.12	7.94	7.78	7.62	7.46	7.31	7.20
240	8.62	8.36	8.17	7.98	7.82	7.65	7.48	7.32	7.20	7.08
250	8.48	8.24	8.04	7.85	7.67	7.52	7.36	7.20	7.08	6.97
260	8.35	8.12	7.89	7.73	7.55	7.40	7.23	7.08	6.96	6.84
270	8.24	8.01	7.81	7.63	7.47	7.31	7.15	7.00	6.86	6.74
280	8.12	7.88	7.67	7.51	7.35	7.20	7.04	6.89	6.78	6.65
290	7.98	7.78	7.57	7.40	7.24	7.08	6.95	6.80	6.69	6.55
300	7.88	7.66	7.47	7.28	7.13	6.97	6.84	6.70	6.58	6.47

DIAMETER										500 H.P.
M.P.H.	R.P.M.									
	1600	1700	1800	1900	2000	2100	2200	2300	2400	2500
100	12.40	12.05	11.75	11.49	11.22	11.00	10.76	10.53	10.35	10.18
110	11.92	11.60	11.30	11.04	10.82	10.60	10.36	10.14	9.97	9.80
120	11.52	11.21	10.94	10.69	10.46	10.25	10.01	9.80	9.63	9.49
130	11.15	10.87	10.58	10.35	10.11	9.91	9.68	9.49	9.31	9.16
140	10.82	10.54	10.26	10.02	9.82	9.63	9.39	9.21	9.04	8.87
150	10.53	10.23	10.00	9.77	9.56	9.35	9.15	8.96	8.69	8.65
160	10.25	9.99	9.73	9.52	9.31	9.11	8.90	8.74	8.56	8.43
170	10.01	9.75	9.50	9.29	9.09	8.90	8.70	8.52	8.38	8.24
180	9.80	9.52	9.28	9.06	8.87	8.69	8.49	8.34	8.17	8.03
190	9.58	9.30	9.09	8.89	8.69	8.50	8.31	8.16	8.01	7.89
200	9.40	9.15	8.91	8.72	8.54	8.34	8.17	8.00	7.85	7.71
210	9.22	8.96	8.73	8.54	8.36	8.18	8.02	7.84	7.68	7.56
220	9.05	8.78	8.56	8.38	8.21	8.01	7.82	7.70	7.55	7.47
230	8.87	8.63	8.40	8.22	8.05	7.87	7.72	7.55	7.43	7.29
240	8.74	8.47	8.28	8.10	7.92	7.75	7.56	7.44	7.29	7.18
250	8.60	8.35	8.15	7.95	7.77	7.62	7.46	7.30	7.15	7.06
260	8.46	8.21	8.00	7.83	7.66	7.50	7.32	7.19	7.05	6.93
270	8.35	8.11	7.91	7.74	7.56	7.40	7.24	7.08	6.95	6.84
280	8.22	7.99	7.78	7.61	7.45	7.29	7.14	7.00	6.86	6.74
290	8.10	7.87	7.67	7.50	7.35	7.19	7.03	6.89	6.77	6.64
300	7.99	7.76	7.55	7.39	7.23	7.07	6.94	6.80	6.68	6.56

DIAMETER RELATION BETWEEN 3-BLADE PROPELLER AND MULTI-BLADE PROPELLERS

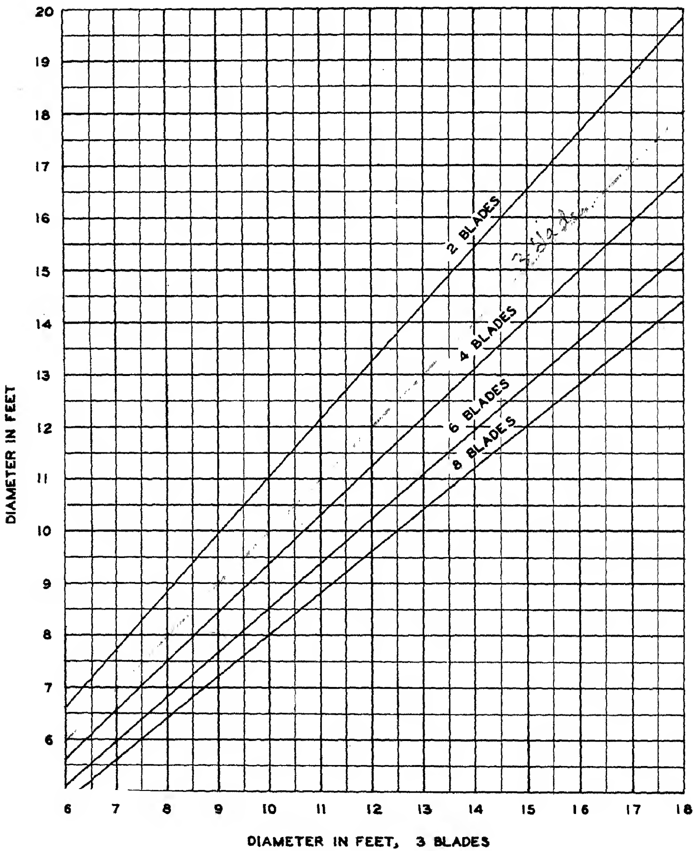

FIGURE 63

INDEX